Pluto Fast Flyby Spacecraft Design and Development

by

J.G.Shirlaw

B.A. Cambridge University England (1987)
M.A. Cambridge University England (1991)

Submitted to the Department of Aeronautics and Astronautics
in partial fulfillment of the requirements for the degrees of
Engineer in Aeronautics and Astronautics
and
Master of Science in Aeronautics and Astronautics
at the
MASSACHUSETTS INSTITUTE OF TECHNOLOGY
May 1994

© Science and Engineering Research Council (UK), 1994. All rights reserved.

The author hereby grants to MIT permission to reproduce and distribute publicly paper and electronic copies of this thesis document in whole or in part, and to grant others the right to do so.

Author ....
Department of Aeronautics and Astronautics
May 23, 1994

Certified by.......
Stanley I. Weiss
Visiting Professor
Thesis Supervisor

Accepted by ......
Professor Harold Y Wachman
Chairman, Department Graduate Committee

MASSACHUSETTS INSTITUTE
OF TECHNOLOGY
JUN 09 1994 Aero

Pluto Fast Flyby Spacecraft Design and Development

by

J.G.Shirlaw

Submitted to the Department of Aeronautics and Astronautics
on May 23, 1994, in partial fulfillment of the
requirements for the degrees of
Engineer in Aeronautics and Astronautics
and
Master of Science in Aeronautics and Astronautics

Abstract

Pluto is the only remaining planet in the solar system that has not been visited by a spacecraft. Because Pluto is now moving away from the sun, having passed perihelion in September 1989, the planets thin atmosphere is beginning to condense onto the planet's surface. This process is expected to be completed between the years 2015 and 2025. In this thesis, a system level design of a Pluto Fast Flyby (PFF) spacecraft is developed. This spacecraft is capable of generating a set of images of Pluto and its moon Charon in the UV, IR and visible bands, and thus conducting an initial survey of Pluto, its atmosphere, and Charon. The spacecraft has a dry mass of 130 kg. The instruments used are based on the payload currently planned by NASA's JPL for use on a mission to Pluto. Using a Titan IV launch vehicle, the spacecraft should rendezvous with Pluto 10 years after launch. The design of the spacecraft in general employed the design methodology found in the Draft NASA Engineering Handbook. As a result of the design activities, a number of improvements to the design methodologies presentation were proposed. Finally using the PFF spacecraft as a baseline, a number of comments on NASA's technology development program with respect to the forthcoming discovery series of missions were advanced.

Thesis Supervisor: Stanley I. Weiss
Title: Visiting Professor

Acknowledgments

I would like to acknowledge the assistance of the following people in the preparation of this thesis:

Toni Smerdon and my father for encouraging and assisting me in applying to MIT.

The Science and Engineering Research Council of Great Britain for providing the funds to support me during my time at MIT.

Professors Joseph Shea and Stan Weiss, for their comments, encouragement and general support in supervising this work. In particular I would like to thank Stan Weiss for accepting the role as my supervisor during Professor Shea's unfortunate illness, and for putting up with my individualistic version of written English in the early version of this work. Also to the many people who assisted in improving the written English by reading various parts of this document.

Allison C Sanlin at the National Research Council, for providing a lot of the material that helped make this thesis, for which no small amount of photocopying was required on her part.

To Professor Richard Battin, for developing my interest in astrodynamics and for his ability to make vector algebra comprehensible.

Professor Walt Hollister for acting as my mentor while here at MIT.

To my Lord Jesus Christ for more things and times than I ever have a hope of remembering or realising

To those poor people who have to read this document. Particularly if it is in its entirety.

And finally all the Americans who have finally realized that they speak American and not English and have accepted the challenge of understanding true English.

Contents

1 Introduction **27**

2 The Planet Pluto **29**

2.1 Peculiarities and Curiosities of Pluto 29

2.2 Pluto and the Publicity for NASA 31

3 The Design Process **33**

3.1 Introduction 33

3.2 The Successive Refinement Spiral 34

3.3 Trade Studies 34

3.4 Applied Design Philosophy 36

4 Science and Mission Objectives **43**

4.1 Introduction 43

4.2 Science Objective 43

4.3 Mission Objective 44

4.4 Program Philosophy 45

4.4.1 Introduction 45

4.4.2 Schedule 47

4.4.3 Science Return 48

4.4.4 Reliability 48
4.4.5 Cost 48
4.4.6 When All parameters Are Acceptable 49

5 Initial Instrument Definition **51**
5.1 Introduction 51
5.2 Required Sensor Systems 51
5.2.1 Neutral Atmosphere 52
5.2.2 Geology & Morphology 53
5.2.3 Surface Composition Mapping 53
5.2.4 Ionosphere 53
5.2.5 Bolometeric Bond Albedo 53
5.2.6 Surface Temperature Mapping 54
5.2.7 Energetic Particles 54
5.2.8 Bulk Parameters (R,M,ρ) 54
5.2.9 Magnetic Field 54
5.2.10 Additional Satellites 55
5.2.11 Typical Instrument Masses 55

6 Mission Concepts **59**
6.1 Introduction 59
6.2 Identification and Quantification of Goals 59
6.3 Perform Functional Analysis 59
6.4 Measurements and Measurement Methods 60
6.4.1 System Characteristics 60
6.4.2 Measurement Methods 61
6.5 Spacecraft Concepts 62

6.6 Selection Rules 64
6.7 Generate Data on the Alternatives 65
6.8 Selection of the Continuing Designs 65
6.9 Conclusion 65

7 System Level Requirements **69**
7.1 Introduction 69
7.2 Mission 70
7.3 Strawman Science Payload 70
7.3.1 Visible Sensor 70
7.3.2 IR Spectrometer 71
7.3.3 UV Sensor 71
7.3.4 Radio Science 72
7.4 Instrument Summary 72
7.4.1 Science Instrument Impact on Spacecraft Design 72
7.5 Orbit 72
7.6 Environment 73
7.7 Launch 73
7.8 Ground Systems Interface 73

8 Spacecraft Flight Operations & Support **75**
8.1 Spacecraft Operations/Mission Profile 75
8.1.1 Introduction 75
8.1.2 Flight Support Team 76
8.1.3 Operations Strategy Trade Study 78
8.1.4 Flight Support Activities 81
8.1.5 Data Downlink Activities 82

8.1.6 Activities During Cruise 83

8.2 Orbit Analysis 83

8.2.1 Introduction 83

8.2.2 Orbit Concepts 83

8.2.3 Gravitational Assists 84

8.2.4 Aerogravity Assist 84

8.2.5 Direct Flight 85

8.2.6 Broken Plane Maneuvers 86

8.2.7 Preferred Orbit Selection 87

8.2.8 Launch Window 87

9 Spacecraft Systems Design **91**

9.1 Introduction 91

9.1.1 Design Approach 92

9.2 Spacecraft Configuration 92

9.2.1 Introduction 92

9.2.2 Instrument Scan Platform 93

9.2.3 Spacecraft Pointed Instruments 93

9.2.4 Pointing Selection 94

9.2.5 Spacecraft Concepts 94

9.3 Functional Analysis 97

9.4 Initial Design Budget Apportionment 97

9.4.1 Margin Allocation 98

9.4.2 Mass Budget 100

9.4.3 Power 102

9.4.4 Pointing 106

9.4.5 Propellant Budget 110

9.4.6 Reliability 112
9.4.7 Cost 113
9.5 Power Subsystem 115
9.5.1 Requirements 115
9.5.2 Power Subsystem Concepts 115
9.5.3 Measurement Characteristics 115
9.5.4 Concept Selection Criteria 116
9.5.5 Solar Arrays 116
9.5.6 Radio-Isotope Thermal Generator 117
9.5.7 Batteries 120
9.5.8 Fuel Cells 122
9.5.9 Fuel Cells Plus a Solar Array 123
9.5.10 Batteries Plus a Solar Array 124
9.5.11 Primary Power Supply Selection 124
9.5.12 Power Regulation 124
9.5.13 Power Distribution 126
9.5.14 Equipment Power Control and Fusing 126
9.5.15 Power Harness 126
9.5.16 Pyrotechnical Devices 127
9.5.17 Risk 127
9.5.18 Cost 128
9.5.19 Subsystem Characteristics 128
9.6 Attitude and Orbit Control Subsystem 128
9.6.1 Introduction 128
9.6.2 Pointing Requirements 130
9.6.3 Spacecraft Platform Stabilisation 135

9.6.4 Actuator Selection 136
9.6.5 Actuator Selection 144
9.6.6 Attitude Determination 145
9.6.7 Safeing Mode Sensors 146
9.6.8 Control Electronics 147
9.6.9 Risk 148
9.6.10 Cost 149
9.6.11 AOCS Summary 149
9.7 Guidance, Navigation and Control 152
9.7.1 Spacecraft-Based Navigation 152
9.7.2 Ground-Based Navigation 152
9.7.3 Preferred Navigation and Control Design 153
9.7.4 Terminal Guidance 153
9.7.5 Risk 154
9.7.6 Cost 154
9.7.7 GNC Subsystem Summary 155
9.8 Command and Data Management Subsystem 155
9.8.1 Introduction 155
9.8.2 CDMS Architecture 155
9.8.3 Architecture Selection 156
9.8.4 Computer System Operational modes 160
9.8.5 Computer Interface Architecture 161
9.8.6 Data Storage Requirements 163
9.8.7 Command and Telemetry Harness 165
9.8.8 CDMS Risk 165
9.8.9 Cost 165

9.8.10 CDMS Design Summary 166
9.9 Launch Subsystem 167
9.9.1 Introduction 167
9.9.2 Titan IV Launch Vehicle 167
9.9.3 ΔV Requirement 168
9.9.4 Upper Stage Selection 168
9.9.5 Upper Stage Guidance 176
9.9.6 Launch System Summary 176
9.10 Propulsion Subsystem 176
9.10.1 Introduction 176
9.10.2 Requirements 177
9.10.3 Fuel Options 177
9.10.4 Propulsion System Selection 180
9.10.5 Blow Down or Regulated System 180
9.10.6 Propulsion Tankage and Equipment Masses 180
9.10.7 Mid-Course Guidance Procedure 181
9.10.8 Risk 181
9.10.9 Cost 182
9.10.10 Propulsion Subsystem Summary 182
9.11 Communications Subsystem 183
9.11.1 Introduction 183
9.11.2 Requirements 183
9.11.3 Communications Architecture 183
9.11.4 Operating Frequency 184
9.11.5 Optical Communications 186
9.11.6 Main Antenna 187

9.11.7 Communication Hardware Architecture 193
9.11.8 Cost 197
9.11.9 Risk 197
9.11.10 Communication Subsystem Summary 198
9.12 Support Structure 199
9.12.1 Introduction 199
9.12.2 Requirements 199
9.12.3 Structure Concept 199
9.12.4 Spacecraft Bus Structure 200
9.12.5 Launcher Interface Attachment 202
9.12.6 Risk 206
9.12.7 Cost 207
9.12.8 Support Structure Summary 207
9.13 Thermal Control Subsystem 207
9.13.1 Introduction 207
9.13.2 Requirements and Assumptions 208
9.13.3 Thermal Control Concepts 211
9.13.4 Louvres 211
9.13.5 Cold Biased System with Heaters 211
9.13.6 Hot Biased Petia Cooling 212
9.13.7 Hot Biased Heat Pipe Control 212
9.13.8 Preferred Thermal Control System 213
9.13.9 MLI 213
9.13.10 Power Regulator Radiator 214
9.13.11 Sun Shade 215
9.13.12 Thermal Control Mass 215

9.13.13 Thermal Control Power Requirement 216
9.13.14 Thermal Control Risk 216
9.13.15 Cost 216
9.13.16 Thermal Control System Summary 217
9.14 Instrument Configuration 217
9.14.1 Introduction 217
9.14.2 Solar and Earth Occultation 218
9.14.3 Spin Axis 218
9.14.4 Preferred Instrument Mounting Direction 219
9.15 First Iteration Design Summary 219
9.15.1 Introduction 219
9.15.2 Budgets 219

10 Design Iteration Changes **225**
10.1 Introduction 225
10.2 Variation of Structure and Antenna Gain 226
10.3 Instruments 227
10.4 Command and Data Management Subsystem 227
10.5 Attitude and Orbit Control 227
10.6 Communication Subsystem 228
10.7 Thermal Control 228
10.8 Power Supply 229
10.9 Propulsion System 229
10.10 Launch System and Upper Stage 229
10.11 Launch Support Structure 230
10.12 Final System Budgets 231
10.13 Risk Summary 231

11 NASA Engineering Handbook Critique 237
11.1 Introduction 237
11.2 Objective of Systems Engineering 238
11.3 Systems Engineering: Science or Art 238
11.4 Systems Engineering and Systems Management 239
11.5 Mission Philosophy to Concept Development 240
  11.5.1 Mission Objective 240
  11.5.2 Program Philosophy 240
  11.5.3 Identifying Goals 241
  11.5.4 Systems Concepts 241
11.6 The Doctrine of Successive Refinement 241
  11.6.1 Requirements Flow Down 242
  11.6.2 Iteration 242
  11.6.3 Defining Goals and Constraints 244
  11.6.4 Budgets 244
  11.6.5 Loop Unrolling 244
  11.6.6 Increase the Resolution of the Design 245
11.7 Design Trade Studies 245
  11.7.1 Trade Studies and the Doctrine of Successive Refinement . . . 245
  11.7.2 Functional Analysis 246
  11.7.3 When to trade or not to trade–that is the question 246
  11.7.4 Making a Tentative Selection 247
11.8 Technical Terms 247
  11.8.1 Definitions 247
  11.8.2 Project Phases 247
11.9 Conclusion 248

12 Technology Development Program 249

12.1 Introduction 249

12.2 Is the PFF a Fair Comparison? 250

12.3 Technology Required for PFF 250

12.3.1 Introduction 250

12.3.2 Micro-Thrusters 251

12.3.3 Inertial Navigation System 251

12.3.4 Star Mappers 251

12.3.5 Communications Subsystem 251

12.3.6 Onboard Computer 252

12.3.7 Data Storage 252

12.3.8 RTG 253

12.3.9 Composite Materials 253

12.3.10 Lens Antenna 254

12.3.11 Thermal Control 254

12.3.12 Electronic Packaging 254

12.3.13 Flight Operations 255

12.4 General Comments on NASA Technology Development 256

12.4.1 Distress Beacon 256

12.4.2 Reaction Wheels 256

12.4.3 AOCS 257

12.4.4 Spreading the Butter too Thin 257

12.4.5 Project Personnel 258

12.4.6 Government Review Process 261

12.4.7 Software Cost 261

12.5 Conclusion 263

13 Future Work **265**
13.1 Introduction 265
13.2 Pluto Fast Flyby Spacecraft 265
13.3 NASA Systems Engineering Handbook 266
13.4 NASA's Discovery Programs 266
13.5 Conclusions 266

14 Conclusion **269**

A Minimum Energy Transfer Orbit **271**

B Minimum Impulse Transfer Notebook **277**

C Solar Radiation Induced Torque Notebook **283**

D Communication Link Budgets **289**
D.1 L Band Down Link 289
D.2 S Band Up Link 291
D.3 S Band Down Link 293
D.4 X Band Up Link 295
D.5 X Band Down Link 297
D.6 Ka Band Up Link 299
D.7 Ka Band Down Link 301

E Computer Program To calculate C_3 **305**
E.1 Make File 305
E.2 array.def.h 306
E.3 definitions.h 307
E.4 Transfer.time.c 308

E.5 Initialise.Planet.c 314
E.6 Compute.transfer.angle.c 318
E.7 Lamberts.problem.c 321
E.8 vector.c 331
E.9 rec.to.clasical.c 334
E.10 universal.c 339

F Lens Mass Calculation **351**
F.1 Assumptions 351
F.2 Circular Cavity Segment Mass 351
F.3 Rectangular Cavity Segment Mass 352
F.4 Waveguide Diameter 353
F.5 Circular Cavity Based Lens Mass 354
F.6 Rectangular Cavity Based Lens Mass 355

G Final Spacecraft Communication Link Budgets **357**
G.1 X Band Up Link 357
G.2 X Band Down Link 359
G.3 Ka Band Up Link 361
G.4 Ka Band Down Link 363

Bibliography **367**

List of Figures

2-1 Hubble Space Telescope Image of Pluto 32

3-1 Successive refinement spiral 40
3-2 Trade Study Process 41
3-3 The Overall Systems Design Process for a Science Mission 42

4-1 Schematic of the Bounding of Program Philosophy Elements 46

6-1 Preliminary Design Trade Tree 63

8-1 Effect of Multiple Spacecraft on Overall Mission Reliability 78
8-2 The current value of the operations support team 80
8-3 Launch Energy vs Flight time to Pluto 86
8-4 Launch Energy (C_3) vs Launch Date for a 1998 Launch and 7-year flight time 88

9-1 Conceptual drawing of a reflector-based spacecraft 95
9-2 Conceptual drawing of a lens based spacecraft 96
9-3 Solar Radiation-induced Torques. 112
9-4 DC Solar Radiation-induced Torques. 113
9-5 Pluto flyby view angle 133
9-6 AOCS Functional Diagram 151

9-7 Onboard Computer States 162
9-8 Maximum ΔV against Mass fraction 170
9-9 Variation of C_3 with Number of Stages and Stage Mass 173
9-10 Discounted Cost of Additional Years of Flight Operations 175
9-11 Variation in thrust against equivalent non-augmented Isp 179
9-12 Reflector Area versus diameter for 0.5, 1 and 2 m focal lengths 193
9-13 Communications Subsystem Hardware Architecture 195
9-14 Conic shell launch interface and upper stage support 203
9-15 Truss based launch interface and upper stage support 204
9-16 Schematic Diagram of the Lens Based Spacecraft in Flight 210

10-1 Revised launch interface and upper stages support 230

11-1 Revised Successive Refinement Spiral Shaded boxes represent changes or additions to the NASA Handbook 243

A-1 Single Impulse Orbit Transfer 272
A-2 Plot of the variation of ΔV with transfer angle 273
A-3 Plot of the variation of flight time with transfer angle 275

F-1 Segment of Antenna Lens 352
F-2 Segment of Antenna Lens 353

List of Tables

4.1 Pluto Mission Science Priorities 44

5.1 Space Sounding Systems Applications 52

5.2 Galileo Science Instrument Payload 56

5.3 Cassini Science Instrument Payload 57

6.1 Performance and System Level Data on the Preliminary Designs . . . 66

6.2 Selection Measurement Data for the Preliminary Designs 67

8.1 Estimated cost of personnel assigned to support flight operations . . . 79

8.2 Summary of Flight Operations crew verses Fire and Forget 81

8.3 C_3 for different launch windows and flight times for a 1998 launch . . 89

9.1 Chosen System Margin Values 98

9.2 Possible Initial Spacecraft Mass Apportionment 101

9.3 Suggested Mass Breakdown Percentages from Selected Sources 103

9.4 Suggested Initial Mass Budget According to Selected Sources 104

9.5 Proposed Initial Mass Budget 105

9.6 Literature-suggested Power Breakdown Percentages 106

9.7 Suggested Initial Power Budget from Selected Sources 107

9.8 Proposed Initial Power Budget 108

9.9 Initial Pointing Requirement Apportionment 109
9.10 Initial Subsystem Cost Apportionment 114
9.11 RTG Material Properties 118
9.12 Required Fuel Mass for Pluto RTG 119
9.13 Costs of the RTG Material to supply 46.8 W 119
9.14 Battery Properties 123
9.15 Alternative Primary Power Supply Characteristics 125
9.16 Power Subsystem Characteristics 129
9.17 Mass characteristics of the AOCS actuator options 145
9.18 AOCS Subsystem Characteristics 150
9.19 GNC subsystem Characteristics 155
9.20 Onboard Computer Throughput and Memory Requirements 159
9.21 Power subsystem Characteristics 165
9.22 Power subsystem Characteristics 166
9.23 Estimated Titan IV Payload Mass vs. C_3 167
9.24 Commercially Available Solid Rocket Motors 171
9.25 Total C_3 Available for Two Solids and a Titan IV Centaur Launcher . 172
9.26 Cost of using different number of identical liquid stages 174
9.27 Propulsions Subsystem Characteristics 177
9.28 Estimated Titan IV Payload Mass vs C_3 178
9.29 Propulsion Subsystem Characteristics 182
9.30 Maximum data return rates 186
9.31 Communications Subsystem Summary 198
9.32 Support Structure Characteristics 208
9.33 Thermal Control Subsystem Characteristics 217
9.34 Spacecraft mass budget after initial systems design work 220

9.35 Spacecraft Final Systems-Level Pad Mass Budget 221
9.36 Spacecraft power budget after initial systems design work 222
9.37 Spacecraft cost budget after initial systems design work 223

10.1 Variation in spacecraft mass with different antenna diameters 226
10.2 Spacecraft Final Systems Level Mass Budget 232
10.3 Spacecraft Final Systems Level Pad Mass Budget 233
10.4 Spacecraft Final Systems Level Power Budget 234
10.5 Spacecraft cost budget after initial systems design work 235

Chapter 1

Introduction

The investigation of the Solar system, some would say, is merely the modern manifestation of mankind's inherent desire to explore. Others would argue that the quest provides us with insights into our world and in particular into the science of planetology. Thus the latter group would argue progress is made in understanding our world and its origins. Whichever of these arguments is favoured, it remains that Pluto is the last of the major planetary bodies of the Sun that has not been visited by mankind or their remote exploring spacecraft. It is within this context that Daniel S Goldin the NASA Administrator[1] said "I'll throw out a special challenge [here}. I believe we can build a spacecraft in three years weighing hundreds, not thousands of pounds, and costing a few hundred million dollars, not billions – and have it arrive at Pluto, the last unexplored planet, in the first years of the 21st century. It can be done."

This thesis presents the system level design of a small scientific spacecraft to carry out a fast flyby of the planet Pluto and its moon Charon before the end of the year 2005. The spacecraft is capable of carrying out a preliminary survey of the planet, its atmosphere and its moon Charon. Subsidiary to this objective is the use of the design technique proposed in the draft NASA System Engineering Handbook, to enable a critique of the handbook to be developed based on actual experience with the proposed methodology.

---

[1] Said in his address to the World Space Congress on the 2nd of September 1992.

The spacecraft requires a launch energy in excess of 305 km^2/sec^2 and therefore must be very light to allow it to be launched by an existing launch vehicle. This fact gives rise to a third objective, which is to use the design of the spacecraft to generate comments on the current activities within NASA in the area of technology development. The thesis takes as a baseline the instrument suite currently planned for inclusion in the mission as foreseen by JPL, the agency within NASA with the task of developing the flight vehicle.

The opening chapters of this thesis describes the background for the Pluto mission, the science requirements and the NASA Engineering Handbook design methodology. The methodology is then demonstrated through a preliminary study of the size of spacecraft that could be sent to Pluto. Having selected a small spacecraft, the detailed work of establishing the mission requirements, constraints and design work is presented along with all the required trade-offs. Having developed a design for the whole spacecraft using the proposed methodology, comments that resulted from the design activity are then summarised. Finally the technological considerations raised by the design are addressed.

Chapter 2

The Planet Pluto

2.1 Peculiarities and Curiosities of Pluto

Pluto[1] was discovered in 1930 by Clyde Tombaugh, at the Lowell Observatory. The planet has only one known moon Charon[2].

The primary interest in Pluto stems from the fact that it is the only remaining planet in the solar system that has not yet been visited by a spacecraft. It is therefore the only planet for which we do not have any more information than Galileo did about Mars and Saturn - only some very blurry images.

However, because of our improved understanding of the universe, these images tell us more than Galileo could have foreseen. The current best images of Pluto are those taken by the Faint Object Camera onboard the Hubble Space Telescope in 1990 (see figure 2-1). Pluto was found to have ten times the mass and double the density of Charon, suggesting that they have very different origins. Pluto has a mass of 1/400th that of the Earth. The reason for the different origins is currently unknown and requires more data, preferably from close-up observations. Pluto and Charon were once considered as a dual planet system, in which the two planets rotate around their common centre of gravity, rather than one about the other. However because of the large mass differential, this interpretation is not currently accepted.

---

[1] The Greek god of the underworld

[2] A son of Erebus who in Greek myth ferries the souls of the dead over the Styx. The moon was discovered in 1978 by astronomers at the US Naval Observatory.

From a 1987 stellar occultation, Pluto's atmosphere's upper limit diameter was computed to be 2286 km. The occultation also showed that Pluto has a clear outer atmosphere with hazy lower regions. Although no direct evidence yet exists, the data is consistent with a methane atmosphere at 67 K. The atmosphere is extremely thin and would only be approximately 10 m deep if held at standard temperature and pressure. From IRAS data taken during 1987, we also know that Pluto has methane ice caps at 54 K, This is the only planet in the solar system cold enough to keep methane solid. There is a dark ice-free equatorial band at 59 K.

Pluto takes almost 248 years to orbit the Sun and passed perihelion on the fifth of September, 1989. Pluto's atmosphere, largely nitrogen and methane, is frozen for most of the orbit, thawing out for approximately 25 years each side of perihelion. Thus, no trace of atmosphere is expected to be detectable after 2015 until 2212. The estimates for the date of "freeze-out" vary between 2015 to 2025 [11, 41]. At aphelion the planet is 50 AU from the Sun.

Other unique features of Pluto are its axial tilt (108 degrees), and the dual planet relationship similar to that of the moon and the Earth. Pluto has a rotational period of 6.3867 days.

Pluto has a density of approximately 2.1 g/cm^3 similar to that of some of the icy moons of the outer planets. Charon does not exhibit the methane ice spectrum of Pluto but appears to have a water ice covering, indicating a body similar to that of the Uranian and Saturnian moons. Charon has a diameter of approximately 1160 km. Because of their different compositions, it is expected that Charon will show the record of ancient meteor impacts, as at these temperatures the water composing its surface acts like terrestrial rock. However, Pluto will only show the most recent impacts since the solid methane has a tendency to relax over geological time scales.

Because of Pluto's low gravitational field, it is likely that liberated atmosphere will collide with Charon. Whether this will produce a noticeable effect is still an open question.

There is a strong variation in the brightness of Pluto as it rotates, the reason for which is not currently known and can be attributed to variations in terrain, chemical composition, or a combination of both. Also, Pluto is believed to have subtle surface markings which can only be examined by a spacecraft encountering Pluto. Pluto's characteristics are very similar to those of Triton and Titan, and the three bodies are some times referred to as the small outer "planets". It is hoped by studying Pluto and Charon that data key to our understanding of how the solar system was formed can be generated.

What ever else is discovered there are bound to be as many surprises in Pluto as there have been with all the other planets encountered so far.

2.2 Pluto and the Publicity for NASA

Although not a scientific rationale for sending a spacecraft to Pluto, another advantage of the mission is the likely public interest that can be attracted by the mission. Images from an unvisited planet make excellent media events and as such are likely to help NASA in the up and coming years of budget cutting. Thus, a mission to Pluto is likely to generate a large political backing, particularly if it can be seen as the vanguard of the "smaller, faster, cheaper" discovery missions.

Figure 2-1: Hubble Space Telescope Image of Pluto

Chapter 3

The Design Process

3.1 Introduction

The process of designing a space system is normally governed by the design philosophy and the engineering practice of the organisation that is conducting the work. The techniques used and the contention resolution process is often summarised as a Systems Engineering Management Plan. However, since this thesis is not being written in an established company, it is advisable to adopt a set of guide lines to follow. Using such a methodology allows the design trades to be consistent and traceable.

The design process that has been chosen for this work is that set out in the NASA Systems Engineering Handbook [31]. This document is currently only in the draft stage. However, by using it as a guideline for the design process of this thesis, experience in the practical application of its methodology can be gained. As a result, any weaknesses or lack of clarity should be exposed. From this experience, suggestions for the document's improvement can be proposed.

The NASA handbook simplifies the design process by suggesting that the process consists of two elements: the successive refinement spiral, and the trade study activities within the spiral.

3.2 The Successive Refinement Spiral

The concept behind the successive refinement spiral is shown graphically in figure 3-1.

The sequence is an iteration of:

- Identify & Quantify Goals.
- Create Concepts.
- Do Trade Studies.
- Select Design.
- Increase Resolution.

The process of refinement is initiated by recognizing a need or opportunity, and then defining a mission objective. The concept of a mission objective is, however, not introduced within the confines of the NASA Handbook [31]

3.3 Trade Studies

A trade study is the heart of the engineering design task. The purpose of the trade study is to select the most appropriate design for further consideration by the project. For example, in choosing the attitude and orbit control subsystem design/philosophy for the spacecraft, the systems engineer will employ a trade study to select which of the various options is the most appropriate for the particular spacecraft being designed. As a result of the trade study, the engineer can narrow the different options that need to be studied at an increased level of detail. It should be noted that as a result of the trades there can be several equally suitable options. In this event several of the designs should be retained for further study until all but one can be eliminated. By conducting the trade, inappropriate designs can be eliminated and the understanding of the remaining designs is increased. The process for conducting a trade study is shown in figure 3-2.

The activities that need to be performed are:

- Define and/or identify the goals, objectives and/or constraints
- Perform functional analysis
- Define measures and measurement methods
- Define plausible alternatives/concepts
- Define selection rules
- Generate data on the alternatives
- Compute measurement characteristics
- Prune the tree[1] according to computed characteristics and selection criteria.

In practice there is an iteration between the definition of measurements and pruning activities. Following the first iteration the subtleties of the design may have been highlighted in the measurement phase, or the most problematic characteristics identified, requiring either new measurements and/or alternatives to be defined. For example, if after the trade study has been completed it is found that too many designs have been pruned from the tree because of the defined selection criteria, then either the selection criteria must be relaxed, or additional alternatives introduced.

---

[1] Pruning the tree is an enhancement of the general elimination process suggested in the NASA handbook.

The essence of pruning the tree is to retain the maximum number of reasonable options for the maximum period of time to avoid"painting oneself into a corner".

It is assumed that "defining the goals and constraints" means establishing the system/subsystem requirements. Furthermore, the functional analysis is assumed to include some tasks to apportion the requirements to the appropriate functional blocks.

3.4 Applied Design Philosophy

A more detailed version of the design procedure implemented in this thesis is shown graphically in figure 3-3. This is a refinement of the upper levels of the methodology of the successive refinement spiral. As such, it introduces more detail of the design methodology than the NASA handbook does.

The overall design process starts with an idea for a mission. In the case of the PFF mission, this is the idea of sending a spacecraft to Pluto. The mission idea can come from the recognition of a need, requirement or market opportunity. In the case of the PFF mission there is also a time-based need, in that Pluto has an atmosphere that will not be in existence in 25 years. Thus, there is a need to explore the planet in the near future.

Once a mission need or idea has been established, the next activity is to determine a set of objectives. This is a quantification of the purpose of the mission. For a science mission the objectives are the science objectives, which include what we wish to discover, and how important each of these objectives are. Included in the science objectives should be specifications of the minimum acceptable and desired level of accuracy in the measurement. Initially these numbers are only useful as guidelines, but they too are important in defining subsequent activities. The final levels of accuracy must be a trade off between what is desired and what is practicable. As what can be practically achieved cannot initially be defined, the levels of desired accuracy are considered "soft" requirements. For example, the Pluto scientist might wish to have images of Pluto with a resolution of better than 50 m. However, this may be impracticable, while a resolution of 2 km could be achieved, which would still provide a large amount of useful information, though not as much as the scientist would wish for.

Once the scientific objectives have been established, the mission objective can be established. The mission objective is based on the science objectives, but introduces programmatic influences such as funding, available launch vehicles, and other operational constraints. The mission objective forms the top level requirements definition.

The instrument definition flows out of the science objectives, combined with the mission objectives. The actual instruments will be designed as a separate activity for most spacecraft as they are funded through a separate process. However a base understanding of their requirements and contents must be established.

The systems engineer uses the mission objective and initial instrument definitions and requirements to generate a set of simple ideas on how to carry out the mission (the mission concept). This is normally based on what are likely to be the mission critical activities. Thus, for the PFF, the critical activity will be achieving the desired arrival time, within the constraints of currently available launch vehicles. The multiple mission concepts, generated by the engineering team, are pruned down to one or two for further study, using high level trade studies.

The mission concept(s) are then broken down to define system level requirements. These are based on a flow down of the mission and science objectives combined with the instrument definitions.

Using the system level requirements, the spacecraft and operational concepts can be generated. These concepts deal with how the spacecraft will look, operate, and what its orbital dynamics could be. Again these concepts can be traded off at a high level of abstraction, or refined by adding in more detail to allow the different options to be compared more accurately. The concepts often evolve by considering the dominant features of that activity. For example, because of the range the spacecraft will be operating over, the PFF spacecraft will be physically dominated by the main mission antenna. The main mission antenna is therefore an ideal place from which to start considering possible spacecraft designs. The development of the spacecraft concepts must be considered one of the black arts of systems engineering blending both experience and imagination.

In some situations the real start of the mission idea is from either the spacecraft concept or the mission designs. The Voyager mission is a good example of the mission design creating a mission idea. Here the mission idea was generated by the discovery that there was the possibility to send a spacecraft to all the outer planets sequentially using gravitational assists. Once this was known, then a mission using this idea could be envisaged, and hence the design process started. An example of the spacecraft generating the mission idea is the case of the current trend of small satellites. Here people wish to build and use small satellites, and therefore the question arises as to what can be done with them. This in turn gives rise to a mission idea, and so to the start of the design process.

Using the spacecraft concepts and the system level requirements, the spacecraft requirements can be generated. These define how the spacecraft should perform. The function of the systems design activity is to flow the spacecraft requirements down into the subsystem requirements, in such a way as to optimise the overall spacecraft performance and ensure that the subsystem requirements are achievable. The systems design work is likely to have to be iterated to ensure that a consistent set of requirements is achieved. This design work also acts as a validation of the initial system level requirements, highlighting any problem areas, where requirements may have to be relaxed. The system design work also allows the various possible spacecraft concepts to be traded off by providing more detailed performance data. As each stage proceeds, the detail available in the requirements increases. As the design and its impacts proceeds down, the initial requirements can be refined.

The operational concepts follow a similar path to that of the spacecraft concepts.

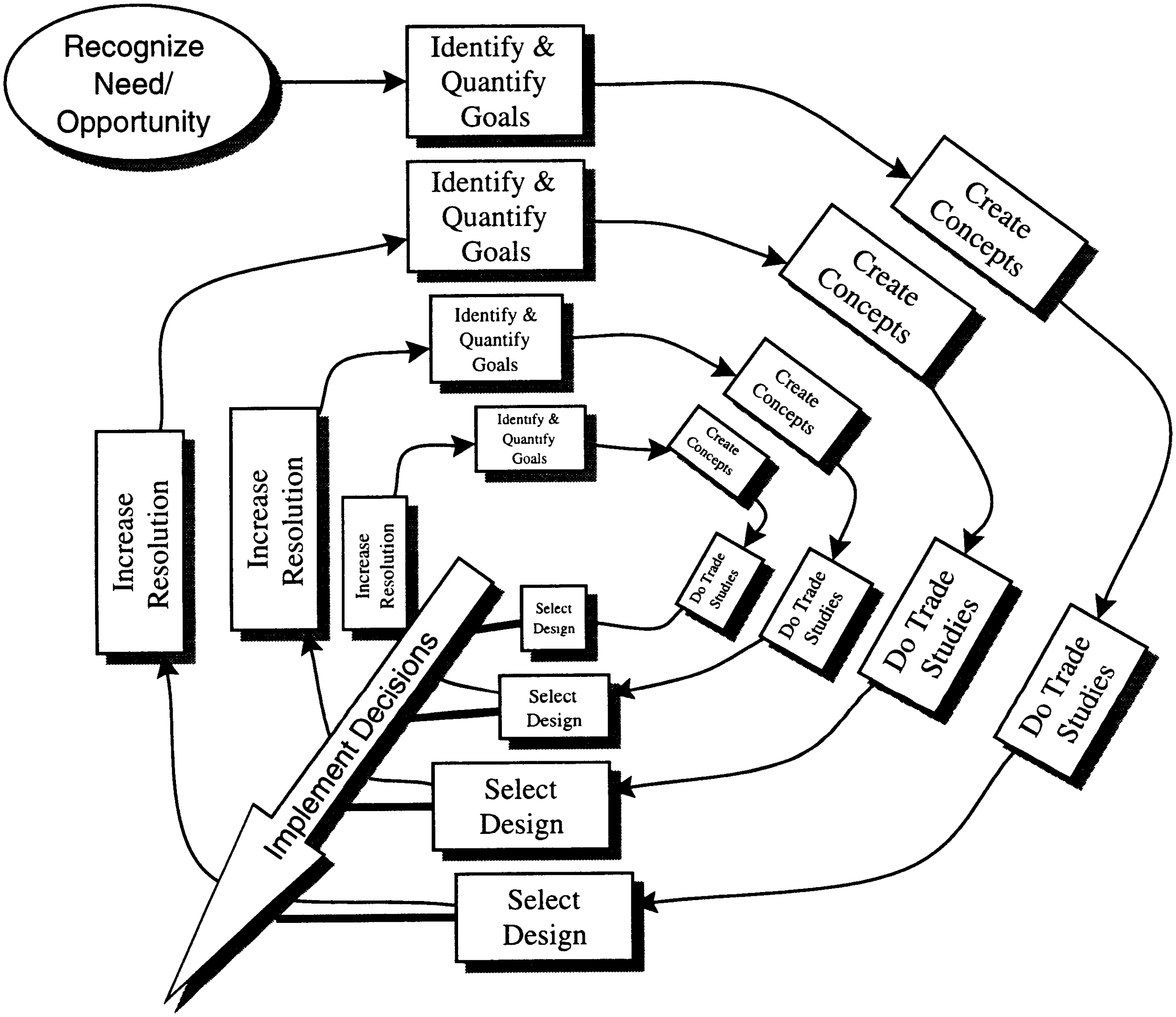
Recognize Need/ Opportunity
Identify & Quantify Goals
Create Concepts
Do Trade Studies
Select Design
Increase Resolution
Identify & Quantify Goals
Create Concepts
Do Trade Studies
Select Design
Increase Resolution
Identify & Quantify Goals
Create Concepts
Do Trade Studies
Select Design
Increase Resolution
Identify & Quantify Goals
Create Concepts
Do Trade Studies
Select Design
Implement Decisions

Figure 3-1: Successive refinement spiral

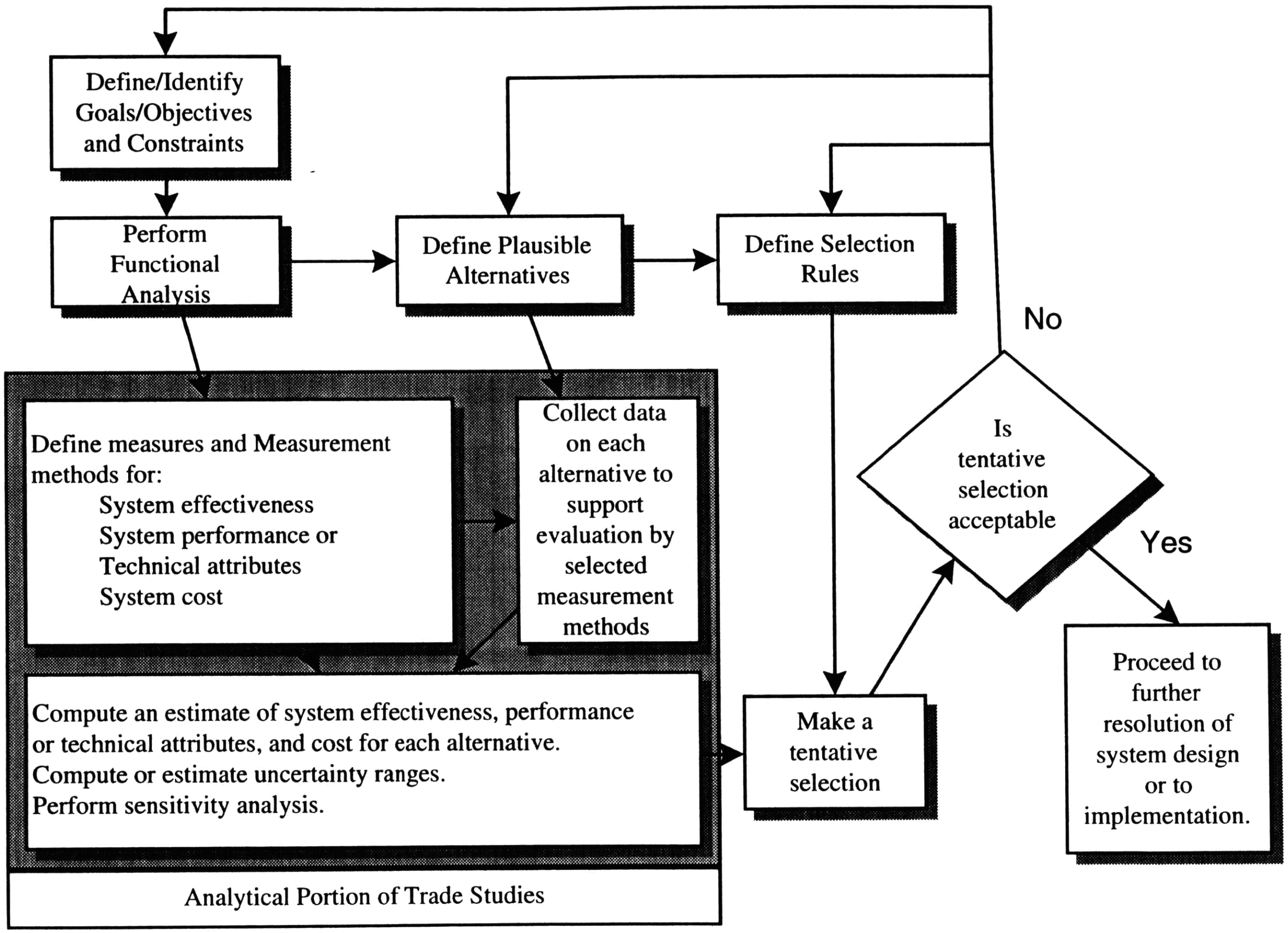
Define/Identify Goals/Objectives and Constraints
Perform Functional Analysis
Define Plausible Alternatives
Define Selection Rules
No
Define measures and Measurement methods for:
System effectiveness
System performance or
Technical attributes
System cost
Collect data on each alternative to support evaluation by selected measurement methods
Is tentative selection acceptable
Yes
Compute an estimate of system effectiveness, performance or technical attributes, and cost for each alternative.
Compute or estimate uncertainty ranges.
Perform sensitivity analysis.
Make a tentative selection
Proceed to further resolution of system design or to implementation.
Analytical Portion of Trade Studies

Figure 3-2: Trade Study Process

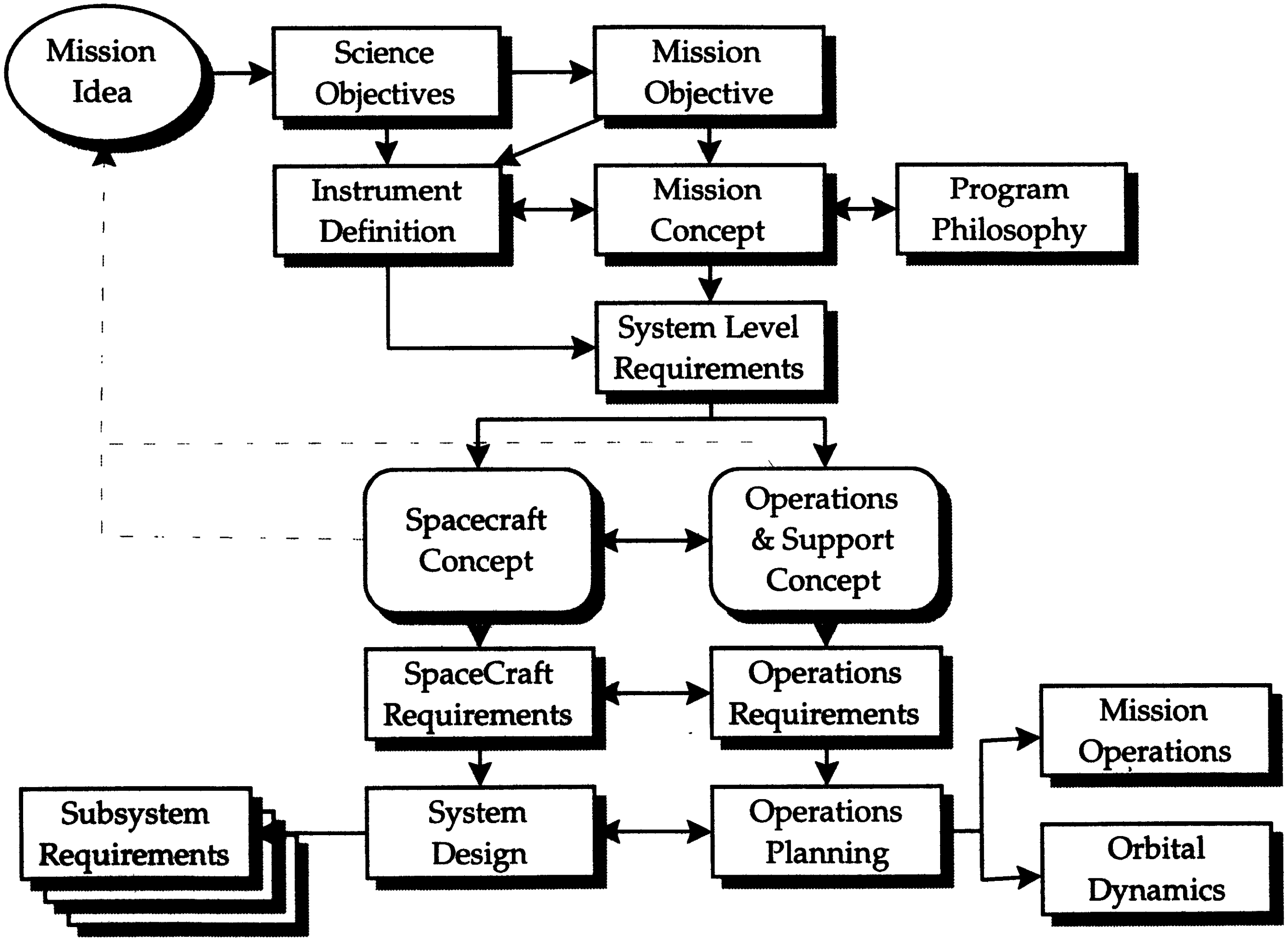
Mission Idea
Science Objectives
Mission Objective
Instrument Definition
Mission Concept
Program Philosophy
System Level Requirements
Spacecraft Concept
Operations & Support Concept
SpaceCraft Requirements
Operations Requirements
Mission Operations
Subsystem Requirements
System Design
Operations Planning
Orbital Dynamics

Figure 3-3: The Overall Systems Design Process for a Science Mission

Chapter 4

Science and Mission Objectives

4.1 Introduction

In conducting any space science engineering project, the initial requirements are derived from the science objective or functional goal and from a mission objective. These are often implicit in small engineering projects. However, in larger systems their identification becomes more important since they act as a focus for the design work and a criterion for evaluating the success of the mission. This idea can be considered an explicit example of a company's mission statement. The mission statement, in this case, acts as a focus for the development and operation of the company in question [20].

4.2 Science Objective

The science objectives, as is normal, come from outside the project design team. The science objectives along with their priority associated with the mission to Pluto are summarised in Table 4.1. The priorities were established by NASA's Outer Planets

1a	Neutral Atmosphere
1a	Geology & Morphology
1a	Surface Composition Mapping
1b	Ionosphere
1b	Bolometeric Bond Albedo
1b	Surface Temperature Mapping
1c	Energetic Particles
1c	Bulk Parameters (R,M,ρ)
1c	Magnetic Field
1c	Additional Satellites

Table 4.1: Pluto Mission Science Priorities

Science Working Group (OPSWG) [36].

4.3 Mission Objective

The Mission Objective for the spacecraft can be stated as follows:

The spacecraft will conduct a Fast Flyby of the planet Pluto and its moon Charon, and return to the Earth scientific data regarding each planet's surface geology, morphology[1], composition and Pluto's neutral atmosphere composition. In addition to this, any of the scientific goals established by the OPSWG, see table 4.1, that can be achieved at no penalty to the mission's cost should also be included.

---

[1] the external structure of rocks in relation to the development of erosional forms or topographic features [29]

The mission shall have a target cost of less than $400 Million per spacecraft including the cost of launching the spacecraft on an existing launch vehicle.

4.4 Program Philosophy

4.4.1 Introduction

Associated with a mission objective is the Program Philosophy. The objective of the program philosophy is to ensure that consistent decision making occurs across the different elements of the spacecraft. The philosophy defines the important criteria and ranks their importance.

For the PFF mission the primary driver is to arrive at Pluto before the Atmosphere condenses out on the planet, and thus, the arrival schedule is the most important element of the philosophy. Although, it should be noted that this is the arrival schedule, rather than the launch or design schedule.

The other key elements of the Program Philosophy are the cost, science return and reliability. The latter is, in a sense, closely linked to the science return. This is not a simple relationship. The first fact that must be considered is that each of these has a bound on its acceptability. For example, if the estimated cost is greater than a given amount (probably of the order of $500 Million), the mission will not be funded. However, if the science return is less than so much, then the mission is also not worth pursuing. Examples of this concept are shown schematically for the cost and schedule in figure 4-1. The diagram shows four main bands:

1. Acceptable level

2. Warning level

3. Cancellation Probable

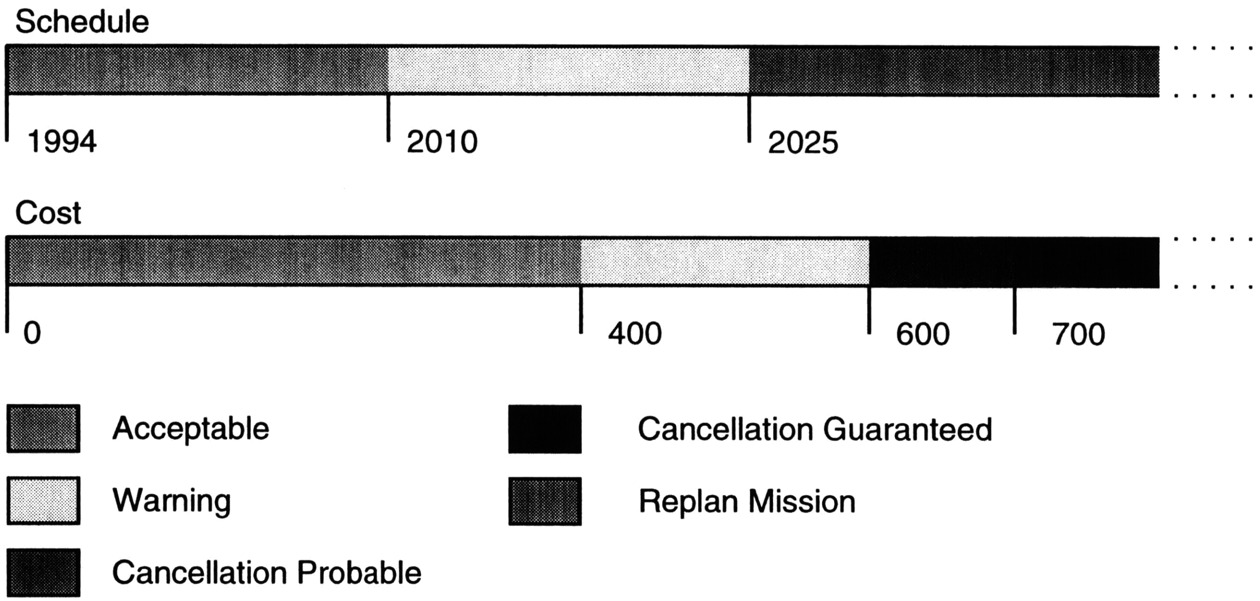
Schedule
1994
2010
2025
Cost
0
400
600
700
Acceptable
Warning
Cancellation Probable
Cancellation Guaranteed
Replan Mission

Figure 4-1: Schematic of the Bounding of Program Philosophy Elements

4. Cancellation Guaranteed

Acceptable Level

The acceptable level specifies the range of the parameter within which no action is required. However, some improvement in the value of each parameter could be considered to move it away from the warning level.

Warning level

If the parameter is in the warning level then remedial action should be carried out to move the value of the parameter back into the acceptable level. It is also likely that the project team will have to justify the value at project review meetings.

Cancellation Probable

If the value is in this range then it does not meet an acceptable standard, and the mission is likely to be cancelled at the next review. However, if the project team can justify the value, and the mission is considered critical enough then the project may be allowed to proceed.

Cancellation Guaranteed

If the parameter is located in this band, the program is no longer acceptable and should probably be cancelled by the project manager, or at a minimum be completely re-evaluated.

4.4.2 Schedule

If the spacecraft's launch schedule slips such that the spacecraft's anticipated arrival date is after that of collapse of the planet's atmosphere then the cost of the mission will be increased to ensure that the spacecraft arrives before this date. However, if the only way to ensure that the spacecraft reaches Pluto before this date is to increase the projects cost such that the additional amount will ensure the program's cancellation, then the mission will have to be completely reviewed. It may still be worth proceeding with the mission, but with different primary science objectives.

4.4.3 Science Return

If the science return is too low then the cost of the mission will be increased, without exceeding the acceptable cost level, to ensure that the science return is more than acceptable. At a minimum the spacecraft must be designed to provide better quality imagery than that currently available.

4.4.4 Reliability

If the reliability enters the warning zone, then the cost of the mission and the schedule can be allowed to slip so that the mission remains viable.

4.4.5 Cost

If the projected cost of the mission exceeds the initial projection, then the mission will be cancelled by Congress. This is one of the few certainties of a project such as the PFF. If the cost reaches a warning level, then the primary option to be used is to slip the spacecraft's schedule as long as this does not involve the spacecraft arriving at Pluto after atmospheric collapse.

If the cost is at an acceptable level, then the reliability and schedule should be improved to the point where the cost is becoming a concern. However, if the cost escalates to the point where cancellation is likely then all the other aspects will be sacrificed, with the possible exception of the arrival date. In this sense, cost is different from all other parameters, in that it is desired to keep it as close to the warning level as possible, whereas reliability, for example, should be as far as possible from the warning level.

4.4.6 When All parameters Are Acceptable

When all the parameters are at an acceptable level, the following order for improvement can be considered: Science Return, Reliability, Schedule, Cost.

Chapter 5

Initial Instrument Definition

5.1 Introduction

The primary science objectives for the PFF mission are given in the science objective section. (See Table 4.1.) The design and nature of the instrument payload is beyond the scope of the current work, as it would be for a typical space mission where the instruments are supplied to the platform manufacturer by outside science teams. However, for the sake of completeness, some comments on the nature of these instruments is appropriate to allow mass and power allocations to be estimated.

5.2 Required Sensor Systems

Table 5.1 [5] shows the different applications of typical space sensors. Using this we can determine the types of instruments that the PFF will need to have.

Each of the major science objectives for the Pluto flyby spacecraft is examined below to determine the type of instrument to use.

Space Sensor System	Applications
Passive UV	Chemical composition
Passive visible	Upper atmospheric temperature and wind-field profiles, ground imaging
Passive IR and microwave	Vertical temperature, species concentration
Active lidar	Vertical wind field, temperature, species concentration, and pressure
Stellar occultation	Composition
Radio occultation	Composition and pressure profiles

Table 5.1: Space Sounding Systems Applications

5.2.1 Neutral Atmosphere

The properties of interest in the neutral atmosphere of Pluto are: composition, pressure profile and temperature profile. Any one of these parameters can be deduced using IR measurements if the other two parameters are known or can be assumed. For example, the temperature of Earth's atmosphere is calculated based on knowledge of the concentration of oxygen molecules at different heights in the atmosphere.

The atmospheric characteristics can also be calculated by observing the change in frequency and/or phase in a RF beam passed through the atmosphere. Thus, to measure all three characteristics, it is necessary to measure the IR emission of the atmosphere and also the frequency and phase shift the atmosphere induces on a RF communications beam from the spacecraft to the Earth.

Along with the basic properties of the atmosphere the presence of trace compounds such as nitrogen, carbon monoxide, carbon dioxide and argon, which are difficult to detect from the Earth, are of interest. These compounds can only be determined using UV occultation. The sun provides a suitably bright source in the UV spectrum. Therefore the spacecraft must, as a minimum, carry an IR spectrometer, UV spectrometer and radio science payload.

5.2.2 Geology & Morphology

The geology and morphology of the planet's surface can be deduced by studying images in the visible part of the spectrum. Additional information can be gained by studying the associated IR spectrum. There is by nature a trade-off between the spectral resolution, the spatial resolution and the mass of the instrument.

5.2.3 Surface Composition Mapping

The surface composition can be estimated from various parameters associated with visible images and IR spectra; for example, the absorption spectrum, reflectivity and emission spectra.

5.2.4 Ionosphere

The study of the ionosphere can be considered as a high-resolution requirement on the study of the atmosphere.

5.2.5 Bolometeric Bond Albedo

The bond albedo is the fraction of the total incident light reflected by a spherical body over all wavelengths. Thus, to measure the bond albedo, a series of radiometric measurements from the planet's atmosphere across a large portion of the spectrum is required.

5.2.6 Surface Temperature Mapping

To map the surface temperature, it is first necessary to find a pass band in the atmospheric absorption spectrum, then using a radiometer to measure the amount of IR radiation emitted in the band of interest. By calibrating the instrument against a known temperature, or several temperatures, the temperature of the surface can be calculated.

5.2.7 Energetic Particles

Two facts about high energy particles are of interest: their type and energy. These can be measured using an advanced form of geiger counter.

5.2.8 Bulk Parameters (R,M,ρ)

The bulk parameters are normally measured by observing the occultation of the radio beam from the spacecraft and the spacecraft's orbit. The diameter of the planet can then be determined from the orbit and the duration of occultation. The mass and J2 can be calculated by measuring the planet's effect on the spacecraft's trajectory.

5.2.9 Magnetic Field

The magnetic field can be determined using a simple magnetometer. However, because the spacecraft itself will generate a magnetic field, it is necessary to mount the magnetometer far away from the spacecraft on a boom. The typical magnetometer boom can be as much as 30 ft long.

5.2.10 Additional Satellites

The search for additional satellites is likely to be based on the use of visible images of the sky surrounding the planet. The presence of satellites of Pluto can then be seen by removing from the images the star systems which form the back drop of the image. This can be done using either known star charts or by using a series of images viewed from different positions. In the latter case the stars appear to be stationary, and therefore, when one image is subtracted from the other, the only objects that remain are moving objects such as satellites. The major impact of this activity is to increase the number of images of the planet and the surrounding space required by the science team.

5.2.11 Typical Instrument Masses

Tables 5.2 and 5.3 show the science instrument payloads for the Galileo and Cassini spacecraft respectively [47]. These two missions were chosen for comparison as they are currently in manufacture or flight, and thus the actual instrument sizes are available.

Using this data, we can estimate that a payload to conduct all the 1a science requirements should have a mass of approximately 22 kg. This is based on the assumption that the IR and visible camera systems can share common optics. To carry out all 1a and 1b science should require approximately 15 additional kg. Finally, to carry out all the primary science objectives should require a payload of approximately 70 kg. At each stage, it has been assumed some improvement in the basic imaging capabilities of the lightest payload has been implemented.

Solid State Imager	28 kg	1500mm f8.5, 800 x 800 CCD map Galilean moons. & monitor atmospheric circulation
Near-IR Mapping Spectrometer	18 kg	0.7-5.2 μm, satellite surface composition, atmosphere temp & composition
UV Spectrometer	4 kg	1150-430 Å atmospheric gases & aerosols
Photopolarimiter-radiometer	5 kg	visible/near-IR bands, radiometer to >42 μm atmospheric particles, thermal radiation
Magnetometer	7 kg	magnetic fields
Energy Particle Detector	9kg	0.02-55 MeV ions, 0.015-11 MeV electrons high energy ions in magnetosphere
Plasma Detector	12 kg	1eV-50 KeV in 64 bands, energy composition & distribution of low energy ions
Plasma Wave	6 kg	6-31Hz, 50Hz-200 KHz, 0.1-5.65MHz electromagnetic waves & wave particle interactions
Dust Detector	4 kg	$10^{-16} - 10^{-6}$ g, 2-50 km/s, measure dust mass velocity & charge
Radio Science	-	determine planet/moon masses and radio & atmospheric structure

Table 5.2: Galileo Science Instrument Payload

Visual IR Mapping Spectrometer	40 kg	320 channels
ISS Imaging	66.4 kg	250 mm fl wide angle & 2000 mm narrow angle 1024 x 1024 element CCD
Titan Radar Mapper	57.5 kg	13.8 GHz 75 W raw power
Ion Neutral Mass Spectrometer	10.8 kg	
Cosmic Dust Analyser	15.1 kg	
Plasma & Radio Wave Spectrometer	24.7 kg	
Plasma Spectrometer	20.1 kg	
UV Spectrometer & Imager	14.9 kg	
Magnetospheric Imaging Instrument	24.9 kg	
Dual Technique Magnetometer	8.7 kg	
Radio Frequency Subsystem	13.2 kg	
Composite IR Spectrometer	36.2 kg	

Table 5.3: Cassini Science Instrument Payload

Chapter 6

Mission Concepts

6.1 Introduction

The design process outlined in the previous section is best illustrated with an example. This is presented as the initial mission concept selection for the Pluto flyby mission.

6.2 Identification and Quantification of Goals

The goals of the mission at the first iteration/refinement level are set out as the general mission objectives as presented in Chapter 4.3. Thus, the overall goal of the mission is to return as much science as possible within the prescribed priority.

6.3 Perform Functional Analysis

The breakdown of the objectives into the various functions necessary to complete the mission is relatively simple and can be simply stated as

- Instrument(s)

- Spacecraft Platform/Bus

The purpose of the spacecraft bus is to provide the instrument package with the necessary support such as power, thermal control, pointing, navigation, guidance, delivery system and communications link back to the Earth. The instruments, on the other hand, are responsible for measuring the various parameters of interest.

6.4 Measurements and Measurement Methods

6.4.1 System Characteristics

The measurements of interest at this level of the mission can be summarised as follows:

- theoretical mass
- current engineering mass
- ΔV
- cost (price)[1]
- reliability
- science return

---

[1] The concept of cost is not to be confused with the vague and uncertain usage of the term "cost" as used in the NASA handbook [31], where often the term is used to mean cost function. Here, the term cost is used exclusively to mean the monetary price of the mission.

6.4.2 Measurement Methods

Theoretical Mass

The theoretical mass of the spacecraft can be calculated based on the assumption that the payload is approximately 20% of the mass of the spacecraft[2].

Current Engineering Mass

As a basic idea the current engineering mass should be calculated by doing an estimate of the mass of each subsystem. However, the number calculated by JPL and collaborators will be used for comparison [36]. These numbers represent a level of detail not normally available at this level of design exploration.

ΔV

The ΔV will be calculated for the different missions using the data presented by JPL [36]. Again, this represents a level of detail not normally available, however a reasonable estimate can be made with the assistance of suitable mission analysis software.

Cost

The cost of the project will be estimated using the costing data in Space Mission Analysis and Mesign [46, page 666]. Specifically:

$$\text{RDT\&E} = 17350 + 1.17X$$

$$\text{TFU} = 198X^{0.77}$$

---

[2] The typical payload mass varies between 15 and 50% [46, Table 10-10]. 20% was selected to reflect of the complexity of the mission. The Cassini Spacecraft only achieves a 16% payload fraction.

/noindentWhere RDT&E is the development cost relationship[3] and X is the spacecraft dry mass. The equations presented are those for the spacecraft bus. A learning curve slope of 95% is assumed for second flight models.

The cost thus presented ignores the launch costs which are likely to be a significant factor for this project because of the large energies required to insert spacecraft into escape trajectories.

Reliability

It is difficult at this point in the planning process to assign reliability to the spacecraft. Thus it was decided to adopt an empirical measure and set the measure of reliability as high, medium or low. Obviously, launching two spacecraft on the same mission increases the reliability, while in designing a light-weight spacecraft reliability is often sacrificed for mass.

Science Return

The science return, as with the reliability, is again a difficult quantity to evaluate. However, breaking it into high, medium or low should suffice for the current trade off.

6.5 Spacecraft Concepts

The following spacecraft concepts can be proposed:

- Small Spacecraft (Sub 200kg)
- Intermediate Spacecraft (Voyager class)

---

[3] in Financial Year 1990 $K

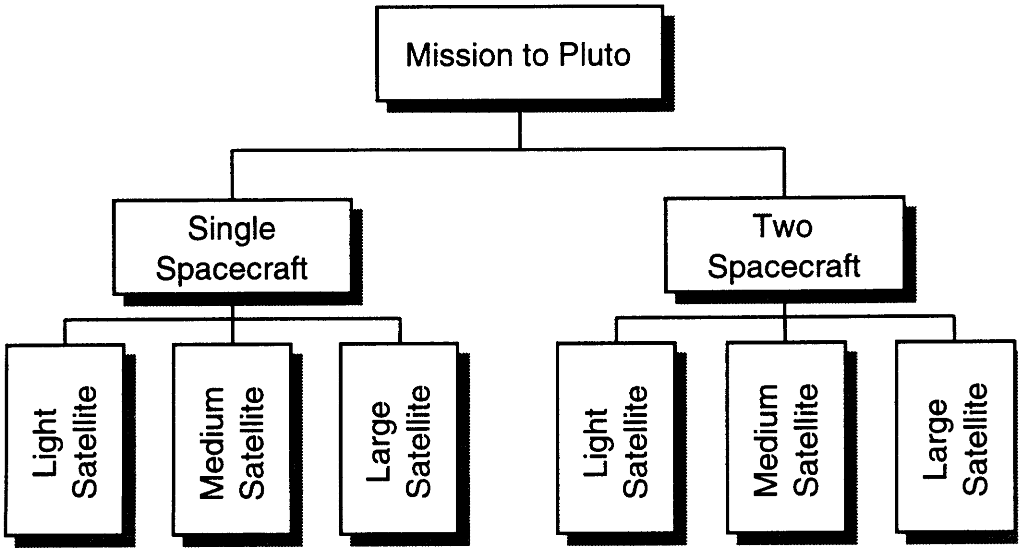
Mission to Pluto
Single Spacecraft
Two Spacecraft
Light Satellite
Medium Satellite
Large Satellite
Light Satellite
Medium Satellite
Large Satellite

Figure 6-1: Preliminary Design Trade Tree

- Large Spacecraft (Galileo/Mars Observer class)

To allow estimation of the mass of the spacecraft it is necessary to know the payload mass and, therefore, the amount of science that each of the spacecraft is expected to return. Let us assume that the science objectives for each mission are set such that the smallest spacecraft must only fulfill the most important science objectives, the 1a objectives, the medium-sized mission should meet all the 1a and 1b science goals, and the largest spacecraft all the primary science goals.

Each of these missions can be flown using either a single spacecraft or a pair of spacecraft. There is no limit to the number of craft that can be used, but conventional wisdom and budgetary constraints normally set two as a reasonable ceiling.

Figure 6-1 shows a possible trade tree for the various Pluto mission possibilities. Obviously, the trade tree represents only a fraction of the possible missions. However, for practical purposes an upper limit to the number of options considered at any given level must be set. As always in engineering this is a matter of judgment.

6.6 Selection Rules

The mission objective is the primary driver for the selection rules at all levels of the design as it defines the priorities of the mission whether they be reliability, science return or cost.

For the purpose of this thesis, the selection rules are primarily governed by the requirements to contain the amount of work and to select a mission with a high disparity between theoretical mass and current engineering mass.

This can be translated into the following selection rules:

1. Only one design shall be selected for further study, with the exception of a pair of missions such that the two missions require only a single spacecraft design, one mission being launched at a later date for the purpose of improved mission reliability and science return.
2. All designs which cannot be launched by existing launch vehicles with an arrival date before 2010 shall be excluded.
3. The design with the largest ratio of the difference between the current design mass and the theoretical mass over the theoretical mass shall be chosen. This is imposed to highlight areas requiring technology development.

Other selection criteria that could be applied to the selection of the spacecraft size are:

1. All designs with a target cost higher that $400 million shall be eliminated
2. All designs with a risk higher than x shall be eliminated.
3. All designs which cannot be launched by existing launch vehicles and arrive at Pluto before 2010 will be eliminated.

4. The number of options for further study shall be less than two, where an option shall be considered as a given single spacecraft mission and its associated dual spacecraft mission.
5. Rational judgment shall be used to eliminate options due to lack of science return.

Because of the other interests in this work, these have not been used. However, if this was an actual project to build the Pluto mission, then the criteria above would be used to replace the criteria used in this thesis.

6.7 Generate Data on the Alternatives

Table 6.1 shows the projected data for each of the alternative missions.

6.8 Selection of the Continuing Designs

Table 6.2 shows the measurement characteristics for each of the mission alternatives.

Using the selection criteria established above, this work will continue with the small spacecraft design option. This was chosen because it has the smallest estimated mass to theoretical mass ratio, and as such presents the most interesting design option.

6.9 Conclusion

Having selected the design, the next phase of the design strategy is to proceed down the refinement spiral. The next activity, therefore, is to define the system level requirements.

Spacecraft Size	Instrument Mass (kg)	Theoretical Mass (kg)	Engineering Mass (kg)	C_3 km^2/s^2	Cost M$	Reliability	Science Return
Small	22	110	69	305	30.7	Low	Low
Medium	37	185		-	41.3	Medium	Medium
Large	70	350	316	144	46.8	High	Medium
2 x Small	22	110	69	305	37.2	Medium	Medium
2 x Medium	37	185		-	57.1	High	Medium
2 x Large	70	350	316	144	67.2	High	High

Table 6.1: Performance and System Level Data on the Preliminary Designs

	Mass ratio	Launch date
Small Spacecraft	0.62	Before 2007
Intermediate Spacecraft	1.0	Between 2003 and 2005
Large Spacecraft	0.90	Between 2003 and 2005

Small Spacecraft	0.62	Before 2007
Intermediate Spacecraft	1.0	Between 2003 and 2005
Large Spacecraft	0.90	Between 2003 and 2005

Table 6.2: Selection Measurement Data for the Preliminary Designs

Chapter 7

System Level Requirements

7.1 Introduction

The first step in the design process must to be to establish the overall requirements for the mission and the subsystems. Thus, the following elements need to be defined within the context of the PFF[46, page 259]:

- Mission
- Payload
- Orbit
- Environment
- Launch
- Ground Systems Interface

The final system's requirements cannot be fully defined, as they require a number of iterations of the system's design to ensure that they are internally consistent.

However, initial requirements can be established which can be refined at a later stage in the design process.

7.2 Mission

The mission objective is summarised in Chapter 4.3. The spacecraft and its subsystems must have an expected design life of at least 10 years (TBC[1]) with a reliability TBD[2].

The spacecraft shall enact a point to point communications architecture with the Deep Space Network (DSN).

The spacecraft and its systems shall provide sufficiently secure communications paths and control instruction encryption to ensure that the mission is not compromised by accidental external interference.

The program is constrained to a budget of $400 Million per spacecraft including launch costs, with a launch date compatible with achieving the mission objectives.

7.3 Strawman Science Payload

The strawman payload proposed for the PFF is summarised below [36, 40]. This is the same science instrument payload that is currently being used by JPL to design their version of the PFF.

7.3.1 Visible Sensor

Pixel size : 7.5 μm

---

[1] To Be Confirmed/Reviewed

[2] To Be Decided

Aperture size: 73 mm

Focal length: 750 mm

Image size: 1000 x 1000 pixels

Digitization: 8 bit

Number of filter wheel positions: 6

Readout time: 2 Seconds

Imaging resolution at flyby: Better than 1 km. (150 m at closest approach)

7.3.2 IR Spectrometer

To keep the science payloads mass down the IR spectrometer is expected to use the same optics as the Visible Camera.

IR spectral range: 1.00 to 2.5 μm

Spectral resolution: $\lambda/\Delta\lambda \sim 300$

Image size: 256 x 256 pixels.

Pixel size: 40 μm

IR resolution: 5 km.

7.3.3 UV Sensor

Frequency range: 55 - 200 nm

Spectral resolution: $\Delta\lambda = 0.5$nm

Spectrometer: Grazing-incidence Diffraction Grating

Aperture: 24 mm

7.3.4 Radio Science

The requirements for the radio science instrument are currently undefined.

7.4 Instrument Summary

Though the details of the instruments are not yet fully defined the allowance for mass power and pointing requirements have been defined to allow work on the design of the spacecraft to proceed [36, 40].

Mass: 6 kg.

Peak Power: 6 W

Pointing Accuracy: 10 μrad

7.4.1 Science Instrument Impact on Spacecraft Design

The instrument mounting on the spacecraft must allow the UV instrument to be pointed at the Sun during solar occultation and let the main mission antenna track the Earth during the Pluto/Earth occultation. This puts either a placement constraint or a turn-rate requirement on the spacecraft.

7.5 Orbit

The orbit is TBD but is baselined as a heliocentric hyperbolic orbit with a closest approach to the Sun of 1 AU.

7.6 Environment

The environment the spacecraft will encounter is TBD. However, a baseline of standard deep space environment should be assumed. Currently, a Jupiter Gravitational Assist is not baselined, however the effect of such a flyby with its inherent radiation hazard should be considered in the design.

7.7 Launch

The launch vehicle and its constraints are TBD. However, the project shall be designed to use a currently available launch vehicle.

7.8 Ground Systems Interface

The ground systems interfaces are TBD.

Chapter 8

Spacecraft Flight Operations & Support

8.1 Spacecraft Operations/Mission Profile

8.1.1 Introduction

The flight to Pluto can be divided into a number of phases:

1. Launch
2. Boost Phase
3. Initial Cruise
4. Mid-course Correction
5. Continued Cruise
6. Final Course Correction
7. Pluto Flyby

8. Post Flyby Activities
9. Spacecraft Shutdown
10. Post Flight Activities(optional)

The levels of activity through these various phases will vary depending on the objectives to be achieved. Various activities in the above list may be repeated. One example of this is the mid-course guidance phase which may involve several small adjustments to the orbit years apart.

8.1.2 Flight Support Team

To support the mission during the flight, a flight support team is required to monitor the status of the spacecraft and to assist in the recovery from any failures that may occur. This team needs to be fully familiarised with the design of all the spacecraft subsystems. Along with the support team, there must be an orbital analysis team that tracks the spacecraft, computes its orbit, and plans and calculates the required ΔV maneuvers to ensure its correct arrival at Pluto.

One of the developing problems for small spacecraft missions is the high cost of operating spacecraft in flight. This problem is not unique to the PFF mission, but is shared with the Discovery missions in particular and with all the current deep-space missions in general. This problem has been highlighted recently by Magellan even though the spacecraft is capable of generating more useful science data, the cost of supporting the mission is now considered too large to be approved by Congress.

Although the basic quoted cost of a spacecraft does not normally include the cost of operating it, these additional costs must be considered when small satellite missions are designed, such as the Pluto Fast Flyby, or any of the Discovery missions. Unlike more conventional missions where the spacecraft's operating costs over its design life are only a fraction of the spacecraft's cost, for small spacecraft the operating cost will be several times the cost of the spacecraft. This is because the cost maintaining a flight readiness engineering team is the same for both large and small spacecraft, as the same basic functions must be provided for both spacecraft. Thus, spacecraft of all sizes need, for example, an engineer who knows the communications subsystem. Large spacecraft may have a much higher data throughput than smaller craft; however, its communications subsystem may cost an order of magnitude more than the one used on a small spacecraft.

Fire and Forget Strategy

One strategy worth considering is a "fire and forget" strategy. That is to use the cost which would have been spent on the support crew on building multiple simple spacecraft, possibly using different suppliers for each subsystem to avoid common failure modes. These spacecraft would be communicated with only 2 or 3 times during the cruise phase to Pluto. These contacts are required to conduct the necessary mid-course corrections. The spacecraft would be targeted to arrive at Pluto in a staggered sequence to ensure that the data could be downlinked in a sequential manner. If a failure occurs in one of the spacecraft which the internal fault tolerance cannot correct, then the spacecraft is simply written off. If the failure is minor, then a small amount of analysis may be carried out. However, a dedicated engineering team is **not** maintained. The idea here is that the cost of the engineering team is transferred into hardware. The question is will the deferred/discounted cost improve the mission performance and if so, by how much? The effect of different numbers of spacecraft on the overall mission reliability is shown in figure 8-1.

The reliability of missions with different numbers of spacecraft is given by:

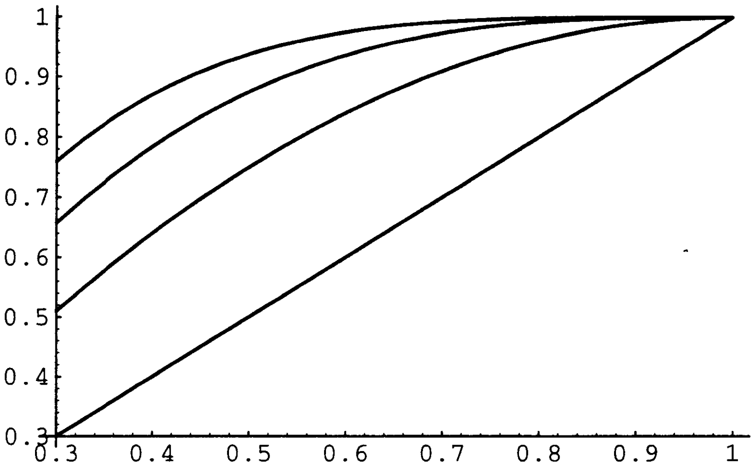

Figure 8-1: Effect of Multiple Spacecraft on Overall Mission Reliability

$$R_{Mission} = [1 - (1 - R_{Spacecraft})^N]$$

where, N is the number of spacecraft and $R_{Spacecraft}$ is the reliability of an individual spacecraft.

8.1.3 Operations Strategy Trade Study

Measures and Measurement Methods

The measurements of interest in selecting the operations strategy are the reliability and the relative cost.

Selection Rules

The selection rule is simply to select the option that provides the maximum reliability for the minimum cost.

Type	Cost \$K/Staff year
Contractor	140
Government	95

Table 8.1: Estimated cost of personnel assigned to support flight operations

Flight Operations Cost

The cost of operating a spacecraft on orbit can be estimated from the cost of contractual staff. Table 8.1 shows the cost of having staff assigned to a project [46, page 730].

Let us assume that to keep a qualified team available, then each member must be employed for half their time by the mission. Furthermore, let us assume that an engineer is required for each of the major subsystems, plus an engineer for mission analysis, and a project manager. This means that at least 6 man years worth of manpower per year is required by the project over the length of the mission.

The equivalent present value of the flight operations personnel can be calculated from [9, page 208]:

$$P = R\frac{(1+r)^N - 1}{r(1+r)^N}$$

where P is the equivalent present value

R is the yearly cost of the operations personnel

r is the discount rate

N is the project length in years.

If we assume that the average cost of the people is \$117K per staff year, then figure 8-2 shows the effect of mission duration on the current value of the flight

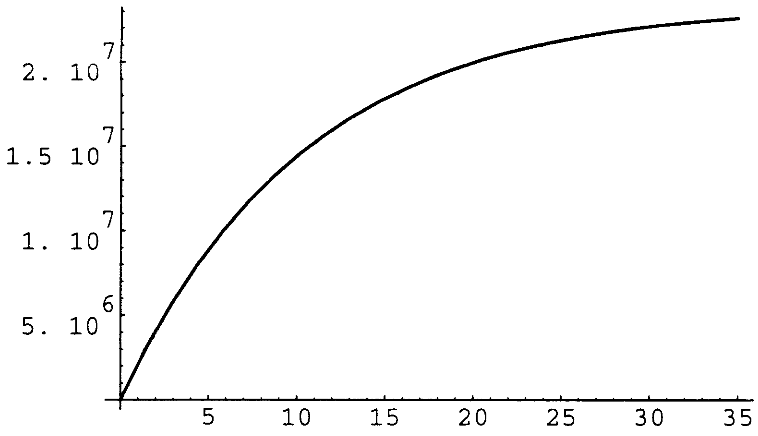

Figure 8-2: The current value of the operations support team

operations crew.

Spacecraft Costs

We can assume that a simple spacecraft with single point failures will cost apprpoximaty $40 million. This is based on the knowledge that a modern large communications satellite costs approximately $80 million. The PFF spacecraft however is far less complex even though it is for a deep space mission.

Let us also assume that to make the spacecraft internally redundant, making it more fault tolerant, then the cost is increased by 50%.

Reliability

Simple spacecraft are assumed to have a reliability of approximately 0.35, based on the assumption that each subsystem has a reliability of approximately 0.95, there being 10 main subsystems. For a single one-up spacecraft where each subsystem includes reliability, then the subsystem should achieve a reliability of 0.99, giving the overall spacecraft reliability of 0.90. Therefore, to achieve comparable reliability a

Type	Spacecraft Cost $M	Operations Cost $M	Reliability
Single	60	35	0.9
Multiple	200	0	0.9

Table 8.2: Summary of Flight Operations crew verses Fire and Forget

fire and forget strategy needs to launch 5 spacecraft.

Summary

Table 8.2 summarizes the data for the two options.

Fire and Forget Conclusions

To achieve the same reliability as more complex spacecraft, it would be necessary to launch 5 of the less-reliable spacecraft. The costs associated with each mission are summarised in table 8.2. It should be noted that these figures do not include launch costs. The preferred option is to maintain a flight operations crew.

However, this analysis should only be treated as preliminary, as the information such as the relative cost and reliability are only estimates. Thus, this trade study should be reviewed once the preliminary design work is complete and more accurate figures are available.

8.1.4 Flight Support Activities

During the cruise phases, to keep the mission to a minimum cost, the spacecraft should be totally self sufficient. The only external interface activities will be to occasionally download status information to the ground and to act as an active target to support ground-based trajectory analysis.

Just prior to the mid-course guidance maneuvers, the spacecraft will receive the appropriate burn commands from the ground as time-tagged information. These will then be executed at the appropriate time. All fault correction activities during the cruise phase will be handled by the spacecraft without assistance from the ground.

Just prior to arrival at Pluto, the observation sequence will be uplinked to the spacecraft. The spacecraft will then execute the appropriate instructions at the appropriate times.

8.1.5 Data Downlink Activities

When is the data from the instruments to be downloaded? There are basically two options if we assume the instruments are pointed by the spacecraft:

- Download during the Pluto flyby. This minimizes the amount of storage required by the spacecraft to store the instrument data.

- Download the data after flyby. This will maximize the time available for data collection and not require the communications subsystem to support a high data rate.

At this stage in the design it is difficult to conduct a study of these two options because the implications on the storage requirements and its system level impacts are not clear due to a lack of detail in the design. The assumed baseline is therefore to store all the data on the spacecraft and downlink it after the flyby.

8.1.6 Activities During Cruise

Knowledge of the amount of active time of the spacecraft while on cruise is required in some of the power subsystem concepts. Therefore, it is assumed that the spacecraft carries out 4 mid-course correction maneuvers during the flight. In addition to this, the spacecraft is tracked for 5 hours each month to provide ranging information and, hence, orbit determination.

8.2 Orbit Analysis

8.2.1 Introduction

A full and detailed study of the trajectory design to Pluto or any other major planet is a complex problem requiring a large number of iterations. As such, this is beyond the scope of this work. However, it is worth considering an initial analysis to understand the size of the problem.

8.2.2 Orbit Concepts

A number of different types of orbits can be considered that will cause the spacecraft to arrive at Pluto. These include:

1. A Gravitational Assist
2. An Aerogravity Assist
3. A Direct Flight
4. A Direct flight using a Broken Plane Maneuver.

8.2.3 Gravitational Assists

The question one must ask is "what is the advantage of using a direct transfer rather than a flyby, giving no consideration to the required transfer time". The simple answer to this is that it avoids the radiation hazard presented by Jupiter, which due to its large magnetic field has a very active set of Van-Allen radiation belts that the spacecraft must pass through to benefit from the gravitational assist. The possibility of an encounter with Jupiter reduces the expected spacecraft reliability and requires the spacecraft to carry additional shielding for sensitive equipment.

The possibility of a reduced grand tour of Jupiter, Uranus and Pluto was proposed by Longuski and Williams [19]. The flight has a 20 year flight time with a required launch in 1996. Because of this rapidly approaching launch date, it is difficult to foresee a development program for a spacecraft that could be completed in time to achieve this launch date. Longuski further notes that the Jupiter/Pluto mission is only achievable every 13 years assuming a $v_\infty = 12$ km/s. For a gravity assist using only Jupiter, the first opportunity does not occur until 2004 [33]. The flight time would be 10.5 years with a closest approach to Jupiter of 15 Jupiter Radii.

8.2.4 Aerogravity Assist

The ΔV achievable from a gravitational swingby is controlled mainly by the approach velocity and the minimum flyby height. These factors control the induced relative local velocity turn on the spacecraft, which in turn changes the heliocentric velocity. For planets with atmospheres, the minimum flyby height is controlled by the height of the atmosphere. It should also be noted in the case of Jupiter, the strong Van Allen belts surrounding the planet strongly influence the flyby height.

In the Aerogravity Assist scenario, the turn angle is increased by using a spacecraft with a lifting body design and flying it through the atmosphere. The aerodynamic lift is then used to turn the spacecraft's velocity. To achieve a positive ΔV from the planet, the gained velocity must be greater than the drag of the atmosphere on the spacecraft. This requirement leads to spacecraft designs which have a very high lift-to-drag ratio. Because of the high L/D requirement it becomes difficult to configure the spacecraft to accommodate other mission requirements such as a large high-gain antenna.

8.2.5 Direct Flight

Let us initially consider what minimum transfer energy is required to just achieve a rendezvous with Pluto.

Minimum Energy Transfer

One of the mission objectives is to arrive at Pluto before the atmosphere sublimates back onto the surface. If this requirement is temporarily ignored and the only mission goal is seen to be to arrive at Pluto, then a minimum energy orbit could be employed. This will then put a minimum on the required ΔV. Appendix A shows the calculation of the minimum energy orbit. The minimum energy transfer will require a C_3 of approximately 121 km^2/Sec^2, with a flight time of 31 years[1]. This is only just in excess of the latest arrival time if an assumed launch date of 1998 is used. The minimum impulse orbit at this travel time is elliptic and as such would provide the minimum flyby velocity, which would be advantageous for instrument viewing, providing the minimum target motion and also the maximum period in which Pluto is in range of the spacecraft's instruments.

Furthermore, because the minimum energy orbit is a elliptical orbit, it may be

---

[1] C_3 is the square of the hyperbolic excess velocity, that is, the velocity in excess of the escape velocity of the Earth [4].

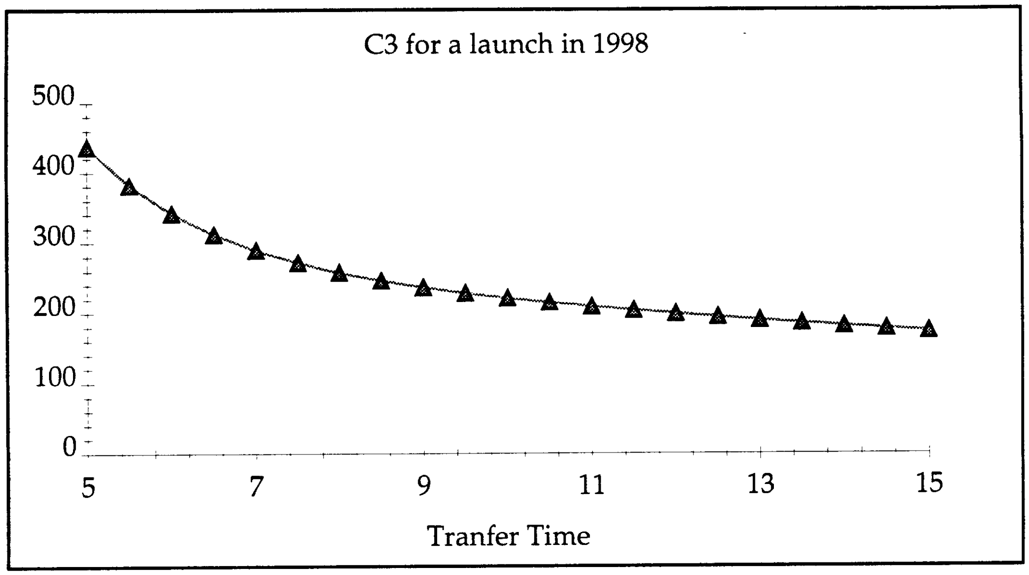

Figure 8-3: Launch Energy vs Flight time to Pluto

worth considering a secondary burn to inject the spacecraft into a Pluto orbit! This would allow a much greater mapping option.

Precise Required Launch Energy

If a launch date of 1998 is assumed, then the launch energy or C_3 is shown in figure 8-3[2]. C_3 is the square of the velocity that must be added to the Earth's Heliocentric velocity to inject it into the correct intercept orbit so that it arrives at the desired time. The optimum launch date is always in late January or early February.

8.2.6 Broken Plane Maneuvers

The normal technique used to insert deep space probes into the desired orbit is that of a Broken Plane maneuver. This technique is utilised because of the high cost of any plane change. In the Broken Plane technique the spacecraft is launched with the majority of the desired velocity towards the target point, but in the same plane as the planet it is leaving. When the speed of the spacecraft has slowed because the probe is traveling away from the Sun, a second burn is executed which rotates the plane of the spacecraft's orbit so that it will now intercept its target [34, 27, 12, 22]. In the case of the Pluto Fast Flyby mission, because of the large ΔV required to inject the spacecraft into the correct trajectory, the spacecraft is travelling at its slowest just prior to the main ΔV and thus the broken plane offers no advantage.

---

[2] Figure 8-3 was calculated using the program shown in appendix E and shows reasonably good agreement with the data calculated by JPL [36].

8.2.7 Preferred Orbit Selection

The preferred orbit is a direct orbit, as this has a window of opportunity for launch every year. It also provides the most flexibility in spacecraft design because as it avoids the problems associated with both Jupiter and Aerogravity Assists.

8.2.8 Launch Window

The variation in the C_3 required to arrive at Pluto, assuming an 1998 launch and a 7 year flight time, is shown in figure 8-4. If the launch window is 18 days, then the required C_3 is increased to approximately 305 km^2/Sec^2 from 290 km^2/Sec^2. This is a variation of approximately 400 m/s in the required ΔV. The length of the desired launch window is a matter of careful optimisation and trade off, which is beyond the current level of the design work. Table 8.3 summarizes the variation of C_3 with flight time and different launch window lengths.

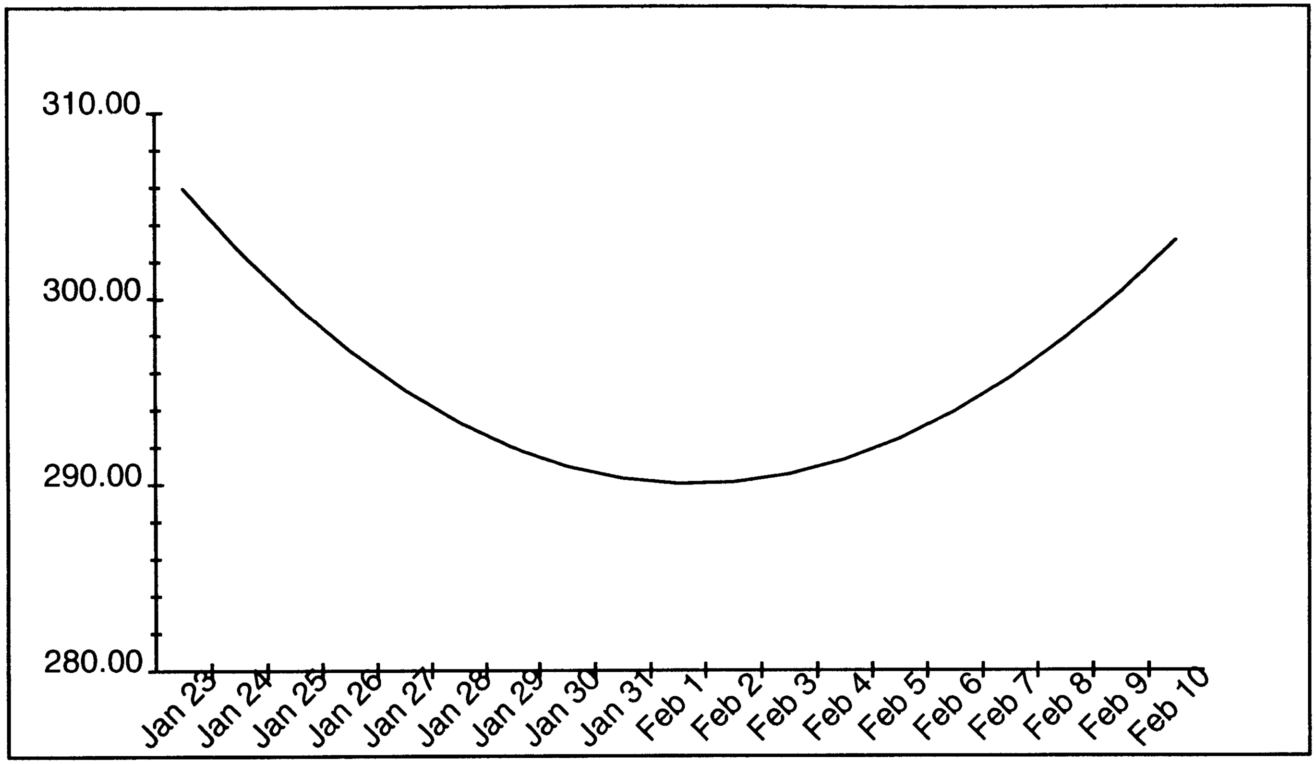

Figure 8-4: Launch Energy (C_3) vs Launch Date for a 1998 Launch and 7-year flight time

	Flight Time (years)								
	7.0	7.5	8.0	8.5	9.0	9.5	10.0	12.0	15.0
1 Day	290	272	258	247	237	229	222	200	174
5 Days	291	273	259	248	238	230	223	200	175
9 Days	293	276	262	250	240	232	225	203	178
13 Days	297	279	265	254	243	236	228	206	181
17 Days	303	285	271	260	249	242	234	211	187
21 Days	310	292	278	268	256	250	241	219	196

Table 8.3: C_3 for different launch windows and flight times for a 1998 launch

Chapter 9

Spacecraft Systems Design

9.1 Introduction

At this level the design spiral and design methodology becomes somewhat clouded, as the issues at this level are not so much the general principles and size of the spacecraft, but how the individual subsystems can be combined to provide the necessary functionality. Thus there are two sets of trade-offs going on in an individual design. The highest level breakdown is how to apportion the requirements to the different sub-systems. The second level is choosing the best equipment design to provide the required functionality for the design. This is where judgment is required about likely solutions.

Wertz and Larson [46] suggest that the process should be to "select a design approach, develop a spacecraft configuration (overall arrangement), and allocate performance [requirements] to the spacecraft elements and bus subsystems. [The systems engineer] then evaluates the resulting design and re-configures or reallocates performance as needed". This is the approach that has been adopted in the systems design activity of the PFF spacecraft.

9.1.1 Design Approach

The design approach adopted at this level of the design simulates a real design environment. The first activity undertaken is developing the spacecraft concepts. Once a limited number of concepts have been selected, the spacecraft is divided into subsystems. These subsystems represent functions on the spacecraft. This allocation of one subsystem per function is done to try and maintain the minimum number of interfaces and to make these interfaces as simple and clean as possible. Once the subsystems have been selected the system level requirements are apportioned to the various subsystems; this activity includes the specification of margins. This forms the initial subsystem requirements. These are of only a preliminary nature due to the lack of information at this phase of the design. Each of the subsystems is then considered in turn to assess how the requirements could be fulfilled and what the impact of these requirements is on the mass and power requirements of the subsystem. The subsystems are designed with no reference to the other subsystems and only to the requirements. This is done to simulate different engineers working in parallel on the task of designing the spacecraft. Once all the subsystems have been designed, the process is iterated to develop a coherent set of designs and to establish baseline subsystem functionality and requirements.

9.2 Spacecraft Configuration

9.2.1 Introduction

The configuration of the spacecraft is really a function of the parameters of the systems themselves combined with the look angle requirements of each of the elements.

The first question in designing the spacecraft configuration is to consider the instruments and their position on the spacecraft. There are two basic options that allow the instruments to view multiple targets in different directions.

1. Inertial spacecraft with instruments on a scan platform
2. Instruments attached to the spacecraft.

The choice of instrument pointing system to satisfy the mission requirements will be based purely on minimising the mass of the spacecraft.

9.2.2 Instrument Scan Platform

If the instruments are mounted on a scan platform, then the spacecraft can be treated as an inertial platform. The instruments are then moved relative to the spacecraft to achieve the desired pointing. Such a system allows the spacecraft to maintain Earth pointing of the main mission antenna. The scan platform has the additional advantage that pointing the instruments only requires the scan platform to be moved. However during such changes in pointing direction the spacecraft must have enough control authority in the AOCS system to maintain the spacecraft in inertial space. The disadvantage of such a design is that the scan platform requires a reasonably large mass and power allocation. A high accuracy scan platform requires very careful thermal control to ensure accurate pointing and therefore is has a high design cost and energy budget requirement.

9.2.3 Spacecraft Pointed Instruments

The alternative strategy is to mount the instruments on the spacecraft. To point the instruments the whole spacecraft is then turned to the required direction. The advantage of such a design is that the spacecraft is lighter since no scan platform is required. However the AOCS actuators must have enough authority to repoint and stabilise the spacecraft within the required time.

9.2.4 Pointing Selection

The pointing mechanism that will give the minimum mass is that of attaching the instruments directly to the spacecraft. This decision must be reviewed when more details are available about the mass penalty placed on the spacecraft by requiring control actuators with sufficient authority to achieve the required repointing speed.

9.2.5 Spacecraft Concepts

As noted in the section on the design procedure, the spacecraft concepts often flow out of the major physical elements of the spacecraft. In the case of the PFF mission the major element is the main mission antenna. Thus two principal spacecraft configurations can be suggested:

1. Parabolic reflector-based spacecraft
2. Lens antenna-based spacecraft

The preferred configuration will be chosen based on minimising the mass of the spacecraft.

Parabolic Reflector-based Spacecraft

The use of a parabolic reflector is the normal choice for this type of mission. Attached to the back of the antenna is a second structure to which all the electronics and RTG are mounted. The bottom of this structure is the launcher interface. The proposed configuration for the PFF mission being designed in this thesis is the reverse of this. The main launcher interface is the outer ring of the antenna. This does however constrain the antenna diameter. The antenna structure is parabolic in shape. This is one of the classical variations of an arch. Therefore the antenna in this configuration

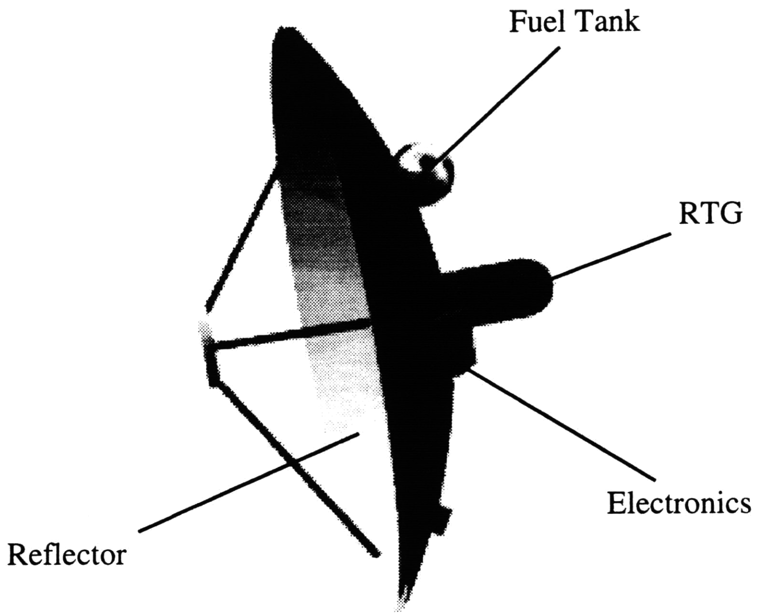

Figure 9-1: Conceptual drawing of a reflector-based spacecraft

should act as an excellent load-bearing path. Rather than mount the electronics equipment on a separate structure, it is proposed to use the back of the main mission antenna as the mounting structure. This will require the antenna to be more rigid than would otherwise be the case, but this is not perceived to be a problem. The most difficult aspect of this configuration will be the thermal control of the spacecraft. Figure 9-1 shows a conceptual view of the spacecraft.

Lens Antenna-Based Spacecraft

Unlike parabolic reflectors, lens systems are very uncommon in spacecraft design. Because the front and back of the lens must be free of obstruction, the only surface available to mount the spacecraft electronics is the edge of the lens. Thus the space-

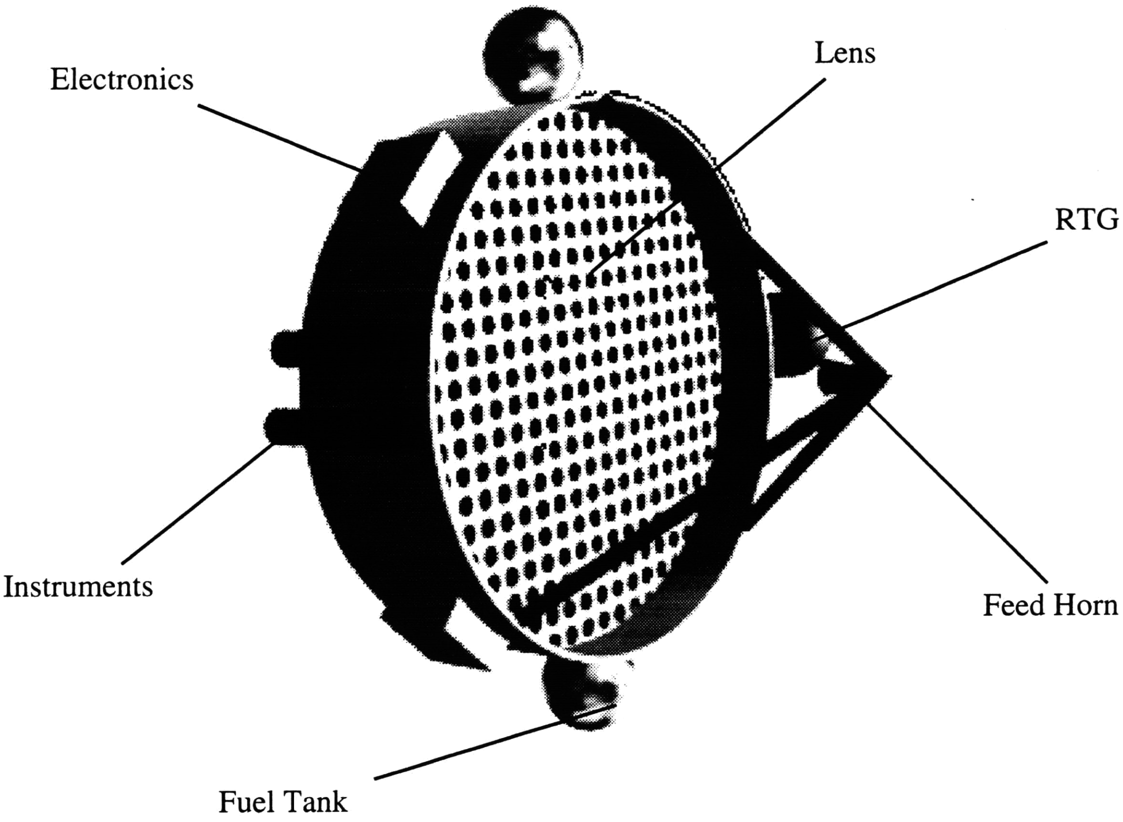

Figure 9-2: Conceptual drawing of a lens based spacecraft

craft configuration envisaged is that of a ring, with the centre of the ring being the lens antenna. The electronics boxes are then mounted on the outside of the ring. Figure 9-2 shows a conceptual view of the spacecraft.

Preferred Spacecraft Concept

At the current level of understanding of the spacecraft it is not possible to make a choice between the two proposed alternatives. Therefore no decision will be made until further analysis of the concepts and the spacecraft as a whole have been achieved.

9.3 Functional Analysis

In designing a spacecraft it is necessary to consider the following functions:

- Power
- Attitude and Orbit Control
- Guidance, Navigation, and Control
- Command and Data Management
- Launch System
- Propulsion
- Communications
- Support Structure
- Thermal Control
- Configuration

9.4 Initial Design Budget Apportionment

The following budgets need to be established in order to develop the initial subsystem specifications:

1. Mass
2. Power
3. Pointing

Budget	Margin %
Mass	10
Power	20
Pointing	10
Propellant	25
Reliability	0
Cost	20
Communications	3 dB

Table 9.1: Chosen System Margin Values

4. Propellant
5. Reliability
6. Cost

Before initial budget apportionment can be made the policy on the allocation of margin must be established[1].

9.4.1 Margin Allocation

The first stage in apportioning the available budgets is to establish the appropriate margin policy, and the levels of margin associated with each of the budgets.

The chosen margins are summarised in table 9.1.

---

[1] The concept of margin allocation and holding is not addressed in the NASA handbook

Margin Policy

The policy can be to either hold the margin at subsystem level or at systems level. For the current work both are equally suitable and as long as the policy is consistent then the outcome is the same. However for a real design it is preferred to keep the margin at systems level to better control its erosion.

The policy for this work will be to keep the margin at the systems level.

Mass Margin

For this preliminary stage of the work a margin of 10% will be used.

Power Margin

The typical power margin for a spacecraft is between 5 and 25%. It is proposed to use a value of 20%, as the power is not well understood, and because the designs used will have little maturity due to the drive to keep the mass down.

Pointing Margin

A pointing margin of 10% has been assumed. Though it would be desirable to have a larger margin, because the spacecraft has very tight pointing requirements the margin must also be kept small.

Propellant Margin

The propellant margin is normally between 10 and 25%. The number chosen for this work is 25% because of the preliminary nature of the analysis of the disturbance torques.

Reliability Margin

Because reliability is not the main mission driver, the reliability of the spacecraft will be considered an outcome of the design rather than a input. Zero margin has been assigned.

Cost Margin

A cost margin of 20% has been assumed. This figure is probably low, given the uncertain and haphazard nature of the costing process.

Communications

The communications link budget margin is required to be at least 3 dB. This is the normal value at this level of the design.

9.4.2 Mass Budget

There are two ways in which it is possible to apportion the various budgets:

- Total spacecraft mass basis
- Apportionment by reference.

Given that the required ΔV is known, and the maximum available thrust is also defined, then it is possible to calculate the allowable mass for the spacecraft. From this figure the “known” mass of the instruments can be subtracted and then the initial apportionment can be done based on standard spacecraft ratios.

The alternative technique is to take as a basis the mass of the instruments, and then scale this figure, using figures for the standard spacecraft ratios. The problem with this approach is that the instrument systems that will be used on the PFF are far

Subsystem	Wertz [46] %	Mass (kg)
Payload	15	6
Thermal Control	2	0.8
Structure	8	3.2
Integration Margin	2	0.8
Other Subsystems	73	29.2
Total	100	40

Table 9.2: Possible Initial Spacecraft Mass Apportionment

smaller and lighter than equivalent spacecraft instruments in use today. This would not be a problem if equivalent miniaturisation had occurred in the other subsystems of the spacecraft.

Wertz and Larson [46, Table 10-10] suggest the ratios given in Table 9.2. They suggest that the payload should be between 15-50% of the dry mass of the spacecraft. Because of the miniaturisation issues a payload fraction of 15% has been assumed.

In his book on spacecraft design, Agrawal[1, page 44] suggests the following relationships:

$$\begin{aligned}
M_{RC} &= (0.01 + 0.0115\sqrt{Y})M_{SC} \\
M_{ST} &= 0.087M_{SP} \\
M_T &= 0.032M_{SC} \\
M_{AC} &= 31 + 0.027(M_{SC} - 700) \\
M_E &= 0.039M_{SC}
\end{aligned}$$

$$M_M = 0.014 M_{SC}$$

where M_{RC} = reaction control system mass
M_{SC} = beginning of life spacecraft mass.
Y = spacecraft life time in years
M_{SP} = spacecraft wet mass
M_T = mass of the thermal control system
M_{AC} = mass attitude control system
M_M = mechanical integration
M_E = electrical integration

Using these relationships approximate percentages can be calculated, assuming that the communications and electrical power subsystems account for any unaccounted mass percentages. While these relationships are actually for a geostationary spacecraft, they are useful references for the PFF design. Typical spacecraft mass percentages are also available from the OACT [16] and the Air Force's Phillips Labs[7]. The suggested figures are shown Table 9.3. The guidance and control allocation has been assigned to the AOCS subsystem. Guidance and navigation for small satellites is normally ground based or subsumed into other systems.

These numbers suggest the masses shown in Table 9.4. There is a reasonably large discrepancy between these figures. Table 9.5 represents a blend of these numbers, and are the numbers used in the subsequent design activities.

9.4.3 Power

As with the mass breakdown, the normal technique for estimating the power requirements of the spacecraft is to use the power requirements of the payload. The baselined power requirement for the instruments when active is 6 W [35]. Table 9.6 shows the

Subsystem	Phillips Labs %	OACT %	Agrawal %
Payload	27.5	26	10
Propulsion	4.3	10	4.6
GN&C	0	0	0
AOCS	6.6	13	22.9
Communications	5.4	4	21.8
C&DH	0	5	1.7
Thermal Control	3.9	2	3.2
Electrical Power	30	23	21.8
Structure	22.3	17	8.7
Integration	0	0	5.3
Total	100	100	100

Table 9.3: Suggested Mass Breakdown Percentages from Selected Sources

Subsystem	Phillips Lab		OACT		Agrawal
	Instrument Based (kg)	Target Based (kg)	Instrument Based (kg)	Target Based (kg)	Target Based (kg)
Payload	6.0	16.5	6.0	15.6	6
Propulsion	0.9	2.6	2.31	6	2.8
GN&C	0.0	0.0	0.0	0.0	0.0
AOCS	1.4	4.0	3.0	7.8	13.7
Communications	1.2	3.2	0.92	2.4	13.1
C&DH	0.0	0.0	1.15	3	1.02
Thermal Control	0.9	2.3	0.46	1.2	1.9
Electrical Power	6.6	18	3.92	10.2	13.1
Structure	4.9	13.4	3.92	10.2	5.2
Integration	0	0	0	0	3.2
Total	21.8	60	23.08	60	60

Table 9.4: Suggested Initial Mass Budget According to Selected Sources

Subsystem	Proposed Value (kg)	Comment
Payload	6.0	Project baseline
Propulsion	3	Dry mass
GN&C	0.0	
AOCS	7.8	
Communications	6	
C&DH	0.0	
AOCS	3	
Thermal Control	2	Passive system
Electrical Power	13	
Structure	10	
Integration	4	5%
Margin	5.5	10 %
Total	60.3	

Table 9.5: Proposed Initial Mass Budget

Subsystem	OACT %	Wertz %
Payload	50	40
Propulsion	1	0
GN&C	0	0
AOCS	7	15
Communications	12	15
C&DH	15	5
Thermal Control	5	5
Electrical Power	10	30
Structure	0	0
Total	100	100

Table 9.6: Literature-suggested Power Breakdown Percentages

power budget relational percentages from the OACT and Wertz et al [16, 46]. If for comparison we assume that the total spacecraft will require 60 W, then the derived power breakdowns are shown in Table 9.7.

In practice none of the suggested budgets are solely suitable, and thus a selection of the suggested values must be made. Table 9.8 shows the modified values that are suggested.

9.4.4 Pointing

The spacecraft needs to point both the antenna and the science instruments. With their shorter wavelengths and higher resolution, the science instruments dominate the spacecraft's pointing requirements. The required pointing accuracy of the instruments

Subsystem	OACT		Wertz	
	Instrument Based (W)	Target Based (W)	Instrument Based (W)	Target Based (W)
Payload	6.0	30	6	24
Propulsion	0.12	0.6	0.0	0.0
GN&C	0.0	0.0	0.0	0.0
AOCS	0.84	4.2	2.25	9
Communications	1.44	7.2	0.75	3
C&DH	1.8	9	0.75	3
Thermal Control	0.6	3	0.75	3
Electrical Power	1.2	6	4.5	18
Structure	0.0	0.0	0.0	0.0
Total	12	60	15	60

Table 9.7: Suggested Initial Power Budget from Selected Sources

Subsystem	Proposed Value (W)	Comment
Payload	6.0	Project baseline
Propulsion	0	No ΔV at Pluto
GN&C	0.0	
AOCS	9	
Communications	7.2	1 W Tx requires 3 W alone
C&DH	9	
Thermal Control	0	Passive system
Electrical Power	7.8	80 % efficient
Structure	0	
Margin	7.8	20 %
Total	46.8	

Table 9.8: Proposed Initial Power Budget

	Error μrad	Comment
Pointing accuracy	7	estimate
Alignment error	1	estimate
Ephemeris error	1	estimate
Margin	0.9	(10 %)
Total	9.9	

Table 9.9: Initial Pointing Requirement Apportionment

is 10μrad [36].

The pointing budget can be broken down into three contributions:

- Pointing accuracy
- Alignment accuracy
- Ephemeris error

The pointing accuracy is the closed-loop ability of the spacecraft to point in a selected direction. Alignment relates the difference between where the spacecraft thinks it is pointing and where it actually is pointing. Such errors are caused by differences between the alignment of the instruments being pointed and the sensors measuring the direction pointed. Ephemeris error deals with the uncertainty in the direction in which to point the instruments to image Pluto, relative to the spacecraft. Table 9.9 gives the initial breakdown of pointing requirements.

A secondary number that must be calculated is the required rate of change of pointing. If we assume that the design driver for this is the ability to track Pluto during the flyby, then by considering the motion of Pluto relative to the spacecraft we can write:

$$\frac{x}{d} = \tan\theta$$

where d is the flyby altitude, x is the position offset, and θ is the view angle. Differentiating this we arrive at:

$$\frac{dx}{dt}\frac{1}{d} = \sec^2\theta\frac{d\theta}{dt}$$

where $\frac{dx}{dt}$ is the flyby velocity, and $\frac{d\theta}{dt}$ is the required roll rate. The target flyby altitude is 15,000 km with a velocity of 18 km/s [44]. This equates to a required roll rate of 0.069 deg/s. An initial rate requirement should be set at 0.1 deg/sec.

9.4.5 Propellant Budget

The spacecraft's propulsion system must provide a ΔV for two main activities, momentum dumping and mid-course guidance maneuvers. The latter are small trim maneuvers performed by the spacecraft to remove any initial ΔV vector errors from the boost vehicle.

Momentum Dumping

The possible disturbance torques on a spacecraft can be summarised as:

1. Aerodynamic
2. Gravity gradient
3. Magnetic
4. Solar radiation pressure

For the Pluto fast flyby the only significant force is the solar radiation pressure. However if the spacecraft is re-routed via Jupiter then magnetic disturbance effects must also be considered. The disturbance torque due to solar radiation pressure can be calculated from [46, page 275].

$$
\begin{aligned}
P_{SN} &= F_s(2 - \alpha_s)\cos i \\
P_{SP} &= F_s \alpha_s \sin i \\
T_s &= A(\mathbf{L} \times \mathbf{P_s}) \\
F_s &= \frac{4.644\times 10^{-6}}{R^2}
\end{aligned}
$$

F_s = Solar flux
α_s = Surface absorptivity
i = Angle of illumination
A = Area illuminated
T_s = Vector torque
R = Range from the sun in AU
L = Distance between centre of solar pressure and C of G

P_{SN} and P_{SP} are the components of the solar radiation pressure normal to and in the plane of the illuminated surface.

Because the orbit of the spacecraft has not yet been fully defined, a minimum impulse trajectory, or worst case, can be assumed. In such a trajectory, the spacecraft will spend more time close to the sun than any of the other direct flight orbits to Pluto, and thus the calculated disturbance torques will be higher than those experienced by the spacecraft. The worst case disturbance torque will therefore be calculated.

Appendix C shows the Mathematica notebook used to calculate the solar radiation torque on the spacecraft.

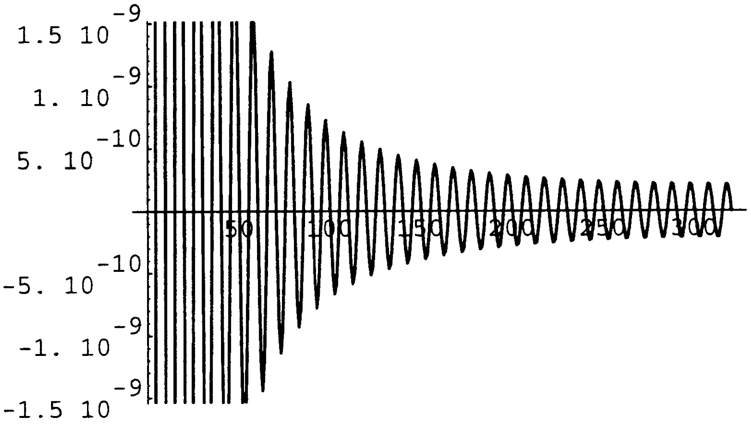

Figure 9-3: Solar Radiation-induced Torques.

The disturbance torque as a function of time is shown in figure 9-3. The oscillatory part will be handled by the AOCS and only the constant part is of consequence for calculating the ΔV required. Figure 9-4 shows the torque bias after passing the torque data through a low pass filter. Integrating this function over the flight time of the spacecraft gives an angular-momentum dumping requirement of 1.6 Nms. This figure could be further broken down to compute the required ΔV. However since the I_{sp} is unknown currently (because the thrusters and propellant have not been chosen) the required angular momentum change will be used.

Mid-course Correction Burn

A preliminary requirement to provide a ΔV of 400 m/s has been baselined [35].

9.4.6 Reliability

In designing a mission to be "quicker, faster, cheaper", one of the key areas that is traded-off is the reliability of the spacecraft. The question of what an acceptable reliability is then arises.

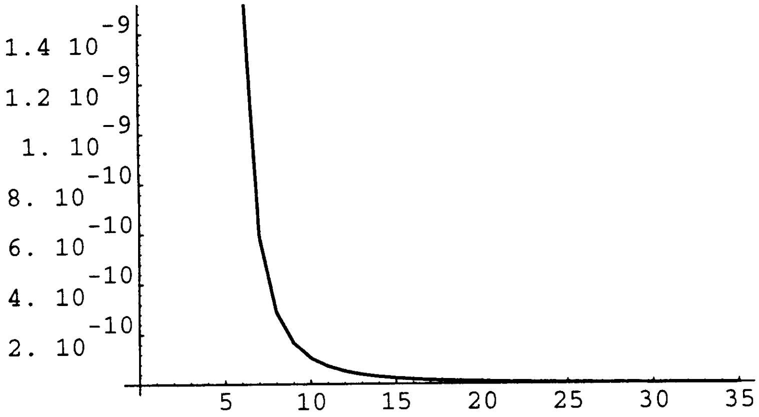

Figure 9-4: DC Solar Radiation-induced Torques.

Because the primary goal is to build a small, light, cheap spacecraft, rather than a conventionally-designed spacecraft, the question to ask at this level of design is what the cost of reliability is . However it is useful to establish an idea of what an acceptable reliability figure would be. For the current work a figure of 0.8 at end of life has been chosen. This is in line with that of a typical scientific satellite (0.81 for HEAO-B [46, page 290]).

9.4.7 Cost

The total target cost for the PFF mission is $400 million including launch [2]. The initial cost apportionment is done on an approximately *pro rata* basis except for the launch vehicle. Table 9.10 shows the provisional design and construction cost requirements[2].

---

[2] It should be noted that most text books on the subject of spacecraft design do not include cost as a design requirement. This is included to be in keeping with its growing importance and the spirit of the first chapter of the NASA handbook [31].

Subsystem	Cost ($ M)	Comment
Payload	0	from separate budget
Propulsion	25	
GN&C	0.0	assumed ground based
AOCS	25	
Communications	25	
C&DH	25	
Thermal Control	5	
Electrical Power	25	
Structure	25	
Integration	5	
Margin	32	(20 %)
Launcher	200	Titan 4 with 2 Star Motors
Total	392	

Table 9.10: Initial Subsystem Cost Apportionment

9.5 Power Subsystem

9.5.1 Requirements

The primary inputs into the power subsystem requirements come from the estimated power required by the other subsystems as shown in the power budget in table 9.8. The other constraints on the system are in terms of the mission-duration, orbit and required lifetime as set out in chapter 7.

9.5.2 Power Subsystem Concepts

There are basically 5 ways of generating electrical power for a spacecraft:

- Solar arrays
- Radio-Isotope thermal generators (RTG)
- Batteries
- Fuel cells
- Magnetic field line generator

Of these we can rule out the use of a magnetic field line generator due to the lack of a suitable strong magnetic field in deep space. This concept is also only in the experimental stage[3].

9.5.3 Measurement Characteristics

The quantity that is of most interest in the selection of the power subsystem design is that of the mass of the subsystem. However, an additional interest is how this quantity changes as the flight time to Pluto changes. The latter is important because the mission profile is not well defined. Thus it would be preferable if the extension of the mission duration only had a small impact on the design of the spacecraft, and in particular the power supply subsystem.

---

[3] The technique is that used by the Italian tethered satellite system.

9.5.4 Concept Selection Criteria

The primary selection criteria is to choose for the minimum mass, for all mission durations between 6 and 30 years. The nominal mission duration is 8 years. Therefore the preferred solution will be one which provides the minimum mass and the minimum mass delta for each additional year.

9.5.5 Solar Arrays

Solar Arrays are the normal generation sources for Earth orbiting satellites and spacecraft operating within the orbit of Mars. Thus, for example, Magellan uses solar arrays as its primary power source.

Array Mass

The typical conversion efficiencies of Silicon Solar Arrays are 14% with a performance degradation of 3.75% per year. The figures for Gallium Arsenide (GaAs) are 18% and 2.75% per year, respectively. Thus, after a 10 year flight time a GaAs solar array would be only 13.6% efficient. If we assume a $\frac{1}{R^2}$ loss for the available solar radiation and given that the available energy is 1369 W/m^2 at the Earth's orbital range, then the available energy from Solar radiation at Pluto is 1.5 W/m^2. Thus to generate the required 46.8 W a 229 m^2 GaAs solar array would be required[4].

---

[4] This assumes that the total surface area of the array is used to collect the light, and that this surface is not required for wiring, structural purposes or thermal control.

The array mass is approximately 3.8 kg/m^2 [13, page 254]. the solar array would thus weigh 14 times the desired spacecraft mass.

To a first order estimate the mass of the array will not change with a change in the mission duration. This approximation is made due to the uncertainty in how the changes in illumination, particularly at UV wavelengths, will effect the cell degradation.

Array Cost

The cost of a solar array can be estimated as 18 \$ K/m^2 [15].

9.5.6 Radio-Isotope Thermal Generator

RTGs are the standard power system used for deep space missions outside the orbit of Mars. These have been used on the Voyager series, Gallileo and Mariner spacecraft among others.

Reactor Mass

The peak power required by the spacecraft will be at Pluto flyby during the radio occultation experiment, if we assume that all instruments are active during this phase. Then the peak power requirement is 46.8 W. The generating power of various RTG materials is shown in table 9.11 [15, page 414].

The conversion efficiencies for a thermoelectric converter are typically between 5 and 8% [46, Page 393]. Thus we can calculate the required thermal mass for each type of material for different mission durations given that the thermal output of a particular material is governed by an exponential decay[5]. The initial mass of fuel

---

[5] This ignores the possibility of the material being converted into a second radioactive material which in turn decays and adds to the heat production

Type	Half-Life	Watts/gm (Thermal)	$/Watts (Thermal)
Po 210	0.378	141	570
Pu 238	86.8	0.55	3000
Ce 144	0.781	25	15
Sr 90	28.0	0.93	250
Cm 242	0.445	120	495

Table 9.11: RTG Material Properties

required can be calculated from the half life by:

$$M_0 = \left(\frac{T_f}{T_{kg}}\right) \times e^{\frac{t \ln 2}{t_{\frac{1}{2}}}}$$

Where t is the mission duration, T_f is the required thermal output of the RTG at the end of the mission, T_{kg} is the thermal output per kilogram of material and $t_{\frac{1}{2}}$ is the half-life of the material. If we assume that the convertor is 7% efficient at EOL then table 9.12 shows the initial mass of each fuel type required for different mission durations.

The Galileo RTG generates 298 W +/- 10% at the BOL and is based on Pu 238 material. Thus the reactor must have a thermal output of 4.68×10^3 W. This requires 8.5 kg of fuel. The mass of the reactor is 56 kg. Therefore we can assume that the casing factor is approximately 6.6. Therefore the Pluto Fast Flyby reactor should weigh approximately 9.9 kg. An upper bound on the mass can be computed by assuming that the reactors beginning of life efficiency is 11% [15, page 414]. This equates to a reactor mass of 15.5 kg. Wertz and Larson [46] suggest a value of 8 W/kg for the RTG mass estimation process. This equates to a mass of 5.85 kg for the whole

Type	10 Years	15 Years	20 Years	25 Years	30 Years
Po 210	436×10^3				
Pu 238	1.32	1.37	1.43	1.48	1.55
Ce 144	191				
Sr 90	0.92	1.04	1.18	1.33	1.51
Cm 242	32×10^3				

Table 9.12: Required Fuel Mass for Pluto RTG

Type	Cost $K
Pu 238	2540
Sr 90	351

Table 9.13: Costs of the RTG Material to supply 46.8 W

reactor. The reactor will be assumed to weigh 10 kg. This being approximately the median value of the three figures.

Reactor Cost

Wertz et al [46] suggest a figure of 16 to 18 K$/W, which equates to a cost of $ 840 thousand for the reactor alone. Using the required material masses from Table 9.11 the cost of the radioactive material alone are shown in Table 9.13.

The base cost of an RTG suitable for supporting the PFF mission is therefore assumed to be $ 0.84 Million.

9.5.7 Batteries

Batteries are normally considered as secondary sources of power for spacecraft, in that they are used when the primary source is temporarily unavailable. They are then recharged from the primary source when it is again available. However, a number of examples do exist of spacecraft which rely exclusively on battery power, such as the Galileo atmospheric probe, and all launch vehicles.

Spacecraft Power Requirement

To size the batteries for a spacecraft it is necessary to calculate the total energy required by the spacecraft. To carry out this estimation it is necessary to decide which units are active during each phase of the mission and hence how much power will be required by each phase.

During the mid-course corrections it will be necessary to supply power to the following subsystems:

- Propulsion
- Communications
- Guidance Navigation and Control
- Command and Data Management System
- Attitude and Orbit Control Subsystem Design
- Power Subsystem
- Thermal Control

Thus during a mid-course maneuver the spacecraft will need 40 W of power, though this could be reduced by powering down the communications subsystem.

However given the loss of the Mars Observer while conducting an orbital maneuver without its communications system enabled, this is an unappealing prospect. For convenience let us assume that each mid-course guidance event requires 10 hours. Thus the battery must provide 400 Wh of power per mid-course correction.

For orbit determination purposes the spacecraft must power up for 5 hours once a month during the cruise phase. During this period the spacecraft must act as an active target, and thus the communications, AOCS and command subsystems must be active. The instruments will remain dormant apart from a short period of say 30 minutes apiece to allow for a full check-out and relay of their status to the ground. Thus the craft will need 193.5 Wh per check-out or 2,322 Wh per year of flight.

During the cruise period, when the spacecraft is not active, a timer must be run. If we assume that a suitable redundant timer would require 100 mW, then the timer would require approximately 877 Wh of power per year.

To calculate the amount of power to downlink the images taken of Pluto it is necessary to make some preliminary assumptions. First let us assume that the communications subsystem can support a downlink rate of 1000 bits per second. The instrument system consists of a 1000 × 1000 pixel array. Each pixel being quantized to 8 bits. Therefore, each image generates 24×10^6 bits of data. Furthermore, if we assume a 3:1 compression ratio, the total data to be downlinked is 8×10^6 bits per image. It will therefore take the system 2.2 hours to down link a single full resolution image. Let us assume that the baseline science return calls for a total of a 1000 images of Pluto and Charon to be generated. Thus to downlink the data will require 84 kWh of power.

The trade-off between power used and data rate is a complex one, (as noted in [39]) in that the power used in the transmitter is interchangeable with the time the transmitter is powered for[6].

---

[6] It is worth pointing out that the OSC design would generate the equivalent of only 20 frames

The variation in the total required power with time stems from the requirement to point the spacecraft and power the command and data management systems while data is being downlinked to the ground. The latter is approximately linearly proportional to the amount of time the transmitter is active. Thus the required power level can be reduced to 16.0 kWh if the rate of the downlink is increased to 2.2 Mbits/sec (the spacecraft would then only require 1 hour to transmit all the science data).

If an allowance of 5 hours for imaging-time is made, then an additional 210 Wh is required to generate the data.

Thus the estimated total power requirement for a 8 year mission is therefore 43 kWh.

Battery Selection

The batteries available to act as primary system batteries are shown in table 9.14. Thus a battery mass of at least 97 kg is required to support the mission. If only the Flyby and Post-fly activities are supported from the battery then 37 kg of battery mass are required. To reduce this to the level of the target 13 kg for the power subsystem would require that the data compression ratio be increased to 9:1 or the science return reduced. The delta in the mass for an extended mission is 6.8 kg/year.

9.5.8 Fuel Cells

A fuel cell chemically reacts hydrogen and oxygen together to form water. As a rule of thumb a fuel cell can generate 1.1 kWh/lb [15]. This is equivalent to 2.4 kWh/kg. Thus to support just the imaging and downlink would require a mass of 6.7 kg. To support the whole mission would require 15 kg. The change in mass for each additional year of the mission is therefore 1.25 kg/year.

---

[39]

Type	Wh/kg
Silver Zinc	130
Nickel Cadmium	30
Nickel Hydride	45
Lithium Thionyl Chloride	440
Lithium Sulfur Dioxide	350
Lithium Monofloride	350
Sodium Sulfur	210
Thermal	200

Table 9.14: Battery Properties

One argument against the use of fuel cells that is not brought out in this discussion is that current uses of fuel cells are short-term lasting normally less than a month. The problem with their use in the PFF craft that would have to be tackled is the leakage rate of the fuel, in particular hydrogen, and the provision of suitable spare fuel.

9.5.9 Fuel Cells Plus a Solar Array

The spacecraft requires 3 kWh of power for every year of the mission. This constitutes an excess of 50% of the power required to operate the spacecraft for its whole mission. The actual demand for power is actually quite low, being of the order of 350 mW. Therefore one possibility is to use a solar array to generate this power, and then supplement it with power from the batteries for the data collection and downlink phase of the mission. The spacecraft would require some additional rechargable battery capacity to store the power required for the orbital navigation activities. Using Nickel Hydride batteries, 4.3 kg of additional battery mass would be required. The power for these batteries is already included in the solar array generating requirement. This type of system would require an array area of approximately 0.5 m^2. The total mass of such a system would be 13.0 kg. The change in mass for an extended flight time can be assumed to be zero.

To keep the solar array pointed at the sun while the timer is the only active system of the spacecraft will require that the spacecraft be spin-stabilised.

9.5.10 Batteries Plus a Solar Array

As with the possibility of utilising the fuel cells with a solar array, so the battery system could be operated with a solar array for the cruise phase of the mission. This would result in a subsystem mass of 43.2 kg.

9.5.11 Primary Power Supply Selection

The selection data for the four alternative sources of primary power supply is summarised in Table 9.15. The preferred design is therefore obviously the RTG as this has the lowest mass and a zero delta for a longer mission, though this will require the electronics located close to the power supply to have some additional radiation protection.

9.5.12 Power Regulation

There are two primary ways in which the electrical power system can condition the bus voltage:

- Peak Power Tracking (PPT)

	Mass kg	ΔMass kg/year	Comment
Solar Array	870	0	Large area
RTG	10	0	Handling problems
Batteries	97		
Fuel Cell	15	1	Fuel containment problems
Fuel Cell and Array	13.0	0	Fuel containment problems
Batteries and Array	43.2	0.0	

Table 9.15: Alternative Primary Power Supply Characteristics

- Direct Energy Transfer (DET)

Peak Power Tracking is normally utilised by varying the operating characteristics of the solar array such that the conversion efficiency of the solar cells changes and thus the power generated varies. The final bus voltage is achieved by using a DC to DC convertor. The problem with this design is that the RTG can be viewed as a constant current source, and as such there is no efficiency curve for the PPT to track along.

The Direct Energy Transfer regulator is much simpler in that it merely shunts the unwanted power to a set of resistors and dissipates the power in that manner. This has the advantage that it is much simpler and more efficient than the PPT, thus this is the preferred design for the probe. The shunt resistors will be connected to a radiator to dissipate the thermal energy generated.

The shunt regulator and control electronics typically have a mass to power ratio of 9 g/W [1, page 373]. Therefore an allocation of 0.5 kg is proposed for the power control electronics.

9.5.13 Power Distribution

With a small spacecraft of this size there is little design activity for the power distribution system. Standard practice is to use a 28 V DC bus, and this is the proposed system for the PFF craft. Because of the simple power regulation system used and the RTG it will be possible to implement a "fully" regulated bus. This will simplify the design of the equipment's electrical interfaces. However, the specification of the peak to peak ripple on the voltage may be higher than on other spacecraft to ensure that the regulator is kept as simple as possible.

9.5.14 Equipment Power Control and Fusing

The switching on and off and fusing of the equipment can be done by either the power subsystem or the equipment itself. This is a subtle architectural question. However, in order to follow the principle of keeping the design simple, with particular reference to the interfaces, it will be assumed that both of these are the responsibility of the equipment.

9.5.15 Power Harness

A standard dual bus system is proposed for redundancy, along with the use of body ground. However the latter is considered TBC. The final choice of grounding is to be made at a later and more detailed stage in the power subsystem design.

The power harness cable will only be required to carry at a maximum 2 Amps.

Thus the cable is likely to be of the order of 0.05 kg/m.

If we assume that the harness must reach around the spacecraft, using the lens-based configuration for convenience, the circumference of the spacecraft yields a length of 9.5 m. If we use a figure of 10 m to account for spur lines etc, then the mass of the harness will be 2 kg.

9.5.16 Pyrotechnical Devices

Pyrotechnical devices will be required by the spacecraft for, among others, separation of the spacecraft from the booster, and possibly to release any covers that protect the instruments during launch. Pyrotechnical devices require large currents to fire and thus specialised circuits are required to fire them. These currents are normally sourced from either batteries or capacitors. For the PFF it is proposed to provide a set of capacitors as part of the pyro firing mechanism. This has the advantage that they can be recharged and fired again if necessary. The capacitors should be charged as one of the last acts on the spacecraft just prior to launch. Because the RTG will be connected at that point in time there should be power available, given that the only subsystem that needs to be active is the CDMS. A nominal 0.5 kg is allocated to the pyro firing subsystem.

9.5.17 Risk

The power subsystem uses well-established technology and therefore is considered to have very little technical risk. The only possible source of technical risk is considered to come from the requirement for a RTG of the appropriate size.

9.5.18 Cost

Using the cost model presented in Wertz et al [46] the cost of designing and developing the subsystem can be estimated from the following relationship:

$$\mathrm{Cost}_{\mathsf{devel}} = 6894 + 0.14X^{0.97}$$

and building the flight model of the power subsystem can be estimated as:

$$\mathrm{Cost}_{\mathsf{build}} = 183X^{0.29}$$

Where X is the product of the power subsystem mass and the BOL power requirement. Because the PFF will utilise an RTG for which these figures are not designed, the mass used in the build cost will be that of the support equipment. The mass of the reactor, calculated earlier, will then be added in. To allow for the development cost the mass of the reactor will be included in the development costs. However, because the reactor is based on the use of radioactive materials with their inherent safety issues, a factor of 1.3 times the base value has been included. This results in an estimated cost for the power subsystem of $ 7.99 Million.

9.5.19 Subsystem Characteristics

The main power subsystem characteristics are summarised in table 9.16.

9.6 Attitude and Orbit Control Subsystem

9.6.1 Introduction

The AOCS subsystem is responsible for attitude sensing and maintenance. That is, it is responsible for ensuring that the spacecraft is pointed in the required direction,

Item	
Power Source	RTG
Electrical Output	46.8 W
Source Mass	10 kg
Power Control	Shunt Regulated
Power Control Mass	0.5 kg
Harness Mass	2 kg
Pyro System	Capacitive system
Pyro System Mass	0.5 kg
Total Mass	13 kg
Cost	$ 7.99 M

Table 9.16: Power Subsystem Characteristics

and for changing that pointing direction to another direction upon command from the main computer. Part of this task is also target-tracking, though the AOCS is not expected to sense the target - merely to provide pre-computed tracking rates.

The orbit-control function of the AOCS subsystem element is considered to be a function of the propulsion system on the PFF. This change in the normal functional allocation is because the only orbit-maintenance carried out by the PFF is a series of mid-course correction burns. The required thrust levels and directions will be computed on the ground. The only role the AOCS plays in the mid-course guidance maneuvers is to ensure that the spacecraft is pointing in the correct direction for the burn to be executed.

The AOCS on the PFF spacecraft is assumed to take control once the spacecraft is released from its booster.

9.6.2 Pointing Requirements

Steady State Pointing Accuracy

The spacecraft is required to point the instruments to an accuracy of 10 μrad. However, because of allowances for system level errors, the AOCS must be designed to achieve an accuracy of 7.0 μrad (see the pointing budget in section 9.4.4). During the cruise phase of the mission, when the instruments are inactive, this requirement can be relaxed if necessary. The secondary limit on pointing accuracy is set by the communications antenna pointing requirements. The antenna beam-width is approximately 0.4 degrees, suggesting a pointing requirement during cruise phase of better than 0.1 degrees.

Spacecraft Moment of Inertia

Just as an estimate of the mass of the spacecraft is required for velocity calculations, so for rotational effects, the moment of inertia of the spacecraft is required. For simplicity the model chosen for the PFF spacecraft is that of a thick disk. The model therefore approximates the lens-based design of the spacecraft with reasonable accuracy. The assumed dimensions are a radius of 1.5 m and a thickness of 0.5 m. This gives the following moments of inertia:

$$I_{cc} = 67.8\,\mathrm{kgm}^2$$

$$I_{aa} = 35.2\,\mathrm{kgm}^2$$

where I_{cc} is the axis at right angles to the face of the disk, and I_{aa} is an axis parallel to the face of the disk.

Disturbance Torque Cancellation

The spacecraft is subjected to disturbance torques which will cause the spacecraft to spin. The AOCS subsystem is responsible for cancelling out these disturbance torques. The main source of disturbance for the PFF spacecraft is solar radiation pressure acting on the spacecraft. The maximum torque occurs when the spacecraft is close to the earth. The applied torque is proportional to the angle between the sun and the Earth, which has a maximum value of approximately 1.5 deg. Thus the peak torque is approximately 1×10^{-6} Nm. The total momentum imparted on the spacecraft over its lifetime by the solar radiation is 11.8 Nms.

Pointing Rates

The AOCS subsystem is responsible for repointing the spacecraft relative to inertial space. The PFF spacecraft requires repointing for the following activities:

- Communications antenna repointing
- Instrument repointing
- Mid-course guidance maneuvers
- Target tracking, or relative motion compensation

Communications Antenna Repointing

The Earth has a circular velocity of 2π Au/year; therefore when the spacecraft is 1 Au from the Earth then the relative maximum rotation rate the spacecraft must have is 200×10^{-9} rad/sec. It is necessary to speed up to this velocity twice a year. The acceleration to obtain this velocity is negligible. The momentum generated by a rotation rate of 200×10^{-9} rad/sec is 7×10^{-6} Nms. Thus for a 8 year mission

112×10^{-6} Nms of momentum will be required if the momentum cannot be stored. This is a relatively small torque requirement and will therefore be ignored in future calculations.

Instrument Repointing

At closest approach the spacecraft provides the best image resolution. Therefore the science team will desire to maximize the number of images of Pluto taken at closest approach. The (maximum) number derives from that required to generate a full disk of the planet.

The imaging time of the instruments can be divided into two phases. The first is the data capture phase. The second is the read phase when the data generated by the instrument is read by the onboard computer. The instrument during the read phase is not imaging the planet. Therefore to maximise the imaging, the spacecraft should be able to repoint during the read phase ready to take the next image. If we assume that the planet is taken as a series of strips, then the spacecraft must be capable of changing attitude by 0.01 degrees during the 2 seconds of the read phase.

The angular position as a function of time due to a torque on the spacecraft is given by:

$$\theta = \frac{Tt^2}{2I}$$

where θ is the angular position, and T is the applied torque. Therefore assuming that the spacecraft is accelerated for 1 second and then decelerated for 1 second, to bring the spacecraft to rest at the end of the 2 second period, then the spacecraft control system must be capable of generating a torque of at least 0.68 Nm. However a system capable of generating at least 0.8 Nm is suggested to provide some margin for controlling the system.

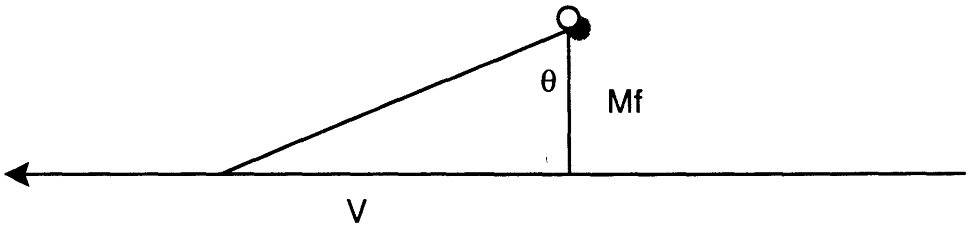

Figure 9-5: Pluto flyby view angle

Let us assume that 500 such repointings per axis are required. Thus the reaction control system requires a capability of generating a total of 680 Nms of momentum, for spacecraft repointing.

Mid-Course Guidance Maneuvers

The attitude changes required by the mid-course guidance maneuvers are considered to be a subset of the instrument repointing activities, and as such generate no requirements of their own. The repositioning will require a total momentum of 13.6 Nms.

Camera Motion Compensation Requirement

The turn rate required by the imaging system to maintain the cameras focused on one spot is constrained by the flyby speed and flyby altitude. With a 15,000 km flyby altitude and 18 km/s velocity, the resulting relative motion of Pluto is 0.064 deg/sec.

To compute the required torque level to track the target the view angle of the target as a function of time must first be calculated. Let us firstly define t to be zero when the spacecraft is at closest approach. Let us further define θ such that it is zero at closest approach. See figure 9-5. θ is therefore given by:

$$\tan\theta = \frac{Vt}{M_f} \tag{9.1}$$

Where V is the flyby velocity[7] and M_f is the distance of closest approach to Pluto. Note that the maximum relative velocity of Pluto is 0.064 deg/sec. To compute the angular acceleration equation 9.1 is differentiated twice:

$$\sec^2\theta\dot{\theta} = \frac{V}{M_f}$$

$$\dot{\theta} = \frac{V\cos^2\theta}{M_f}$$

$$\ddot{\theta} = -2\frac{V\cos\theta\sin\theta}{M_f}\dot{\theta}$$

$$\ddot{\theta} = -2\frac{V^2\cos^3\theta\sin\theta}{M_f^2}$$

To find the maximum required acceleration we differentiate and set $\frac{d^3\theta}{dt^3} = 0$:

$$\frac{d^3\theta}{dt^3} = 6\frac{V^2\cos^2\theta\sin^2\theta}{M_f^2}\dot{\theta} - 2\frac{V^2\cos^4\theta}{M_f^2}\dot{\theta}$$

$$\frac{d^3\theta}{dt^3} = \left(\frac{V^2\cos^2\theta}{M_f^2}\dot{\theta}\right)\left(6\cos^2\theta - 2\sin^2\theta\right)$$

$\frac{d^3\theta}{dt^3} = 0$ when $\theta = \pi/6$ rad. Thus the maximum rate of angular acceleration required is 46×10^{-6} deg/sec^2. This is much smaller than the other requirements and thus can be safely ignored.

---

[7] Note that because of the low gravitational mass of Pluto we can assume that the spacecraft travels in a straight line at a constant velocity as a first approximation

9.6.3 Spacecraft Platform Stabilisation

The spacecraft stabilisation is responsible for maintaining the desired pointing attitude of the spacecraft. There are three basic spacecraft stabilisation concepts:

1. Spin stabilisation
2. Momentum biasing
3. 3-Axis stabilisation.

Other techniques such as gravity-gradient and magnetic-gradient stabilisation are possible; however, these techniques can be ignored for the current discussion because of the lack of either a suitable gravity field or magnetic field for most of the spacecraft's cruise phase.

Spin Stabilisation

In spin stabilisation the spacecraft is spun about its main axis. This introduces a gyroscopic stiffness to the spacecraft, and thus any moments applied to the spacecraft are translated into a nutation of the spin vector. The key problem with this type of design is that the instrument would either have to be mounted on a separate despun platform or one must use the spin motion to scan the target. The typical accuracy of a spin stabilisation system is 0.1 deg or 2 mrad.

Momentum Biasing

Momentum biasing the spacecraft is similar to spin stabilisation except that rather than spinning the spacecraft, a momentum wheel is placed on the spacecraft. It is spun up to a high speed to achieve a similar momentum to that of the spin-stabilised spacecraft. Again the typical pointing accuracy of the spacecraft is 0.1 degrees.

3-Axis Stabilisation

In 3-axis stabilisation the induced forces on the spacecraft that must be opposed are counteracted by the use of either reaction wheels, which store the induced torque, or by thrusters, which generate opposing torques. Pointing accuracies of up to 0.001 deg or 17μrad can be achieved using a 3-axis system.

Stabilisation Selection

The only design that can achieve the desired stabilisation accuracy is the 3-axis design and thus this is the preferred option.

9.6.4 Actuator Selection

Introduction

For the PFF mission we can basically consider three types of AOCS actuators:

- Control Moment Gyros
- Reaction Wheels
- Thrusters

Control Moment Gyros

A control moment gyro can exert between 25 and 500 Nm of torque, which is far in excess of that required by the PFF spacecraft for its repointing activities. In addition, given that each unit weighs more than 40 kg, we can conclude that these are not suitable for the PFF.

Reaction Wheels

Reaction wheels can typically generate torques of 0.01 to 1 Nm. The maximum torque required by the PFF is 0.8 Nm, required for instrument repointing.

The problem is that a suitable reaction wheel is likely to weigh at least 10 kg, so the weight of the AOCS would be in excess of 30 kg.

If a set of thrusters are used to provide the high peak torques for repositioning and a reaction wheel is used to provide on-station torques, then the mass of the reaction wheels required can be reduced to 3.5 kg per axis with a peak power requirement of 16.3 W. These wheels are capable of generating 0.09 Nm of torque[8].

Maximum Stored Momentum

As the spacecraft tracks the Earth during cruise phase, the momentum wheels must store the imposed momentum until the direction of the torque on the spacecraft reverses and the momentum on the wheels can be off-loaded. Thus, it is necessary to calculate the maximum momentum that the spacecraft must store.

If we assume that the torque on the spacecraft is approximately sinusoidal, with a peak of 1×10^{-6}Nm, and that the period is half a year, then the maximum momentum of the spacecraft is 5 Nms. As this level of momentum is greater than the wheels' capacity to store it, the excess momentum will have to be dumped.

Momentum Dumping

To dump momentum, the spacecraft will require a set of thrusters and propellant. The torque these thrusters produce must be less than the maximum torque of the wheels, unless we permit the spacecraft to spin for a short period of time and thereby lose its pointing.

---

[8] Based on Teldix RDR 3 reaction wheel [47]

Thrusters

In the thruster only scenario, low pressure thrusters are used to provide all torques on the spacecraft. The following factors control the sizing of the control thrusters:

1. Thrust induced oscillation
2. Disturbance torque cancellation
3. Required roll rates

Thruster Induced Oscillation

Let us assume that the control system can never achieve a static situation; that is, the spacecraft always has some roll rate. For example, assume that the spacecraft starts with an initial clockwise roll rate. The spacecraft will then continue to roll clockwise until it reaches the limit of the spacecraft's pointing accuracy. At this point the spacecraft AOCS system will execute a burn to induce a counter-clockwise roll. When the spacecraft achieves the correct pointing the control system has two options: fire a second thruster to reduce the roll rate or leave the current roll rate as established. Whichever scenario is executed, the thrusters can never be exactly matched and the spacecraft will have some residual roll rate, which will be maintained until the spacecraft again reaches the limits set on the acceptable pointing accuracy.

The first question to answer is what is the maximum roll rate and hence thruster force, that will allow the spacecraft to maintain the required pointing accuracy.

Let us assume that the actuator can be activated and deactivated instantaneously. The limit on the time the thruster is active is therefore dominated by the control system.

The maximum controllable rotation rate is one which will take the spacecraft from one end of the pointing box to the other, within the cycle time of the controller.

For example, consider the case of the spacecraft having a slow roll rate. When the spacecraft reaches the limit of its pointing accuracy, the AOCS will pulse the thrusters. This will induce a roll rate in the opposite direction to the original one. If this rate is the maximum controllable rate, then when the AOCS computer next examines the attitude of the spacecraft it will be at the other end of the pointing box, thus necessitating a second thruster firing. This maximum roll rate limit sets a limit on the maximum size of the thrusters that can be used for on-station pointing maintenance.

The minimum torque from a set of thrusters is given by:

$$T_{min} = F \times \text{Moment Arm} \times \text{Duty Cycle}$$

The induced rotational speed is therefore:

$$\omega_{induced} = \frac{T_{min}}{I}$$

Assuming that the duty cycle is 1 /controller bandwidth:

$$\omega_{max} = \frac{7\mu rad}{\text{duty cycle}}$$

Thus, the maximum allowable thrust F from the thruster pairs is given by:

$$F_{max} = \frac{7\mu rad \times I}{(\text{Duty Cycle})^2 \times \text{Moment Arm}}$$

The spacecraft's pointing box's width is 7μrad. Thus, if we assume that the controller has a 100 Hz bandwidth[9], then the maximum thruster size that can be employed to avoid putting the spacecraft into an oscillatory mode is 1.6 N. Employing a factor of safety of 10, this limits the selection to > 0.16 N thruster.

---

[9] Note that the minimum duty cycle time of the thruster is typically 5 ms, and as such this implies a higher degree of controllability than available.

There are a number of thrusters available in this thrust range, such as cold gas thrusters, mono-propellant thrusters and electro-thermal thrusters, such as resistojets.

Time Between Thruster Firings

If the spacecraft AOCS subsystem has initiated a burn to reacquire correct pointing, the AOCS subsystem will later be required to initiate a second burn to cancel out the roll rate induced by the first burn. However, as noted previously, the thrusters will not balance each other out exactly. The imbalance in the control can be assumed, on average, to be half the minimum commandable rate. Thus, the time between thruster firings will be,

$$t = \frac{I\theta_{max}}{F_t L S} - \frac{S}{2}$$

where I is the moment of inertia of the spacecraft about that axis, F_t is the thruster force, L is the thruster's moment arm and S is the minimum on-time of the thruster. The minimum value of S is typically 5 ms [46, page 648]. Therefore, with no disturbance torques present, the thrusters will fire twice every 0.2 seconds. Since the imaging period for the instrument is 4 seconds, the spacecraft will have reached its pointing limits approximately 20 times during that period. This is likely to lead to an excessive amount of image blurring. To increase the time between firings to the order of 5 seconds (ie, greater than the camera integration time) requires a thruster with a force of less than 5 mN. Currently, this size of thruster does not exist, but it should be possible to build such a thruster, particularly if the design is simple, such as for a cold gas system. Such a thruster is assumed to weigh 0.1 kg [46, extrapolating from table 17-10].

Station-Keeping Fuel Requirement

From the definition of I_{sp} we can calculate the mass of fuel used each pulse:

$$m_p = \frac{F_t S}{I_{sp} g}$$

While hydrazine is more commonly used, Cold gas presents a worst case, mass with very reasonable probability of development, so assuming an Isp of 50 seconds, then the thruster must use 5.1×10^{-8} kg/burn. This equates to a mass of 3.2 kg of fuel per axis for a 10-year mission. If the pointing control requirement is reduced for the cruise phase of the mission to that required only to maintain the communications antenna pointing requirement, the time between firings is reduced to once every 27 minutes. This reduces the fuel required to 0.02 kg per axis.

Disturbance Torque Cancellation

The spacecraft is subject to disturbances from solar radiation pressure. The resulting torque must be opposed by the reaction control system.

If T_d is the applied external torque to the spacecraft then:

$$T_d = I\dot{\omega}$$

$$\dot{\omega} = \frac{T_d}{I}$$

Thus, assuming an initial angular offset and velocity of zero:

$$\theta = \frac{T_d t^2}{2I}$$

When the spacecraft reaches the limit on its angular accuracy then the spacecraft must be returned to the correct pointing. The maximum torque on the spacecraft is 1×10^{-6} Nm. Thus, if we try to maintain the maximum attitude accuracy, the spacecraft will fire its thrusters after 16 seconds.

The minimum size of thruster required to control the disturbance torque, assuming that the thrusters are fired in pairs and a minimum pulse of 5 ms, is given by:

$$F_t = \frac{\sqrt{2\theta_{max} I T_d}}{LS}$$

The minimum required thrust is 3 mN and the total momentum imposed on the spacecraft by the solar radiation pressure is 11.8 Nms. Therefore, to cancel out the disturbance torque the spacecraft must execute a total burn of 800 seconds. This equates to a fuel requirement of 0.2 kg of fuel.

Required Roll Rates

During a number of phases of the mission, such as mid-course burns and flybys, the spacecraft must reorientate itself. Each reorientation will require the spacecraft to execute two burns. The first to spin the spacecraft to initiate the reorientation and the second to cancel the spin rate.

To generate the 680 Nms of momentum required for repointing a cold gas based system with an Isp of 50 seconds would require approximately 3 kg of fuel. An allocation of 3.5 kg is made to allow for additional maneuvers and two axis turns.

The thrusters required for this operation are of the order of 0.5 N thrusters. The problem with using this size of thrusters comes from considering the problem of imbalance between the pairs. Assume that the thrusters are active for 0.85 seconds to initiate and stop the turn. If the thrusters are mis-balanced by half the minimum pulse width, then the station-keeping thrusters need to generate a total impulse of 2.5 mNs. With the 5 mN thrusters, this will require a burn of half a second. This is just sufficient to allow the spacecraft to achieve correct pointing within the 2 seconds required between frames. More detailed analysis is required to ensure that the spacecraft can control differences in the roll thrusters.

The use of different propellants other than the cold gas system analysed above is possible, because of their higher Isps, these offer smaller fuel requirements. However, because of the simplicity and low mass of fuel required by the cold gas system, mono and bi-propellant systems have not been considered. The choice, however mono-propellant hydrazine would afford integration of fuel supplies for AOCS and ΔV thrusters and should be considered for future design iterations.

Propellant Tanks

A typical mass fraction for a high pressure system is 0.64, so the tank mass is 0.36 times that of the propellant. In the PFF's case, this is likely to be low due to the small mass of propellant and relatively high mass of associated hardware, such as mountings.

Fuel Pipes, Valves and Other Paraphernalia

If we model the pipe as a cylinder, then the allowable stress can be calculated from:

$$\sigma = \frac{pr}{t}$$

where p is the operating pressure, r the pipe radius and t the wall thickness. If the pipes are assumed to be made of aluminium, $\sigma = 300 \times 10^6 N/m^2$ (allowing for a 40% safety factor) and the density is 2.85×10^3kg/m^3. With an input pressure of 300 psi, or 2.1 MPa, and a radius of 2 mm ,the required wall thickness is 0.014 mm. If 1 mm is assumed to be a reasonable manufacturable thickness the pipe mass is approximately 0.05 kg/m. Assuming 10 m of piping (as with the power bus), this equates to 0.5 kg of piping. As such, the spacecraft will require at least 12 thrusters to allow for redundancy, and thus 12 solenoid valves plus 12 filters, a set of fill and drain valves and 12 normally open squib valves so that we can shut off any line in the event of a failure, and a normally closed pyro valve. Assuming each of these weighs 25 grams, then approximately 1 kg must be allowed for sundries.

Thruster System Aggregate Mass

The spacecraft requires 0.06 kg for station-keeping, 0.2 kg for solar radiation torque cancellation, and 3.5 kg for attitude changes. A total propellant load for the AOCS system of 4 kg is assumed. The tankage mass allocation is 1.4 kg. Adding 3.4 kg for thrusters, piping and other devices, gives an overall mass requirement of 8.8 kg.

Electrical Power for the Thrusters

The only power required by the thrusters is to operate the valves. Each valve will typically require 1 W and because the thrusters are fired in pairs, an allocation of 2 W per axis has been assumed.

Reaction Wheels with Momentum Dumping

To dump the momentum stored in the reaction wheels, 0.2 kg of fuel from the cold gas system is required. Because only 1 set of thrusters is required, as compared to the two for the thruster-only system, 2.3 kg is sufficient for tankage, fuel lines, thrusters and other sundry equipment.

9.6.5 Actuator Selection

The choice of actuator should be based solely on the mass of the system. The five basic options are as follows: control moment gyros, pure reaction wheels, pure thrusters, or a combination of the latter two. Table 9.17 summarises the different masses and power requirements of the options. The chosen option is the thruster only system.

Actuator	Mass kg	Power W	Comment
CMG	120	-	
Reaction Wheels only	40	95.8	Peak power
Thrusters only	8.8	6	Assuming cold gas
Reaction Wheels with Thrusters	22.8	32.6	
Reaction Wheels with dumping	42.5	95.8	Peak power

Table 9.17: Mass characteristics of the AOCS actuator options

9.6.6 Attitude Determination

The attitude determination system must measure the attitude of the spacecraft in space. Thus, the system must provide a measurement accuracy of better than 10×7^{-6} rad or 1.5 arc seconds. The only units that can measure this type of accuracy are star trackers and star mappers. The problem with these types of units are that the update rate is relatively low, on the order of seconds. The question is, is this good enough?

A currently available suitable star mapper could be the modus sensor, which weighs 6 kg and requires 10.5 W. However, star trackers in 3 kg range are currently being bread-boarded. It can be reasonably safely assumed that these devices will be available in time for the PFF. These units are predicted to require 11 W.

High Rate Attitude Data

The only way in which we can provide high rate attitude data is via an Inertial Navigation System (INS). Fortunately, because the PFF will have a very accurate reference system in the form of the star mappers, the INS can have a relatively high drift rate. The INS is only required to provide accurate pointing direction information rather than full positional information. Therefore the accelerometers of the INS are not strictly required but because they add little mass to the system will be included. The obvious choice for mass and power reasons is a strap-down system.

The maximum allowable drift rate generates a false acceleration which would cause the spacecraft to mis-point between updates. If the drift rate is d, then the pointing error is given by:

$$\text{Pointing Error} = \frac{dt^3}{6}$$

Thus to have a pointing error of less than 7×10^{-6} rad after 1 second would require the INS's drift rate to be less than 8.7 deg/hr. For safety, we will add a factor of 20 to this and require the INS to have a drift rate of better than 0.44 deg/hr. This is equivalent to an error of 0.36×10^{-6}rad after 1 second.

The mass of a suitable INS is approximately 1.6 kg and will require 17.5 W (this is a Honeywell RLG system).

9.6.7 Safeing Mode Sensors

In the event of the spacecraft switching to a safeing mode the spacecraft is required to orientate itself so that it is pointed at the sun, an easy target to find. For safety, we will need a set of sun sensors onboard the spacecraft. In this mode, the spacecraft cannot be required to maintain tight pointing. Typical sun sensors have an accuracy of approximately 0.1 deg, which is comparable with cruise mode pointing requirements[10]. However care must be taken in selecting the sensors to ensure that they will correctly detect the Sun, even at 31 AU.

---

[10] As an aside, it is interesting to consider what safeing mode should be used with an optical communications system which has an inherently tight beam and so would be difficult, if not impossible, to communicate with in sun pointing mode.

The mass of four such sensors that can provide full coverage is approximately 1 kg. They will require 0.25 W of power; however, as these will not normally be operational, we can neglect the power requirement.

9.6.8 Control Electronics

The AOCS control electronics must implement the control laws designed for the spacecraft's control, using the sensors as inputs and the thrusters as controllers. The logic can be implemented using either digital or analog hardware. However, because the PFF uses star trackers as part of its sensor suit, the controller must be digital to process the information.

A suitable computer such as the HEAO computer weighs 4.5 kg and requires 15 W of power. This is capable of generating control commands every 320 ms. The computations require 16 Kbytes of memory.

To calculate the required processing power, let us assume that the orientation and spin rates are stored as quaternians. The first action must be to calculate the current angular position and velocity of the spacecraft, given the previous position, velocity, current, and previous angular acceleration. First, the body rates from the INS must be converted into a quaternian position via equations of the form:

$$\dot{e}_0 = -\frac{1}{2}(e_1 p + e_2 q + e_3 r) + k\lambda e_0$$

where

$$\lambda = 1 - (e_0^2 + e_1^2 + e_2^2 + e_3^2)$$

and p, q, r are the body rate accelerations.

Each execution would require approximately 18 floating point operations. There are four equations; let us assume the equations take 10 iterations to converge, thus, the conversion requires 720 FP operations. Similar calculations are required for position and acceleration. Finally, the resulting body rates and accelerations must be integrated to calculate the current position. Let us assume this takes 40 FP operations. The result of this processing can then be fed to the control algorithm. Let us assume a second order control law which will require approximately 20 FP operations to calculate the desired response. Thus, the PFF control system must be capable of executing approximately 800 FP operations per command cycle. Thus, we need approximately 3 KFP ops/sec to provide thrust controls every 250 ms. This is a typical control rate [45, page 212]. This gives us a control bandwidth of 2 Hz, which is relatively small. If this is increased to 10 Hz, then an execution rate of 16 KFP/sec is required.

This low processor speed requirement would make the system ideal for incorporation as a subtask in the CDMS. Therefore, this has been assumed in assessing the mass and power requirements of the AOCS subsystem.

9.6.9 Risk

The main risk for the AOCS system as selected is the availability of the microthrusters required for station-keeping. Although these are very simple, they do not currently exist at the thrust level required by the PFF and must therefore be considered a high risk item. The large number of firings that such a thruster will be required to perform will also be a major problem in the design and development of the thrusters. An alternative way to provide the low levels of thrust required by the spacecraft is to use valves that can pulse open for periods shorter than 5 ms. To manage the risk with a high level of confidence in the outcome, both strategies should be pursued.

The star mappers proposed for use by the AOCS subsystem are currently only in the bread-board stage. This is therefore a technical risk which must be carefully monitored. However, the risk level is assessed to be low enough not to require additional action.

9.6.10 Cost

The cost of the AOCS subsystem can be broken down into two categories: the cost of sensors and the cost of the control system. The cost of the sensors is based on the weight of the sensors[11] using the following relationship:

$$\text{Cost}_{\text{determination}} = 4225 + 4329X^{0.46} + 2275 + 1617X^{0.39}$$

The cost includes a multiplication factor of 1.3 to account for the fact that the star mappers are a new design.

The cost of the reaction control system is also based on the dry mass of the system (4.8 kg) using the following relationship:

$$\text{Cost}_{\text{reaction}} = 935 + 153X - 364 + 186X^{0.73}$$

The total cost of the AOCS system is therefore estimated as 27.85 M$.

9.6.11 AOCS Summary

Table 9.18 shows a summary of the key performance and data of the PFF AOCS subsystem. The system is shown schematically in figure 9-6.

---

[11] Reference [46] suggests this should be the dry mass. However, if this figure is used the AOCS system cost is 50M$ which is too high. Hence, the assumption of equipment mass is assumed.

Item		Comment
Sensors	INS	Required for fast update
	4 Star Mappers	Used to update INS
	4 Sun Sensors	Used for safeing mode.
Actuators	2 Sets of thrusters	
	5 mN Cold gas	Station-Keeping
	0.5 N Cold gas	Roll Thrusters
Control Electronics	None	Allocated to CDMS
Sensor Mass	14.6 kg	
Sensor Power	50.75 W	
Actuator Mass	4.8 kg	
Actuator peak power	6 W	
Total Mass	19.4 kg	
Power Requirement	56.8 W	
Cost	27.85 M$	

Table 9.18: AOCS Subsystem Characteristics

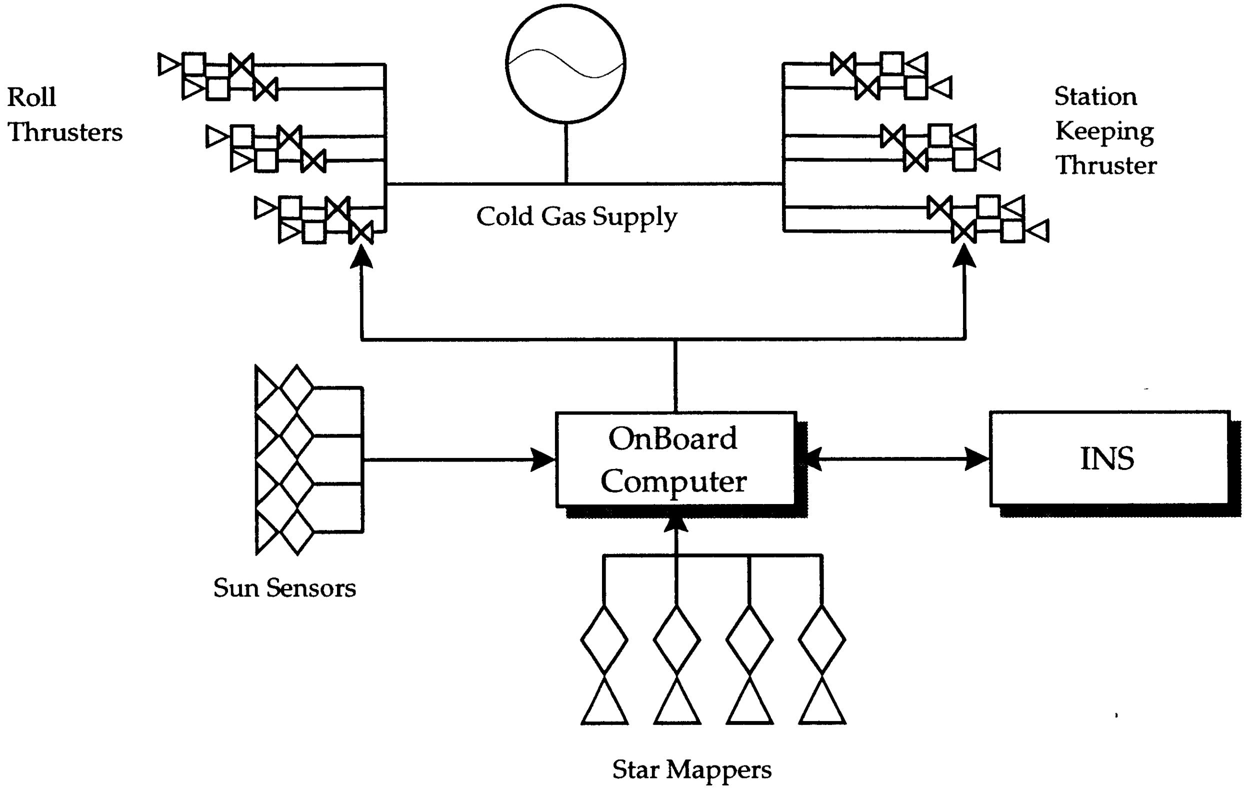
Roll Thrusters
Cold Gas Supply
Station Keeping Thruster
Sun Sensors
OnBoard Computer
INS
Star Mappers

Figure 9-6: AOCS Functional Diagram

9.7 Guidance, Navigation and Control

The guidance, navigation and control activities of the spacecraft can be implemented in one of two basic methods:

- Spacecraft-Based
- Ground-Based

9.7.1 Spacecraft-Based Navigation

For the spacecraft to conduct autonomous guidance and navigation, the spacecraft must be capable of computing accurately its own position and that of its target, plus implementing flyby optimisation activities that ensure that its arrival is in the correct orientation to Pluto to maximize the imaging options of the spacecraft. The spacecraft needs to then compute the optimum burn time and ΔV required. These activities require a large amount of computational power. However, since the arrival criteria are preset, there is little option for reconfiguring the arrival parameters to improve/optimize the imaging options. Because the desired imaging sequence will not have been selected prior to launch, then this information will have to be unloaded to the spacecraft prior to arrival at Pluto.

9.7.2 Ground-Based Navigation

In the ground-based navigation scenario the spacecraft provides position information to the ground and also acts as an active target to allow its range to be determined. This information is then fed to ground-based engineers who can then compute the optimum mid-course correction burns for the spacecraft to execute. The course correction burns are then relayed to the spacecraft, in the form of time-tagged commands.

These are then executed by the spacecraft at the appropriate time. This type of design has the advantage of requiring little onboard processing power.

9.7.3 Preferred Navigation and Control Design

The preferred design is to use a ground-based Navigation, guidance and control strategy. This is with the exception of the level of autonomy necessary to ensure the safe and correct operation of the spacecraft when not in contact with the ground.

9.7.4 Terminal Guidance

Upon arrival at Pluto, the spacecraft will begin taking a sequence of images of the planet and of its moon Charon. Prior to arrival the spacecraft will have received a set of time-tagged instructions relating to the images to be taken along with the pointing direction for each of these images. The spacecraft is fitted with a high accuracy navigation system and so can be assumed that it will point at the desired direction. However, because of errors in the knowledge of the spacecraft's and the target's exact positions in space, there is a question of whether the spacecraft images the desired target. More simply, is the target where the controllers on Earth think it is relative to the spacecraft?

Typical spacecraft position accuracies in space are 20 km [48]. The other critical problem in the pointing of the spacecraft's instruments is a knowledge of the ephemeris of Pluto and Charon. This can be a particularly large source of error in the instruments' target acquisition. The knowledge of the ephemeris of the spacecraft and of Pluto can be improved using pre-encounter optical navigation images, where Pluto is imaged against the known star background. Using this technique, the a priori ephemeris error for Galileo's encounter with the asteroid Gaspra was reduced to 5 km [23, 42]. The Galileo encounter accuracy was hampered by the failure of the spacecraft's main mission antenna to deploy, and thus it can be expected that the accuracy in a fully operational mission would be improved beyond this figure.

An error of 5 km in the relative position of Pluto would induce an offset of approximately 330 pixels when the edge of Pluto is imaged. This is an acceptable level of accuracy. However, to ensure that an 1σ a priori ephemeris knowledge of Pluto's position to better than 5 km is known will require analysis beyond the level of the current design iteration. Included in this analysis must be a computation of the number of images that will be required for optical navigation.

It is believed that the use of an optical navigation technique to refine the calculated position of both the spacecraft and Pluto should provide sufficient accuracy in the instrument pointing instructions to ensure a successful flyby.

9.7.5 Risk

The guidance and navigation systems are not implemented on the spacecraft, but as operational procedures and ground-based operations. The only question that is uncertain is what accuracy the optical navigation technique will provide on the a priori knowedge of the relative position of Pluto and the spacecraft. The subsystem is therefore considered only to have a moderate level of technical risk and to be free of programmatic risk.

9.7.6 Cost

All of the activities associated with the guidance and navigation of the spacecraft occur after the launch of the spacecraft. The only cost of the system is associated with ensuring that the appropriate operational procedures are developed and documented. A cost of \$0.2 million is allocated to this subsystem to cover interface and compatibility activities.

Item		Comment
Guidance System	Ground-based	
Terminal Guidance	Optical navigation assisted	
Cost	$ 0.2 Million	interface activities

Table 9.19: GNC subsystem Characteristics

9.7.7 GNC Subsystem Summary

A summary of the GNC subsystem is presented in table 9.19.

9.8 Command and Data Management Subsystem

9.8.1 Introduction

The roles of the CDMS and the Onboard Computer are extremely intertwined, hence these two functions are examined together in this section. The simplest conceptual way to consider the two units is that the CDMS acts as the Onboard Computer's (OBC) interface to the world. Thus it passes signals from the OBC to the various subsystems, and relays back status and telemetry information to the OBC.

9.8.2 CDMS Architecture

There are a number of possible architectures for the CDMS. These vary between centralised control and distributed control. Thus, the following system architectures are proposed:

- Classical Design with a command decoder and execution unit, a main command computer, and an AOCS computer. The instrument data storage unit is considered as a separate subsystem.

- Medium Complexity Design whereby the command decoder is included in the Onboard Computer, but AOCS and instrument data-storage are separate.
- Simplified Design whereby AOCS functions are separate, but all other data related activities are handled by CDMS.
- All functions integrated into the OBC.

9.8.3 Architecture Selection

Selection Criteria

The selection criteria for the preferred architecture is the design with the minimum mass that can provide the necessary functionality to the spacecraft, while keeping the interfaces as simple as possible.

Functional Analysis

The CDMS needs to perform the following functions:

- Housekeeping data collection
- Subsystem control
- Master clock generation
- Timed command sequence execution
- Telemetry and data formatting

Autonomy Requirement

The complexity of the CDMS is a function of the level of autonomy of the spacecraft. For example, consider two extremes, the first a spacecraft with no autonomy at all. The CDMS's only function is to execute time-tagged commands at the appropriate point in time. The other extreme is a spacecraft which is capable of high levels of autonomous decision-making.

The autonomy issue is central to the redundancy architecture of the spacecraft. For example, if the CDMS does not have any hardware monitoring capability and autonomy then the telecommunication subsystem must be actively redundant, ie, the receiving side of the communication system must have two active paths, such that if one of the receivers fails the spacecraft can still receive orders from the ground. This has implications on the power requirement for the spacecraft. If the CDMS has a high level of autonomy however, it may be possible to operate the communications subsystem with only one active receive chain. In the event of a detected failure, a second receiver can be powered up and made the master unit. However, the question of how the CDMS can determine whether the receiver has failed or not is a complex one. The only clear way that such a failure can be determined is when the CDMS is not able to detect a signal (transmitted from the ground) that should be there. However, since communication between the spacecraft and the ground occurs only at infrequent intervals, failure detection is made that much harder. The question then becomes, what happens in the event of a non spacecraft or non-communications failure occurring which causes the spacecraft not to receive the uplink. For the current level of work this discussion is beyond the level of detail required. For the current purposes the CDMS is assumed to be capable of operating fully autonomously during routine operations of the spacecraft. Major system-failures will cause the spacecraft to enter a safeing mode until the ground controllers can provide instructions to rectify or bypass the problem.

Computer Processor Power Requirements

The required computer throughput and memory-size is shown in table 9.20. The table assumes that the word length is 16 bits. Therefore, approximately 3 Mbytes of memory will be required by the OBC. If we assume that 25% of this memory is executable code and that it is programmed in Ada, then approximately sixty-thousand lines of code will be required.

Computer Mass and Power Requirements

Examples of advanced computers currently becoming available are a 0.3 MIPS machine weighing 5 kg and requiring 16 W [25]. To increase the processing power to 3.0 MIPS, the computer would weigh 9.0 kg and require 25 W [7]. The proposed system only requires a throughput of 0.1 MIPS. Therefore, a mass alocation to the CDMS of 5 kg and 16 W is proposed. This allocation is assumed to cover a redundant unit.

Architecture Selection

The choice of the OBC architecture is beyond the level required to establish the system budgets. However, the architecture does need to be established for the subsystem requirements. The baselined design is that of the simplest system possible that integrates all the functions into the OBC. This is possible because the processing speed of small computer systems currently available are greater than the total expected work load the PFF will require.

Function	Memory Kbits	Throughput KIPS	Comment
Command Processing	10.0	1.0	Command link is low rate
Telemetry Generation	7.0	1.0	Telemetry link is low rate
Command Execution	20.0	3.0	All flyby commands pre-stored
AOCS	10.0	16	From AOCS design
Star Tracker Info	34.0	2.0	
Telemetry Gathering	5.0	10.0	
Autonomy	50	20.0	High level required
Fault Detection	34.0	20.0	
Power Management	3.4	5.0	
Thermal Control	2.6	3.0	
Orbit Control	2.0	1.2	
Instrument Control	10.0	1.0	
Subtotal	188.0	63.2	
Margin	94	31.6	50%
Total	282.0	94.8	

Table 9.20: Onboard Computer Throughput and Memory Requirements

9.8.4 Computer System Operational modes

The different modes that the onboard computer of the spacecraft can be in are shown in figure 9-7. It should be noted that the safe mode can be reached from any other mode. These event lines are not drawn, however, in order to simplify the diagram.

The main modes of operation are:

Off: The spacecraft is fully powered down.

Initialise State: This is entered on power up or after exiting safe mode.

Safe Mode: The spacecraft is pointed at the sun - entered when a major system failure prevents the spacecraft from being able to correct fault itself.

Ground Test: Supports the check-out of the spacecraft when on the ground.

Launch Mode: State of spacecraft while attached to launcher, exited when the pyros are fired to release the spacecraft from the launcher.

Cruise Mode: The normal operating mode of the spacecraft, the spacecraft is operating completely autonomosly.

Flyby Imaging Mode: Spacecraft is in tight pointing mode and instruments are activated or warming up. Includes data transfer from the instruments to Onboard storage.

Communications Mode: Spacecraft communicating with the Earth for telemetry downlink or tracking purposes.

Mid-Cource Correction: Execution of time-tagged burns uplinked from the ground to ensure correct encouter with Pluto.

Instrument Data Return: Return of instrument data to the ground post Pluto Flyby.

9.8.5 Computer Interface Architecture

The question we must next address is the preferred interface architecture of the onboard computer.

There are basically 3 options:

- Centralised
- Ring
- Bus

The interface architecture chosen will predominantly depend on what is available and suitable. That is, the PFF mission cannot afford to design a specific onboard computer for its mission, and thus must utilise what is available, or will be available for its mission. Thus, the interface architecture, will be dependent on what the chosen computer uses. Of the possible architectures only the Centralised structure does not require some form of intelligence in the subsystems to interface with the OBC. In the Bus and Ring architectures the other subsystems must implement some form of communications protocol, as compared with the Centralised architecture where the subsystem is only required to provide connections to the appropriate sensors which then can be sampled by the OBC. The Centralised architecture is very desirable when the number of subsystems and sensors associated with those subsystems is small. The other architectures basically trade off the mass of the wiring harness for local electronics. The preferred design is the centralised system because it keeps the interfaces relatively simple and because the PFF has a relatively small number of equipments.

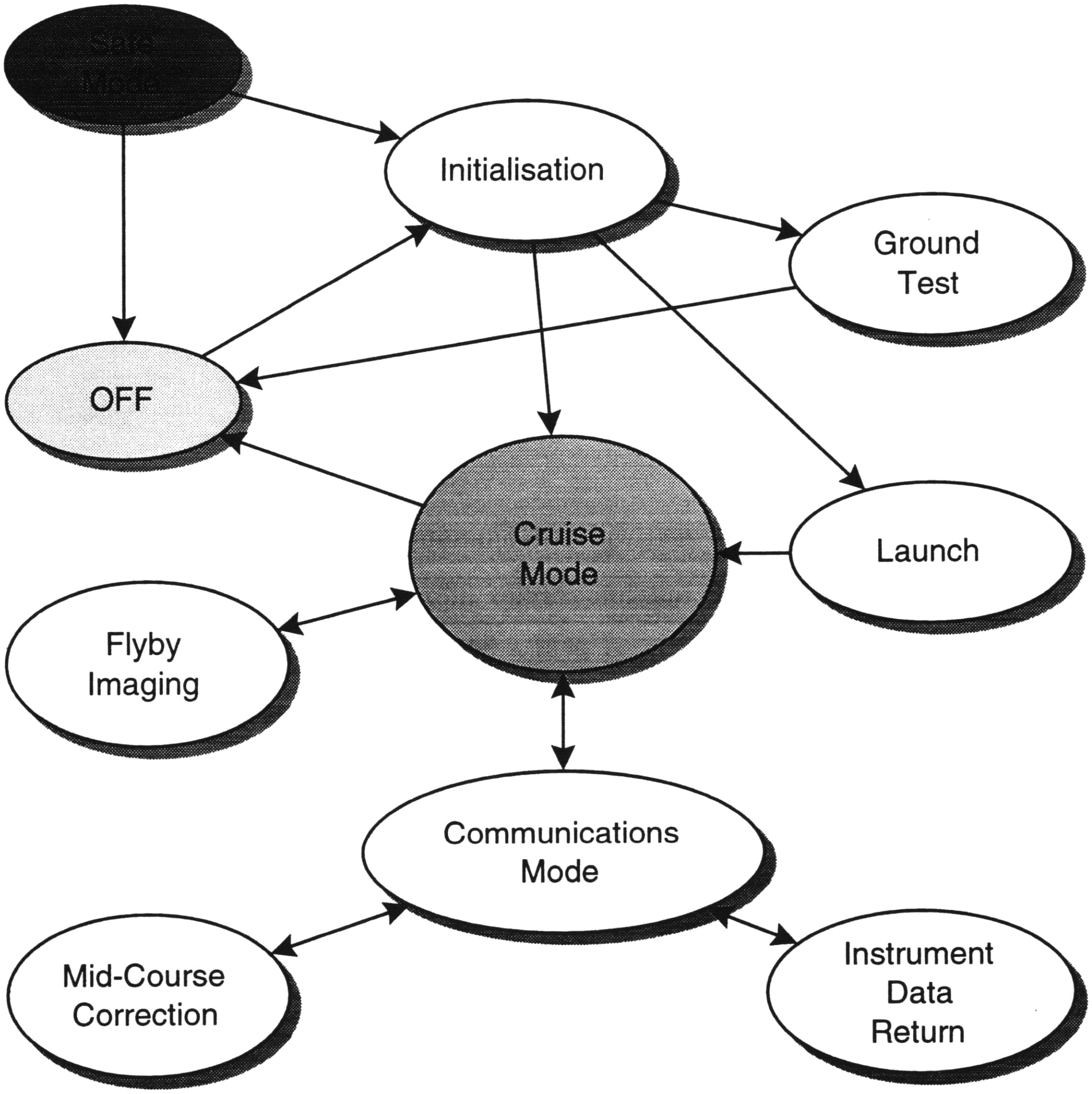
Safe Mode
Initialisation
Ground Test
OFF
Cruise Mode
Launch
Flyby Imaging
Communications Mode
Mid-Course Correction
Instrument Data Return

Figure 9-7: Onboard Computer States

9.8.6 Data Storage Requirements

The visible instrument can record a single image every 4 seconds during the flyby. Each image contains 1000x1000 pixels in three colours.

The flyby velocity is 18 km/s. Pluto has a radius of 3×10^3km. Based on this, Pluto will fill 100 pixel square 100 hours before closest approach. Given this information and the fact that Pluto has an estimated revolution period of 56.3 days, it would be desirable to image Pluto at this point since these would be the only images of one side of Pluto, assuming there is only one spacecraft.

This slow imaging activity will provide an oportunity to download the images in nearly real time. This could be advantagous for storage since that these images will not consume storage capacity at the time of closest aproach.

Let us assume that the science team requires a data set equivelent to a 1000 frames. This equates to 22.35 Gbits, or 2.8 Gbytes, of data that must be stored.

System bandwidth

At closest approach it is expected that the science team will wish to generate a full mosaic of Pluto[12]. Thus, the CDMS must read out the image data, compress the data, and then store it to the onboard recorder. Each image is a 1000 × 1000 frame. The instruments use a 8 bit quantization, thus each frame consisting of 3 colours, is 22.8 Mbits in size. The read time for the instrument is 2 seconds, giving a data rate of 11.4 Mbit/s.

Data Compression

The use of data compression by the spacecraft will allow the amount of storage and the time to transmit the data to the ground to be considerably reduced. Because the data are a set of images which tend to have a very high level of redundancy, a 3:1 image compression ration has been assumed [36].

---

[12] At closest approach Pluto is 40 frames wide.

It would be advantageous for the onboard computer to implement the compression algorithms as a software function, as this will allow the compression algorithms to be updated during the voyage to take account of the on-going research in this field. However, there is a speed penalty associated with the compression algorithms implementation in software. This issue is currently TBD.

Data Storage Hardware

The large data storage required by the PFF mission has in past deep space missions been achieved by use of tape recorders. However, currently emerging technology offers two other alternatives. The first of these new technologies is solid-state memory, which uses a large amount of static silicon memory to store the data. Because the data is stored in the state of a set of transistors the read and write speeds are very high, allowing high data transfer rates to be achieved. The problem or danger for solid state memory is from Single Event Upsets (SEU). The second new technology is based arround the use of conventional personal computer hard disks. These devices are mounted in a suitably designed enclosure to protect them from the space environment to form the flight hardware. Because of the rapid development of this technology driven by the consumer nature of personal computers these devices offer high capacities at a low price. Table 9.21 summarises the mass and power required by each of the storage options.

The preferred option is the hard drive memory system as this presents the minimum mass and power requirements.

Unit	Mass kg	Power W	Comment
Tape Recorder	10	30	
Solid State Memory	19.5	20	Power Estimated
Hard Drive	4.5	16	Power Estimated

Table 9.21: Power subsystem Characteristics

9.8.7 Command and Telemetry Harness

Assume a mass of the electrical cable used by the spacecraft to be 0.05 kg/m. Then assuming that each subsystem will require approximately 15 lines and that the average distance between the CDMS and a subsystem is 3 m, then the mass of the wiring harness will be 11 kg.

9.8.8 CDMS Risk

A large number of processors in the range required by the PFF are available [46, Table 16-10]. Thus, the computer hardware is not seen as a high-risk part of the design.

The range of low mass and power storage systems compatible with the baselined PFF data storage system is currently expanding very rapidly. Therefore, little risk is foreseen from the baselined data storage unit.

9.8.9 Cost

The hardware costs for the CDMS are based on the parametric model for the TTC parametric model [46, page 729] and utilises the mass of the subsystem.

Item		Comment
Main Computer	SCI FTP-3200	
Computer Mass	5 kg	Including redundancy
Computer power	16 W	
Data Storage	Hard Disk-based	
Storage Mass	9.0 kg	
Storage Power	16 W	
Harness Mass	11 kg	
Computer Code lines	60,000	Ada code assumed
Cost	$ 32.8 Million	Dominated by software costs

Table 9.22: Power subsystem Characteristics

$$\text{Cost}_{\text{Hardware}} = 1955 + 199X + 93 + 164X^{0.93}$$

The flight software cost can be calculated using the following formula [46, Table 20-8]:

$$\text{Cost}_{\text{Software}} = 375 \times \text{KLOC}$$

Thus, the total cost of the CDMS subsystem is estimated as $ 32.80 Million. Two-thirds of this cost are associated with the flight software.

9.8.10 CDMS Design Summary

The command and data management system developed in this section is summarised in table 9.22.

Payload Mass kg	C_3 km^2/sec^2
4536	12
3200	32
2273	50
1520	70
1015	90
404	110

Table 9.23: Estimated Titan IV Payload Mass vs. C_3

9.9 Launch Subsystem

9.9.1 Introduction

The main responsibility of the launch system is to place the spacecraft in the correct orbit to intercept Pluto. The launch system comprises two elements, the main launch vehicle, which is a conventional rocket, and a set of upper stages. The latter are required to give the spacecraft the additional C_3 necessary to achieve the fast flyby orbit.

9.9.2 Titan IV Launch Vehicle

The baseline launch vehicle for the Pluto mission is the Titan IV launcher, which is the most powerful launcher available. Table 9.23 shows the estimated C_3 for the Titan IV [18]. The uprated Titan IV with the new solid rocket motors (SRMU) is not proposed, as currently the program status is uncertain. The use of the uprated SRMUs would improve the achieved C_3.

Using a linear regression analysis, the function of C_3 against payload mass x can be approximated by:

$$\begin{aligned} C_3 = \quad & 1.73312\,10^7 + 120.905 \ln(x) + 10902.1 \ln(\tfrac{23860+x}{3540+x}) - \\ & 1.84089 \times 10^6 \ln(\tfrac{63460+x}{28360+x}) + 9.01432 \times 10^6 \ln(\tfrac{226460+x}{71460+x}) - \\ & 2.60947 \times 10^7 \ln(\tfrac{860460+x}{314460+x}) \end{aligned}$$

The constants in the arguments of the log functions arise from the masses of the various stages of the Titan IV. The payload limit is approximately 5000kg.

9.9.3 ΔV Requirement

The C_3 required to inject the spacecraft into a Pluto intercept orbit is approximately $305 \text{km}^2/\text{s}^2$ for a 7 year flight time [40, page 4]. Since a Titan 4 can only impart a maximum C_3 of 110 km^2/sec^2 (with a payload of only 404kg) then the spacecraft and any associated boosters must impart at a minimum 48.7 km^2/sec^2, or a ΔV of 6.976 km/s. This figure is the minimum ΔV required from the upper stage. The selected upper stage will to be required to provide a much larger ΔV to account for the reduced C_3 from the Titan. The reduced C_3 from the Titan VI is a result of the spacecraft and upper stage weighing more than 404 kg.

9.9.4 Upper Stage Selection

There are basically three choices for the upper stage selection: several stacked commercial upper stages, a stack of specially developed upper stages, or an integrated propulsion system on the spacecraft.

Integrated Upper Stage System

The integrated upper stage could be either a separate set of tanks which are ejected after the boost phase, or a totally integrated design that remains attached to the main spacecraft.

The advantage of using an integrated design rather than a separate set of upper stages is that duplicate units like the thrusters will not be required.

The Necessity for Multiple Upper Stages

The mass of propellant required to generate a ΔV is given by:

$$m_p = m_f \left[\exp^{\left(\frac{\Delta V}{I_{sp} g}\right)} - 1 \right]$$

If we assume that the ratio of propellant to propulsion hardware is a constant, then the maximum possible ΔV occurs when:

$$\Delta V = I_{sp} g * \ln \left(\frac{1}{1 + M_{frac}} \right)$$

where

$$M_{frac} = \frac{M_p}{M_{propulsion}}$$

and $M_{propulsion}$ is the wet mass of the spacecraft. A graph of the maximum available ΔV against mass fraction is shown in figure 9-8 for an Isp of 300 seconds. The figure shows the maximum achievable ΔV for a range of mass fractions between 85 and 95 %, which are the limits of current and near-future technology.

To achieve the required 6.97 km/sec ΔV, using a liquid hydrogen and oxygen system (Isp = 450), a mass fraction of better than 96% would be required. This is not achievable with current technology; thus, the use of a single stage upper stage is not possible, and therefore the integrated system is not possible.

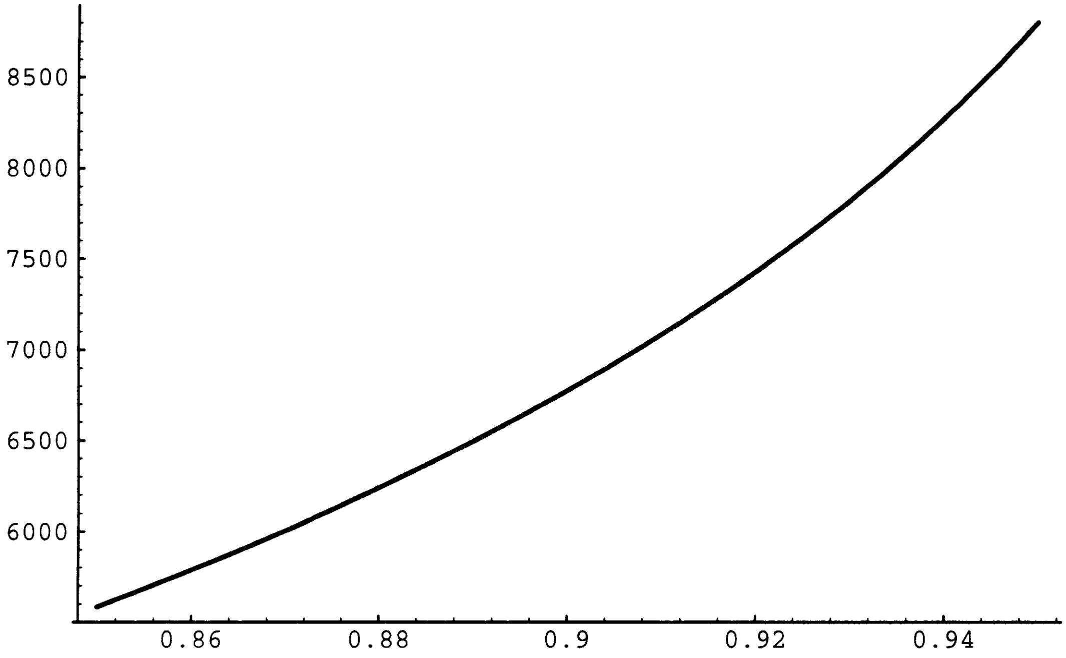

Figure 9-8: Maximum ΔV against Mass fraction

Solid Rocket Upper Stages

Table 9.24 shows a selection of commercially available upper stages and their key performance characteristics. The cost of each motor is calculated using the following formula [46, page 272]:

$$\text{Cost} = 72.5X^{0.72}$$

where X is the dry weight of the motor. This figure does not include any wrap costs, nor a reduction for learning curve. These two are assumed to cancel each other out as a rough approximation. However, a factor of 1.25 is included to cover the use of a composite motor casing.

Table 9.25 shows the achievable C_3 for various combinations of solid motors, when used in combination with a Titan IV SRM launch vehicle. The cost of any of the

Motor	Dry Weight kg	Propellant Mass kg	Isp S	Cost $M
IUS SRM-1	624	9,750	295.5	7.46
Leasat	328	3330	285.4	4.70
Star 48A	129	2430	283.9	2.40
Star 48B(S)	126	2011	286.2	2.07
Star 48B(L)	131	2011	292.2	2.15
Star 75	566	7500	288.0	6.96
IUS SRM-2	270	2725	303.8	4.08
Star 13B	7	40	285.7	0.29
Star 30BP	33	510	292.0	0.90
Star 30C	35	585	285.2	0.86
Star 30E	40	620	290.1	0.98
Star 37F	69	1080	291.0	1.53

Table 9.24: Commercially Available Solid Rocket Motors

combinations shown in the table is less than \$ 4M.

Liquid Fueled Upper Stages

There are two basic strategies to building a liquid fueled upper stage. The first is to optimise the ΔV generation capability of the stages when combined. The alternative is to design a single stage that is then stacked to form the multiple stage system. The latter strategy has the advantage that it keeps down the development cost of the upper stage stack.

Let us assume that the fuel to be used is N_2O_4 and MMH. These two fuels are

	2nd Stage							
1st Stage	None	Star 13B	Star 27	Star 30BP	Star 30C	Star 30E	Star 31	Star 37F
Star 13B	63.5	112.5	232.9	250.5	249.9	250.5	220.8	237.1
Star 27	225.6	237.5	257.7	261.1	256.5	255.5	217.9	234.7
Star 30BP	247.4	256.1	262.1	262.8	257.4	256.1	217.0	233.9
Star 30C	247.9	256.7	261.1	261.4	256.0	254.6	215.7	232.6
Star 30E	248.9	258.2	261.7	261.7	256.2	254.8	215.6	232.6
Star 31	221.37	238.2	250.9	251.6	246.5	245.2	205.3	223.1
Star 37F	237.6	250.9	256.4	256.3	250.8	249.4	209.4	227.2
Star 48A	192.3	211.3	229.0	229.2	223.7	222.1	175.4	195.1
Star 48BS	199.3	218.4	237.1	238.2	233.0	231.6	187.4	206.8
Star 48BL	201.2	220.5	239.1	239.9	234.6	233.2	188.3	207.9
Star 62	184.8	204.4	222.6	222.1	216.4	214.6	167.9	186.8

Table 9.25: Total C_3 Available for Two Solids and a Titan IV Centaur Launcher

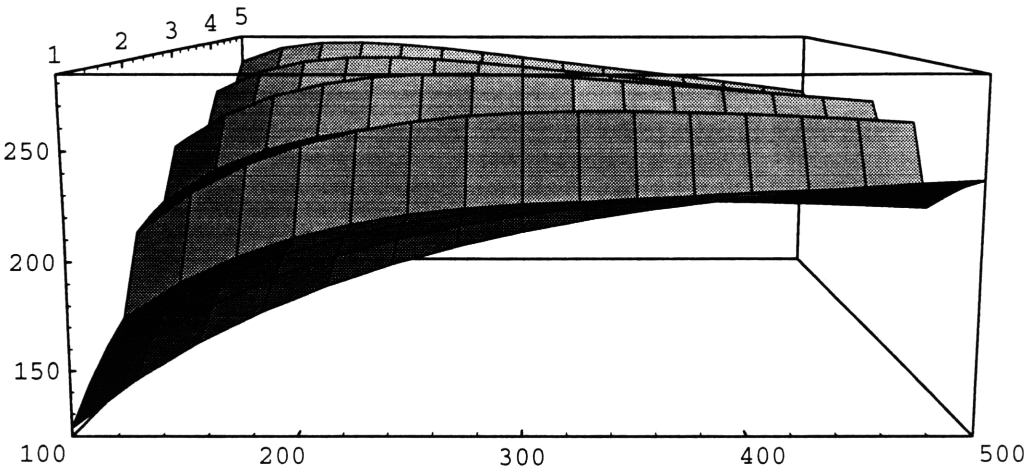

Figure 9-9: Variation of C_3 with Number of Stages and Stage Mass

chosen since they do not require cryogenic storage. The exact choice of fuel is left for a second round trade-off study. These two fuels give a typical Isp of 310 seconds.

Using this information and assuming that the mass fraction of the propulsion system maximum is 90%, then the peak C_3 available from one stage is approximately 240 km^2/s^2, for two stages it is 260 km^2/s^2, for three stages, 270 km^2/s^2 and four stages is 275 km^2/S^2. The variation of the available C_3 is shown in figure 9-9.

The development cost of such an upper stage can be calculated from [46, page 728]:

$$\text{Cost}_{\text{development}} = 0.0 + 0.0312X$$

Where X is the total impulse of a stage. The total impulse is assumed to be given by the Isp times the mass of the propellant. Thus, for a two stage unit the development cost can be estimated as 2.9 M\$. The cost of each flight unit can be calculated using:

$$\text{Cost}_{\text{production}} = 0.0104 \times X$$

	Stage Mass kg	Max C_3 km^2/S^2	Development Cost M$ FY92	Unit Cost M$ FY92	Total M$ FY92
1 Stage	590	239	5.1	1.7	6.8
2 Stages	330	260	2.9	0.91	4.7
3 Stages	240	270	2.1	0.64	4.0
4 Stages	180	275	1.6	0.47	3.5

Table 9.26: Cost of using different number of identical liquid stages

Thus, the cost of each stage is 0.91 M$.

The cost of the various number of stages is shown in table 9.26 assuming a 95% learning curve.

From table 9.26 it can be seen that the cost of designing each of the stages is much larger than the production unit costs. Therefore, the option of using a number of individually optimised stages can be excluded.

Upper Stage Selection

The choice of an upper stage can be narrowed down to a trade-off between using a set of specially designed liquid stages, and a set of commercially available upper stages. The selection criteria for this are extremely difficult to define. The baseline requirement is for the cheapest system that will ensure the arrival of the spacecraft before atmosphere freeze out.

There is some performance advantage to be gained from using a multi-stage liquid system. However, the cost of the liquid system is much higher. For comparison, a Star 30 E can provide a total C_3 of 248 km^2/s^2 for a cost of just over $ 1 Million. A stack of two Star 30BP motors would give 262 km^2/s^2 and would cost approximately $ 1.8 Million, while a comparable two stage liquid providing a total C_3 of 260 km^2/s^2

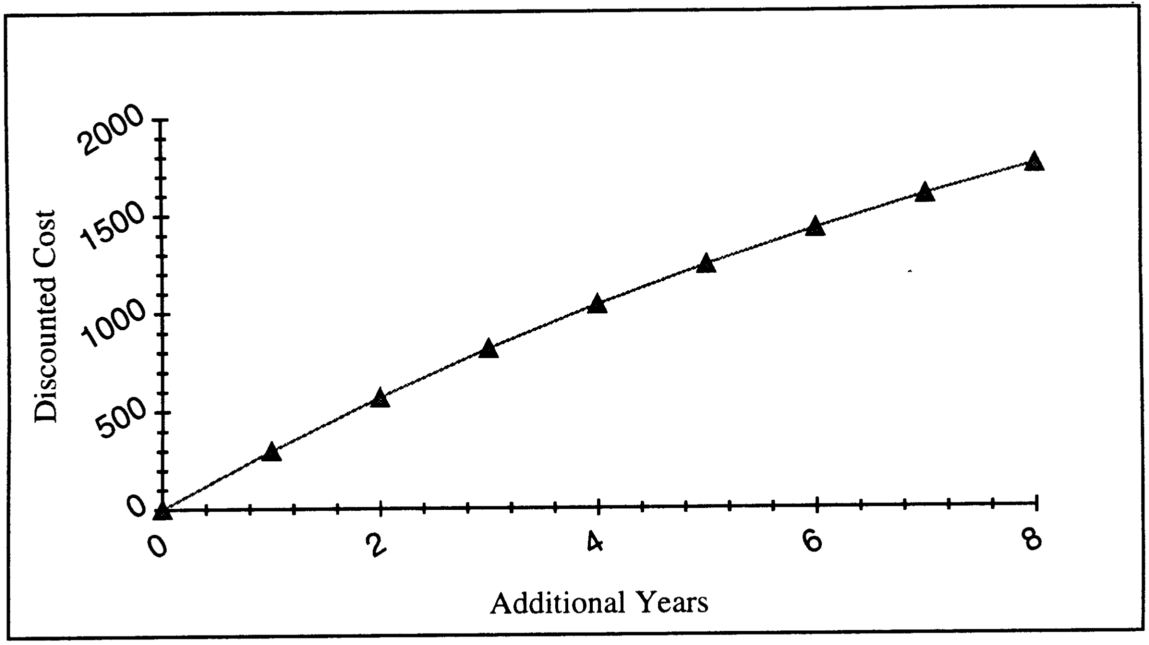

Figure 9-10: Discounted Cost of Additional Years of Flight Operations

system would cost 4.7 $M.

Because the liquid upper stage provides a higher overall C_3, and hence shorter flight time, it may be possible for the total cost of the mission to be less for a spacecraft using a liquid upper stage than a spacecraft with a solid upper stage. The saving comes from the reduced cost of the flight operations. Figure 9-10 shows the cost of each additional year of flight operations, discounted back to the date of launch. It is based on a 6 man year manpower requirement and a 8 year nominal flight time. As can be seen, because of the discounting of costs, the provision of a shorter flight time can not be justified by the decreased cost of operations support.

The use of a single Star 30E solid rocket motor will cost less than $ 1 million and cause the spacecraft to arrive within 9 years of launch. Using a single solid is attractive in order to keep the system simple. The Star 30E provides the maximum C_3 of all the single stages configurations considered and has therefore been baselined as the upper stage.

9.9.5 Upper Stage Guidance

The control of the upper stage during orbital injection can be either from a set of dedicated electronics which are connected to the motor or the onboard AOCS system can double as the guidance electronics. The natural choice is to use the onboard electronics and sensor systems. Given that the spacecraft has a very accurate control system this should be more than satisfactory. The one remaining question is whether the spacecraft has enough control authority to ensure the ΔV is applied in the correct direction.

For the present, it will be assumed that the spacecraft's roll thrusters have enough authority. In addition, any misalignment of the thrust vector can be recovered using the onboard propulsion system, that is necessary to carry out the mid-course guidance maneuvers. The next phase of the design effort should examine this issue in detail.

9.9.6 Launch System Summary

Table 9.27 presents a summary of the proposed launch system and upper stage.

9.10 Propulsion Subsystem

9.10.1 Introduction

The onboard propulsion system is required to execute mid-course guidance maneuvers to correct for any initial misalignment of the thrust vector from the solid rocket motors, and fine guidance to ensure the correct rendezvous of the spacecraft with Pluto.

Item		Comment
Launch Vehicle	Titan IV Centaur	
Upper Stage	Star 30 E	
Total C_3	249 km^2/Sec^2	
Transfer Time	9 years	9 day launch window
Launcher Cost	227 $ M	[18]
Upper Stage Cost	1 $ M	Mass estimate

Table 9.27: Propulsions Subsystem Characteristics

9.10.2 Requirements

The requirements for the propulsion system are that the fuel used must be storable for a long duration, as the mid-course correction burns will not occur until several years into the flight of the craft.

An initial allocation of 400 m/s of ΔV is required from the subsystem [36]. This number will be refined in later stages of the design, and is dependent on the expected launch vehicle and upper stage injection accuracy which are currently TBD. The spacecraft is expected to execute four mid-course guidance maneuvers, each with a ΔV requirement of 100 m/s.

9.10.3 Fuel Options

Table 9.28 lists the various fuels available for the PFF mission along with typical Isp, thrust levels, and the mass of fuel required to impart a ΔV of 400 m/s on a 60.3 kg dry mass spacecraft.

Propellant	Isp Sec	Thrust Level N	Propellant Mass kg	Comment
Cold Gas	50	0.05-200	76	
Hydrogen Peroxide	200	0.05-5	13.6	
N_2H_4	200	0.05-5	13.6	
H_2&O_2	450	5-1000	5.7	Not storable
N_2O_4&MMH	320	5 - 1000	8.2	
Hybrid	255	50-75,000	10.5	Not Well Developed

Table 9.28: Estimated Titan IV Payload Mass vs C_3

Electric Propulsion Systems

Most electric propulsion systems use power from the spacecraft bus to increase the potential energy of the propellant. The working fluid's potential energy is then converted to kinetic energy using a conventional rocket nozzle. Ion engines are the one exception to this where the electrical power is converted directly into kinetic energy of the working fluid.

The power required from the electrical power system is given by:

$$P = \frac{F I_{sp} g}{2\eta}$$

where F is the thrust level and η is the thruster's conversion efficiency. The power required can be converted into additional dry mass of the spacecraft by recognising that the power system weight is approximately 0.2 kg/W. Let us assume a value of η of 0.9. This corresponds to a typical Resistojet efficiency [38]. Using this information, it is possible to ask what thrust level an electric thruster provides for the same wet

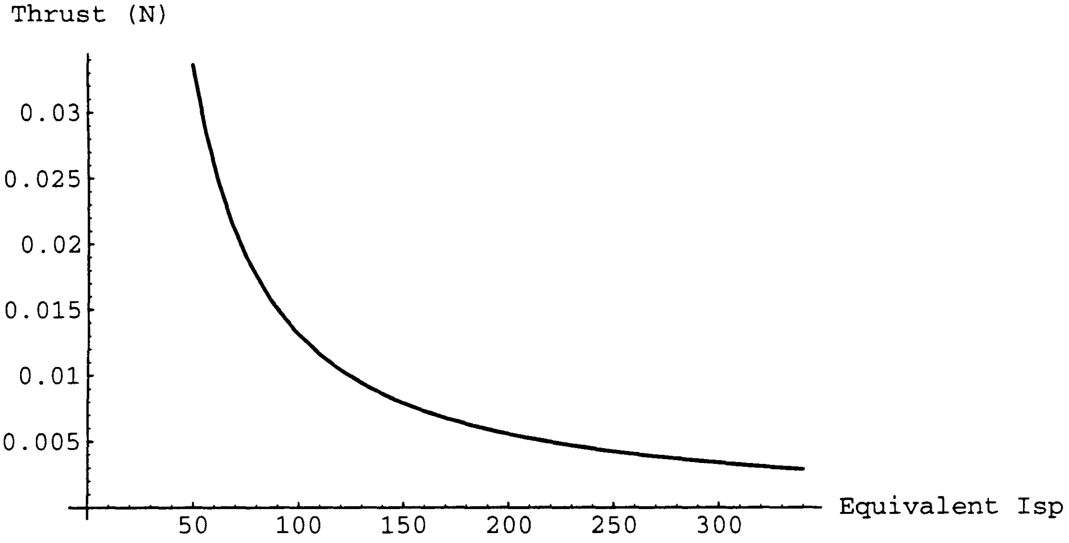

Figure 9-11: Variation in thrust against equivalent non-augmented Isp

mass, and ΔV requirement. Figure 9-11 shows the relationship between thrust level and equivalent non-augmented Isp for a electric thruster with an Isp of 2000 seconds.

The amount of fuel required for a given ΔV is given by:

$$m_p = m_f \left[e^{\frac{\Delta V}{I_{sp} g}} - 1 \right]$$

The mass flow rate through the thruster is given by:

$$\dot{m} = \frac{F}{I_{sp} g}$$

Thus the length of the thruster burn is given by:

$$t = \frac{m_f I_{sp} g}{F} \left[e^{\frac{\Delta V}{I_{sp} g}} - 1 \right]$$

Thus, for a 0.005 N electric propulsion system with a Isp of 2000 seconds, a 100 m/s ΔV requires 14 days. A non-augmented propulsion system with only an Isp of 220 seconds would have no mass penalty associated with it, compared to the electrical propulsion system, but could produce a thrust of greater than 5 N. This would then only require a burn lasting 21 minutes. One of the current limiting factors of electrical propulsion systems is that the lifetime of the thrusters is extremely limited. Setting aside any considerations of technical maturity, it is safe to conclude that an electric propulsion system is unlikely to provide a suitable propulsion system when compared to non-augmented systems.

9.10.4 Propulsion System Selection

The selection criteria for the propulsion system is to select a fuel that minimises the weight of the spacecraft, is well-developed and is storable. Using table 9.28, the natural choice is therefore a bi-propellant system, using either N_2O_4 and MMH or N_2H_4 and UDMH.

9.10.5 Blow Down or Regulated System

The choice of whether to use a blow down or regulated systems will be left to a lower level trade, and is therefore TBD.

9.10.6 Propulsion Tankage and Equipment Masses

The typical mass of a small 5 N thruster is 0.1 kg [38]. Because the spacecraft is based around the use of a large lens structure, it is not possible to place a single thruster along the axis of the spacecraft. Therefore multiple thrusters will be required around the rim of the bus. Therefore the PFF spacecraft will require either 3 or 4 thrusters. As an initial estimate 3 such thrusters are baselined to be placed 120 degrees apart around the rim of the bus structure.

The spacecraft will be fitted with a series of isolation valves rather than check valves. This requirement is a result of the inquiry into the loss of the Mars Observer. An allocation of 0.5 kg is made to allow for the filters, fill and drain valves, and isolation valves required by the system.

Liquid propulsion systems are typically 85 to 93 % propellant by mass [46]. Therefore because the system is relatively small let us assume a value of 85%. This equates to a tank mass of approximately 1.5 kg. Because of the configuration of the spacecraft an additional allowance for pipeage of 0.01 kg/m is added.

9.10.7 Mid-Course Guidance Procedure

The mid-course correction instructions will be computed on the ground before unloading to the spacecraft as time-tagged data. At the appropriate time the spacecraft will reorient its major axis in the direction of the desired ΔV. The spacecraft can now either spin up so as to be spin-stabilised for the burn or maintain a 3-Axis pointing control. The selection between these two is not considered a critical issue at the current time and is therefore left as TBD. The selection of the stabilisation during mid-course burns is likely to be dependent on the required actuator control torques to control thruster misalignment. Once the desired pointing and stabilisation has been achieved, the burn sequence will be executed for the precomputed duration. Once the burn has been successfully executed the spacecraft will return to 3-Axis stabilised Earth pointing to conduct a ranging test to establish the new orbit.

9.10.8 Risk

The technology behind the proposed propulsion system is well established, and therefore the subsystem is considered to have minimal technological and programmatical

Item		Comment
ΔV	400 m/s	
Propellant	N_2O_4 and MMH	
Engine Thrust	5 N	
Isp	320 Sec	
Propellant Mass	8.2 kg	
Number of Thrusters	3	120 degree spaced
Stabilisation	Spin	during course correction only
Dry Mass	2.4 kg	
Power Requirement	3 W	Required for valve activation
Cost	\$ 1.29 Million	

Table 9.29: Propulsion Subsystem Characteristics

risk.

9.10.9 Cost

The cost of the propulsion system is based on the use of the cost model for the attitude and reaction control, via the following relationship:

$$\text{Cost} = 935 + 153X - 364 + 186X^{0.73}$$

This gives an estimated cost for the propulsion system of \$ 1.29 Million.

9.10.10 Propulsion Subsystem Summary

Table 9.29 presents a summary of the propulsion subsystem for the PFF mission.

9.11 Communications Subsystem

9.11.1 Introduction

The communications subsystem provides the link between the Earth and the spacecraft. Its tasks are to pass instructions from the controllers to the spacecraft's CDMS and to relay onboard status and instrument measurements back to the Earth.

9.11.2 Requirements

The communications system has the least defined requirements of all the subsystems. We can say that it must transmit all the information generated by the spacecraft with a Bit Error Rate (BER) of less than 10^{-6}. However the data rate at which this must be achieved is not specified. The only requirement is that the ground network will not be occupied for a large period of time, and therefore it should not be too low.

The ground based station can be assumed to be the Deep Space Network (DSN). We can assume this because it is the primary network used for all deep space missions and provides the maximum antenna gains available.

9.11.3 Communications Architecture

The communications architecture is a simple point to point design. However, because of the rotation of the Earth and the long communications time, the Earth-based network will require multiple ground stations. This is part of the service provided by the DSN.

9.11.4 Operating Frequency

The ground station network chosen for operation with the PFF mission is the Deep Space Network. This limits the frequencies available to the spacecraft to the following:

- L Band (1.668 GHz)
- S Band (2.295 GHz)
- X Band (8.420 GHz)
- Ka Band (32.00 GHz)

Frequency Selection Criteria

The optimum selection criteria for selecting the frequency would yield the lightest equipment while providing a reasonable transmission data rate. However, to simplify the process, the selection criteria that will be used is the one that provides the highest return data rate. The higher data rate is attractive as it limits the amount of time for the communications network to return the data. This is particularly important for the PFF because of the low data rates and the large quantity of the image data to be retrieved.

L Band

The L band system would utilise the 70 m DSN subnetwork[21]. This is the largest set of antennas available. However because of the low frequency the gain available from the antenna is only 60.2 dBi. However this band does have the advantage of low atmospheric interference and low attenuation. A full link budget for the down link is shown in Appendix D. The DSN does not support L band uplinks.

S Band

The S band like the L band can utilise the 70 m subnetwork. This provides a gain of 63.34 dBi. The 34 m network can also be used as a backup, however the available gain is only 56.9 dBi. This option of a second network is attractive as it would ensure that if one of the networks is unavailable for either technical or organisational reasons, then a backup set of antennas would be available. Again at S band the atmospheric effects are relatively small.

X Band

The X band link like the S band can use either the 70 m or the 34 m subnetworks.

Ka Band

Ka band links are only available from the 34 m subnetwork. The disadvantage of using Ka band is the high value of the rain attenuation. However, because of the sighting of the receiving antenna, the maximum weather-induced attenuation is only 0.46 dB, and a 27.9 K effect on the system noise temperature. A second advantage of using Ka band is that the electronics on the spacecraft scale with frequency and thus the electronics associated with the RF chain are both smaller and lighter at Ka band, when compared to those at the other frequencies proposed.

Frequency Selection

The available down link data rate are summarised in table 9.30. Also shown in the table is the time taken to transmit 1 Gbyte of data.

As can be seen, the use of L and S band is not really practical. Thus only X and Ka band are appropriate. The preferred system is the Ka band as this will provide

Frequency Band	Data Rate Bit/sec	Transmit Time
L Band	19	14.3 years
S Band	72	3.8 years
X Band	120	200 days
Ka Band	260	382 days

Table 9.30: Maximum data return rates

a lower equipment mass. However X band should not be ruled out at this point in time[13].

9.11.5 Optical Communications

The use of higher frequencies into the visible band are very attractive for spacecraft communications because of the high bandwidths and large antenna gains available for a given physical antenna size. There are currently plans for the DSN to include optical communications capabilities. However, these are unlikely to be available in the time frame of the PFF mission[26]. To overcome this problem, the PFF could be designed to use RF for close to Earth communications and then to transfer to optical communications when the spacecraft is far enough away, provided that the ground based antennas will have been constructed. For this to be a practical approach it would be necessary to guarantee that the ground based network would be complete. Given the technical problems that still have to be solved, the large expense of such a network, particularly in the current era of tight budget constraints on NASA, this must be considered a high risk option, and has therefore been excluded from further consideration.

---

[13] This is a good example of where the trade tree is pruned rather than a single design selected

9.11.6 Main Antenna

The main spacecraft antenna provides the primary gain for the communications subsystem.

There are three main types of antenna used by spacecraft [17]:

1. Parabolic Reflector
2. RF Lens Antenna
3. Phased Array

Phased Array

Structurally a phased array would appear roughly as a flat plane, with a number of small feed elements covering the surface. The advantage of phased arrays is that they can be electronically pointed, though in the PFF this is not a function that is particularly important.

Ka band frequencies cannot currently be used with a phased array because of the problems associated with building the feed elements. Ground-based military systems do use Ka band phased arrays. However, they use individual feed horns for each element and therefore the mass would be prohibitive for space applications.

There are two ways in which we can build the array. One is to use distributed amplifiers, where each feed element of the array has its own amplifier. However the problem with this type of design is that because of the low power being transmitted (3 W), the size of the amplifiers is likely to be small and thus the boxes and wiring harness associated with each amplifier are likely to present a high mass penalty. This type of arrangement is normally only considered for high power applications. The alternative is to generate the transmit beam via a single amplifier, and then to divide this out to the different elements. The problem with this type of architecture is the losses in the splitters and phase shifters required to ensure that the beam is properly focused.

Lens Antenna

The lens antenna requires a series of varying length waveguide sections to shift the phase of the beam.

For a simple lens the length of an individual element is given by

$$d = d_0 + \frac{r^2}{2F(1-\eta)}$$

where d_0 is the length of the central element of the lens, F is the focal length and r is the radius of the elements from the centre of the lens, and

$$\eta = \left[1 - \left(\frac{\lambda}{\lambda_c}\right)^2\right]^{\frac{1}{2}}$$

The bandwidth of the lens is given by:

$$\text{Bandwidth} \simeq \frac{200\eta(F/D)}{(1+\eta)(D/\lambda)}\text{Percent}$$

To keep the lens as narrow as possible then we want to make λ as close as possible to λ_c. If we assume that the maximum data rate the antenna must support is 2000 bits/second, the required bandwidth as a percentage is $24 \times 10^{-6}\%$ at X band. Thus let us assume a requirement of 0.001 %. Rearranging the equation for the bandwidth we have:

$$\eta \simeq \frac{\text{Bandwidth}}{\frac{200F\lambda}{D^2} - \text{Bandwidth}}$$

If we assume a focal length of 1 meter, then at X band η is 0.00032, and 0.0012 at Ka band. This equates to a max d of $d_0 + 1.25$ m. Because of the very low value of η the thickness of the lens is almost independent of the frequency.

Zoned Waveguide Lens

To achieve a minimum weight waveguide lens, the lens needs to be built using the concepts of lens zoning [32]. The idea behind the lens zoning is that when the length of the lens exceeds a multiple of the waveguide wavelength, then the induced phase shift can be produced by a shorter length of waveguide.

The zoning length, that is the length of waveguide, that introduces a phase shift of 2π is given by:

$$d_\lambda = \frac{\lambda}{(1-\eta)}$$

Therefore, again due to the low values of η, the maximum required length of waveguide is λ. Hence, the maximum waveguide element's thickness is $d_0 + \lambda$. Let us therefore assume that the average thickness of the lens is $d_0 + \lambda/2$. The only question remaining is what is the minimum thickness of the lens that will allow the lens to retain its structural integrity.

If we treat the lens as a doubly-curved shell then the theoretical buckling stress is given by:

$$\sigma_{cr} = 0.6\gamma\frac{Et}{R}$$

where γ is a correction factor and is given by:

$$\phi = \frac{1}{16}\sqrt{\frac{R}{t}}$$

$$\gamma = 1.0 - 0.901(1.0 - e^{-\phi})$$

The maximum stress must be at the edge of the disk, thus we can assume that the induced stress is given by:

$$\sigma = \frac{Mg}{2\pi Rt}$$

If we assume that the maximum acceleration is 5g, and R is 1.5 m, then all that remains to be calculated is the mass, as a function of the thickness. If we model the lens as a sheet with a given fill factor, then the sheet's mass can be modeled as:

$$M = f\pi R^2 t\rho$$

This is convenient as now the induced stress is independent of the thickness. Inserting a thickness of 5 mm then we find that the induced stress is 1.8 $\mathrm{KN/m^2}$ assuming a 17% fill factor, and the critical stress is 9.9×10^6 $\mathrm{N/m^2}$ giving us a large safety margin. The average thickness is therefore 0.023 m at X band and 0.009 m at Ka band. Using the formulas established in Appendix F, the X band lens should weigh 42 kg, while the Ka band would weigh 49.4 kg. This assumes that aluminium is used. Ideally it would be nice to build this out of composite. However it is difficult to see how this could be done easily. Typically composite is used as face sheets, where the material is in the form of long sheets. For the lens the maximum length is into the material.

Manufacturing the lens

The lens antenna could be made a number of ways. The most obvious is to manufacture the lens by bonding a set of waveguides together[14]. The alternative is to form a solid sheet, then etch out the waveguides, possibly using spark erosion to ensure an accurate sizing of the guides.

Parabolic Reflector

The parabolic reflector is the most common of the large antenna designs used in spacecraft applications. It has the advantage of being very simple and light weight. These designs can be either centrally or offset fed. For the PFF we need only consider the centrally-fed design.

There are two possible arrangements for the feed structure. Either the main reflector can be fed directly by a feed horn placed at the focus, or the main reflector can be fed from a sub reflector placed at the focal point, which is in turn fed by a feed horn at the centre of the main reflector. The latter is the classical cassegrain design. Either alternative is suitable for this application, and needs further detailed study. For the current we will assume that the antenna is directly fed.

Reflector Mass

The shape of the reflector is described by [6]:

$$r = \frac{2F}{1+\cos\theta}$$

Integrating this with respect to θ ,the surface area of the parabola can be computed [37, page 653] as

---

[14] Rather than use either circular or rectangular waveguide, it would be preferred to use hexagonal waveguide as this will give a better packing structure. The form of the electromagnetic waves in such a structure would be an interesting mathematical problem.

$$S = \int_0^{\phi} 2\pi r \sin\theta \sqrt{r^2 + \left(\frac{dr}{d\theta}\right)^2}\, d\theta$$

$$S = \int_0^{\phi} \frac{2\pi F \sin\theta}{1+\cos\theta} \sqrt{\frac{4F^2}{(1+\cos\theta)^2} + \frac{2F\sin\theta}{(1+\cos\theta)^2}} d\theta$$

$$S = \frac{8F^2\pi}{3}\left(\frac{1}{\cos^3\frac{\phi}{2}} - 1\right)$$

where ϕ is the value of θ that gives the required antenna diameter. Assuming that the antenna has a focal length of 1 m and a 1.5 m diameter requiring $\phi = 73.74$ deg, the antenna has a surface area of 8 m^2.

Let us assume that the reflector is manufactured as a honeycomb panel with carbon fiber epoxy face skins using four ply face skins. Let us further assume that the face sheet is 1 mm thick, giving a face skin volume of $0.032m^3$. The density of a graphite epoxy sheet is 1620 kg/m^3; the face sheets will therefore weigh 26 kg. An aluminium honeycomb normally has a density of 80 kg/m^3 [46, Page 453]. Thus if we assume an approximately 2 inch (5 cm) thick panel, the honeycomb weights 32 kg, giving the antenna a total mass of 58 kg. If we increase the antenna focal length to 2 m, by utilising a sub-reflector in a cassegrain configuration, then the mass of the main reflector is reduced to 53 kg, though the mass of the sub reflector must be added. The variation of reflector surface area against diameter for 0.5, 1 and 2 m focal lengths is shown if figure 9-12.

Antenna Selection

The selected antenna design is the Lens design due to its lower weight. However this needs to be tempered against the structural mass of the spacecraft which must be added to the lens design to support the electronics. The reverse side of the reflector antenna would act as the main spacecraft mounting surface.

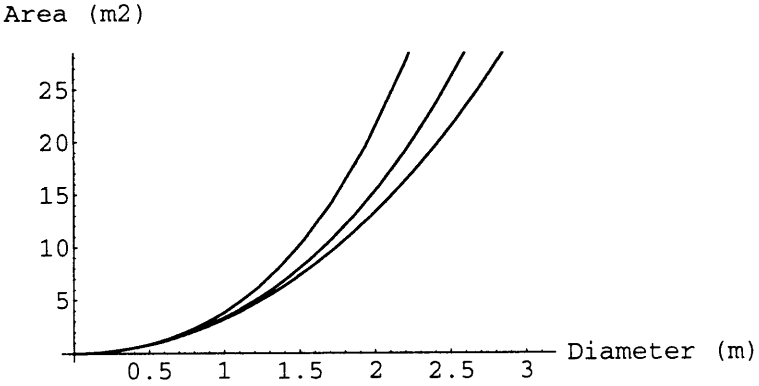

Figure 9-12: Reflector Area versus diameter for 0.5, 1 and 2 m focal lengths

Total Antenna Mass

The rest of the mass of the antenna structure must be added to the mass of the lens. The feed horn, support struts, and mounting attachments are important considerations.

For the horn we can assume a mass of approximately 1.5 kg, scaling a C band horn. Each strut must be 1.8 m long, and assuming they are 3 cm diameter, 1 mm thick composite tubes, each will weigh 0.3 kg each. The waveguide feed will be approximately 20 mm by 10 mm, using 1mm thick walls and a length of 2 m for a mass of 0.7 kg. Thus the total antenna mass is approximately 52.5 kg at Ka band, when attachments are included.

9.11.7 Communication Hardware Architecture

The communications architecture of this type of spacecraft is very simple and has a conventional block diagram. Figure 9-13 shows the proposed block diagram.

The blocks making up the communication subsystem electronics are:

- Low Noise Amplifier (LNA)
- Diplexor
- High Power Amplifier (HPA)
- Modulator
- Demodulator

Diplexor

The diplexor (which is a simple low and high pass filter) separates out the receive and transmit frequencies. A mass of 0.5 kg is assumed for this unit.

HPA

The high power amplifier takes the output of the modulator and amplifies it up to the correct transmit power. The output of this device is currently proposed as 3 W. There are two choices of technology: the Traveling Wave Tube Amplifier (TWTA) or the Solid State Power Amplifiers (SSPA). The SSPA is the preferred choice for the PFF as it provides a high level of reliability and a low mass when compared to a TWTA. The disadvantage of the SSPA is its relatively low efficiency of 25% at X band and 15% at Ka band, as compared to the typical TWTA's efficiency of 50%. SSPAs for Ka band are available up to 10 W. The estimated mass of each SSPA is 1.2 kg.

Modulator

The modulator converts the data stream from the OBC into a RF representation of the data and introduces error correction coding. As a base line, BPSK modulation is

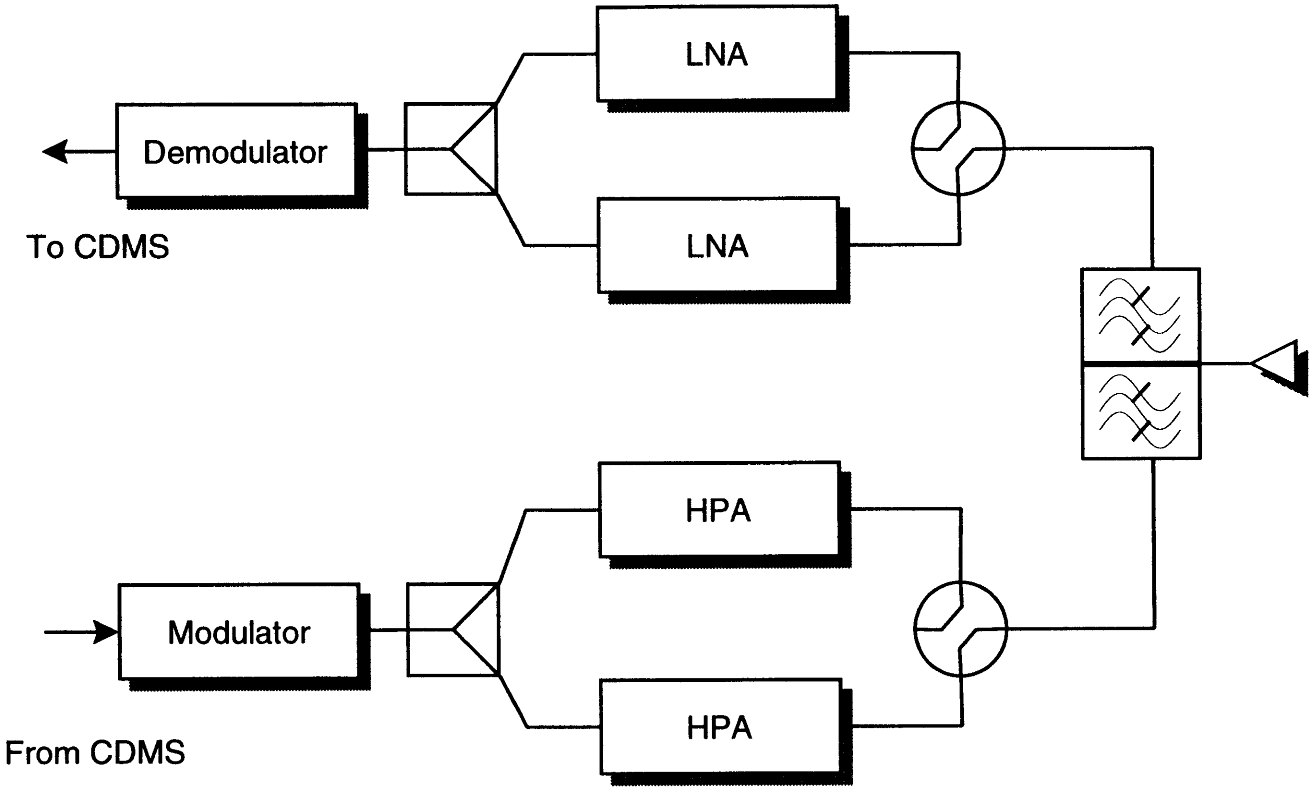
LNA
Demodulator
To CDMS
LNA
HPA
Modulator
From CDMS
HPA

Figure 9-13: Communications Subsystem Hardware Architecture

chosen with a Reed-Solomon(255,223) code convoluted with a long constraint length convolutional (7,1/2) code. This gives a required Eb/No of 2.6 dB at the required BER [21].

The Modulator must also accept from the demodulator the ranging tone loop back, such that the ranging tone can be inserted into the return carrier. The modulator must therefore interface with the SSPA, the OBC and the demodulator. The output of the modulator should be compatible with driving the SSPA at maximum output.

Demodulator

The demodulator takes the RF input and demodulates it. It then decodes the data stream and passes it to the OBC. The demodulator also extracts the ranging tone and passes the tone to the modulator for insertion onto the return link. The uplink utilises an RS(255,223) block code to improve the link performance and requires a Eb/No of 6.4 dB for a 10^{-6} BER [21].

LNA

The LNA is the first stage in the receive chain and provides the primary amplification; it dominates the signal to noise ratio in the rest of the receiver. A noise figure of approximately 1.6 dB should be achievable for the PFF LNA [30].

Equipment mass

The Modulator, Demodulator and LNA are often built as a single unit and the combined weight is estimated as 1.5 kg requiring 12 W. The RF switch required to interface to the SSPA is assumed to weigh 0.2 kg and an allowance of 0.2 kg is made for the interconnection cables. The antenna feed waveguide is included in the mass of the antenna.

9.11.8 Cost

Using the standard parametric cost model, the cost of the communications electronics can be calculated from:

$$\text{Cost}_{\text{electronics}} = 2346 + 239X + 112 + 197X^{0.93}$$

A factor of 1.2 has been added to this calculation to cover the use of Ka band equipment. The equivalent equation for the cost of the antenna is:

$$\text{Cost}_{\text{antenna}} = 1523X^{0.59} + 30.0 + 345X^{0.59}$$

A factor of 1.5 has been added to this calculation to account for the fact that a lens based design is to be used. As noted earlier this is a deviation from the normal use of such a system. In both of the above equations, X represents the mass of the equipment. The total cost of the communications subsystem is estimated as \$ 23.81 million.

9.11.9 Risk

The electronics for the communication subsystem are considered a moderate risk element of the design since they are based upon well established designs. The largest risk for the communications subsystem is the lens antenna. This type of antenna has been used in space on previous missions, but normally for multibeam antennas rather than the single narrow beam system proposed here. Because it has been used before, the technical risk can be considered moderate. For similar reasons, the programmatic risk is also considered moderate. Because of these risks the estimated cost for this element of the subsystem includes a large multiplication factor. Note if the development of the lens becomes an unacceptable risk during the program, then

Item		Comment
Electronics Mass	4.8 kg	
Antenna Design	Lens Antenna	
Transmit Power	3 W	
LNA Noise Figure	1.6	
Antenna Diameter	1.5 m	
Antenna Beamwidth	0.43 Deg	at Ka Band
Antenna Mass	52.5 kg	
Polarization	Circular	
Power Requirement	24 W	
Cost	$ 23.81 Million	

Table 9.31: Communications Subsystem Summary

the lens can be replaced with a parabolic reflector, if the ring bus design is preserved. The instruments however would have to be mounted facing in the opposite direction, to account for the reversed feed direction, and therefore flight direction.

9.11.10 Communication Subsystem Summary

The performance characteristics of the Communications subsystem are summarised in table 9.31.

9.12 Support Structure

9.12.1 Introduction

The support structure provides the mounting points for the instruments, electronics and other units of the various subsystems. The structure provides the primary path for distributing loads around the spacecraft and it also acts as the attachment point for the launcher interface.

9.12.2 Requirements

The maximum acceleration of a Titan IV is +3.3, -6.5 g axial and 1.5 g lateral [18]. A Star 30E solid rocket motor has a peak thrust of 40,990 N and an average thrust of 35,185 N. The mass of the PFF and Star motor casing is 100.3 kg. Assuming the Star motor at burnout is generating its average thrust level, the maximum acceleration[15] of the spacecraft is 35.8 g. This is likely to be a critical design driver for the equipment design[16]. Note that because of the high thrust levels, it is unlikely that the AOCS system will have enough control authority to control the upper stage during orbital insertion; therefore the spacecraft should be spin stabilised during this phase of the mission.

9.12.3 Structure Concept

The concept proposed for the PFF is that the edge of the main mission antenna act as the interface attachment point. The launcher interface adapter ring must therefore be sized such that it is the same diameter as the main antenna. The spacecraft is then launched nose down.

---

[15] For this to be true the motor must generate maximum thrust when more than 3% of its fuel remains.

[16] JPL have a similar problem with an estimated acceleration of 20 g at thruster burn out.

As noted earlier there are two types of antenna proposed, a lens antenna and a parabolic reflector. Consider the parabolic reflector first. When inverted the reflector appears very much like a dome or 3D arch. Since this is a very good load-bearing structure, it is proposed that the main antenna form the structural surface. Thus, the electronic packages would be mounted to the back of the antenna. This necessitates that the structure be slightly stronger than normally required, but this is not anticipated to be a problem.

The lens antenna obviously cannot be used in the same way as the reflector; however, the edge of the antenna can be utilised. It is proposed to build a ring around the edge of the lens. The ring then acts as a structural stiffener for the lens and, in appearance, would resemble the classical thrust cylinder utilised as the primary structure by many of today's spacecraft. The preferred design for the main antenna is that of the lens; therefore, only this design will be considered further in this section.

9.12.4 Spacecraft Bus Structure

The main spacecraft structure can be modeled as a simple thrust tube. To minimise the weight of the structure, let us assume that the structure is constructed from carbon fibre composite with an aluminium honeycomb core.

Critical Compression Limit

Using a general instability model for the failure of such a panel, the effective Young's modulus and thickness are given by [1, page 216]:

$$\bar{t} = \frac{\sqrt{12}h}{\sqrt{\frac{E_1 t_1}{E_2 t_2}} + \sqrt{\frac{E_2 t_2}{E_1 t_1}}}$$

$$\bar{E} = \frac{E_1 t_1 + E_2 t_2}{\bar{t}}$$

The critical buckling stress is then given by:

$$P_c = 1.2\gamma\pi\bar{E}\bar{t}^2$$

where

$$\gamma = 1 - 0.9\left(1 - e^{-\phi}\right)$$

and

$$\phi = \frac{1}{16}\sqrt{\frac{r}{\bar{t}}}$$

with r as the radius of the shell and σ_c as the critical buckling stress.

The thrust tube must be able to withstand a load of $60.3 \times 35.8 \times 9.81 = 21.2$ KN. If the structure is constructed from 1 mm thick face skins with a 1 cm honeycomb, the critical load will be 6245.8 KN, giving a safety factor of nearly 300.

Critical Bending Moment

Let us assume that the equipment has its centre of gravity 10 cm out from the bus. The imposed moment on the spacecraft is then

$$M = 60.3 \times 6.5 \times 9.81 \times 1.6 = 6.2 \text{ KNm}$$

$$M_c = 0.6\gamma\pi\bar{E}r\bar{t}^2$$

Using the above dimensions the critical moment is 4.8×10^6 Nm, giving a safety margin in excess of 750.

Bus Mass

The density of the face sheets is 1490kg/m^3 [1, page 245]. The density of the aluminium core is 80kg/m^3 [46, Fig 11-40]. Assuming the bus is 0.5 m high, the bus will have a mass of 17.9 kg. The largest part of this mass is the face skins. For comparison a 3 mm thick solid aluminium structure would also be capable of supporting the desired launch loads with a reduced safety margin. The equivalent aluminium structure would have a mass of 39.6 kg.

9.12.5 Launcher Interface Attachment

The support structure must include an adapter ring to join the launch vehicle, injection motors and spacecraft together.

Two possible concepts for the launch adapter are proposed.

1. Two conical thrust tubes.
2. Two rod based cones.

The two concepts are shown graphically in figures 9-14 and 9-15.

Assumptions

In order to design the upper stage support and launch adapter, several assumptions must be made. The first assumption is that the mechanical interface diameter of the Centaur upper stage is assumed to be the same as the ORBUS 21 used on the Titan III [18], 2.311 m. The Star 30E motor has a diameter of 0.762 m and a length of

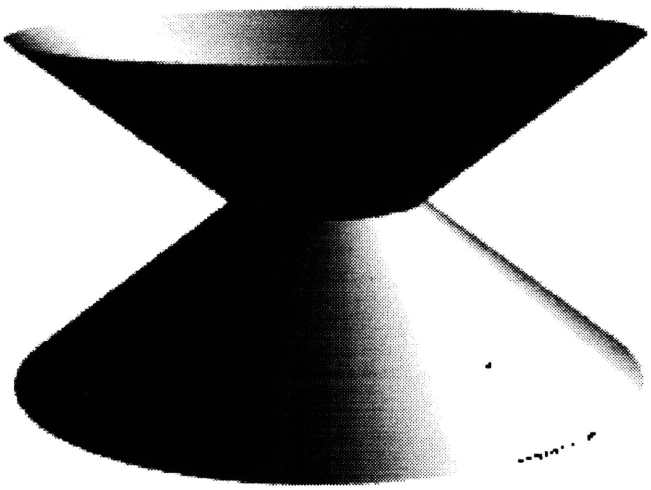

Figure 9-14: Conic shell launch interface and upper stage support

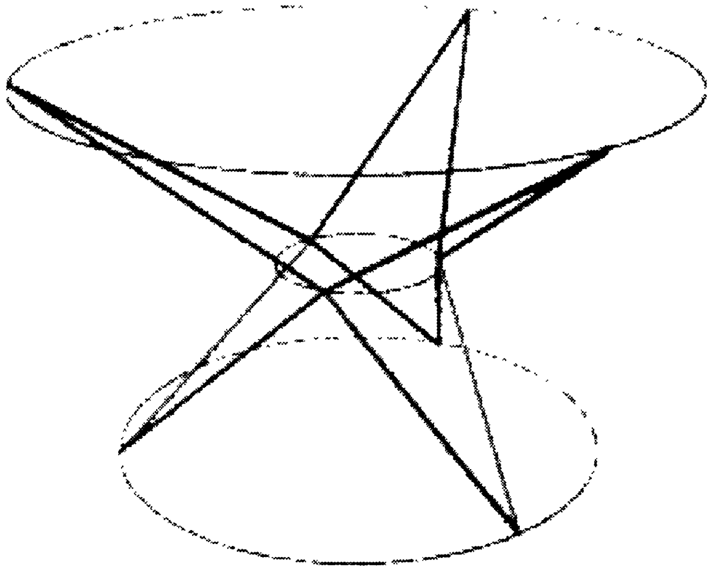

Figure 9-15: Truss based launch interface and upper stage support

1.683 m. The attachment ring of the Star motor is assumed to be at the mid-point of the motor.

Thrust Cone

A thrust cone can be modeled as an equivalent cylinder [1], using:

$$r_e = \frac{r_{min}}{\cos\alpha}$$

where r_{min} is the Star motor diameter for both of the cones. The cone angle (α) is 51.2 degrees for the upper cone and 52.5 degrees for the lower cone. This gives an effective radius of 0.608 m and 0.626 m, respectively. If the shell is constructed using a composite honeycomb with 1 mm thick face skins and 10 mm thick honeycomb, the thrust cones will withstand forces in excess of 7.7 MN. Such a design provides a safety factor of greater than 350 and 150 for the lower and upper cones, respectively. The mass of the upper cone is 20.2 kg, while the lower cone would have a mass of 20.8 kg. Additionally the mass allowance for pyrotechnical separation mechanisms and fastenings must be added; a total mass of 5 kg is allowed. Thus the total launch support mass is 46 kg.

Thrust Rods System

Assume that 6 rods, each 1.62 m long, are used on each level. The support rods on the upper level are inclined to the vertical by 56.3 degrees. Therefore each rod must sustain a force of 6.4 KN.

The critical buckling load of a column is given by:

$$P_{cr} = \frac{\pi^3 E r^4}{4L^2}$$

Therefore, if each rod is 30 mm in diameter then the critical buckling load is 34 KN, giving an overall safety factor of 10. Each rod would weigh 3.2 kg. The mass of the interface attachments must be added. Let us assume that the motor, launcher and spacecraft simply require mounting brackets, rather than a ring structure as shown in figure 9-15, allowing the equivalent of a solid cube of aluminium of 50 mm on a side for each mounting with its associated pyro mechanism. The total mass of the launch support system would be 41.6 kg.

This type of design has the advantage over the cone system of a simpler separation mechanism, requiring the firing of only 3 bolts per separation plane.

Launch Support Structure Selection

The choice of a launch support configuration is difficult because of the similarities of their estimated mass. At this level of the trade study it is therefore unwise to make a choice. For purposes of a baseline design the rod-based design is chosen; however, a mass allowance of 45 kg is proposed. One particular concern of the rod-based system is the effect of torsional loads on the structure and the attachment mechanism. Both of these considerations would require detailed analysis in the next level of the design iteration.

9.12.6 Risk

The support systems proposed for the PFF spacecraft are extremely simple and can be well approximated by simple analytical models. The support system is therefore considered to present no technical risk. The use of composite materials for the structure is a relatively new technique for the American space engineering community and so there is the possibility of some schedule risk. However, these technologies have begun to be used for commercial satellites and are well established in Europe. It is therefore believed that this risk can be ignored.

9.12.7 Cost

The cost of the spacecraft's structure and the launch interface support structure can be calculated using the following parametric equation, based on the mass of the structure:

$$\text{Cost} = 3300 + 520X^{0.66} + 172X^{0.65}$$

This equation includes a factor of 1.25 in the development and test phase and 2.0 in the production costs to account for the use of composite materials. This results in a total estimated cost for the spacecraft bus and launch support system of $ 13.46 million.

9.12.8 Support Structure Summary

A summary of the support structure is presented in table 9.32.

9.13 Thermal Control Subsystem

9.13.1 Introduction

The thermal control subsystem is responsible for ensuring that the temperature of the spacecraft and its associated electronics is kept within the desired operating range. Thus, the thermal control subsystem must protect the spacecraft from the "cold" of space and the heat of solar radiation. The subsystem must also dissipate any heat generated by the spacecraft's equipment.

Item	Comment
Bus Structure	Thrust cylinder
Bus Material	Composite honeycomb
Bus Mass	17.9 kg
Launch Support	Rod based truss
Support Material	Aluminium rods
Support Mass	41.6 kg
Cost	$ 13.46 million

Table 9.32: Support Structure Characteristics

9.13.2 Requirements and Assumptions

Temperature limits

The typical allowed temperature range for electronic equipment is 0 to 40 deg C [46, Table 11-40]. However, the propulsion subsystem will require a tighter control on the temperature between 7 and 35 deg C. This is to maintain the hydrazine in a usable form.

The IR sensor will require a direct link to a cold surface to ensure that the sensor is at the correct operating temperature of 77 K.

Solar input

The main external thermal input to the spacecraft is the Sun. Thus, the thermal input to the spacecraft varies between wide extremes of 1358 W/m^2 just after launch and 1.5 W/m^2 when the spacecraft arrives at Pluto.

In cruise mode, the main antenna will be pointed at the Earth and as a first approximation it will be the main thermal energy absorbing surface of the spacecraft.

Let us therefore assume that the main mission antenna can be thermally isolated from the spacecraft bus. The only thermal input to the bus will therefore be the electrical power dissipated by the electronics.

This is actually a simplification because at several stages the spacecraft must change its pointing such that it cannot be considered to be effectively Sun pointing. The two main stages at which this occurs is during the flyby of Pluto and during the mid-course guidance maneuvers. At Pluto, the spacecraft must re-orientate so that the instruments are targeted towards the planet. However because of the low solar input at Pluto, the effect on the spacecraft can be ignored at this level of the design activity. The mid-course correction burns are of sufficiently short duration that the impact of the solar radiation will be ignored for the time being. However, full analysis of the thermal control regime during mid-course guidance burns will be required to ensure that the chosen design will maintain the spacecraft within the desired temperature ranges. Similar analysis will be needed during launch and orbital injection, when the spacecraft is close both to the Earth and the Sun. Both these analyses will be left for more detailed studies at a lower level in the design process.

Thermal Dissipation Requirements

In cruise mode, when only the CDMS and AOCS subsystems are active, the spacecraft must dissipate approximately 15 W of thermal energy. However, at Pluto, and during ranging activities, the thermal control subsystem must dissipate 43.8 W[17]. The energy not supplied to the electrical subsystems must be dissipated by the electrical power supply. For dissipation purposes, because of the geometry of the lens based spacecraft, the electronic assemblies will be considered to be always only in view of deep space. See figure 9-16.

---

[17] This is the total power generated by the power subsystem less the power transmitted by the spacecraft as RF energy.

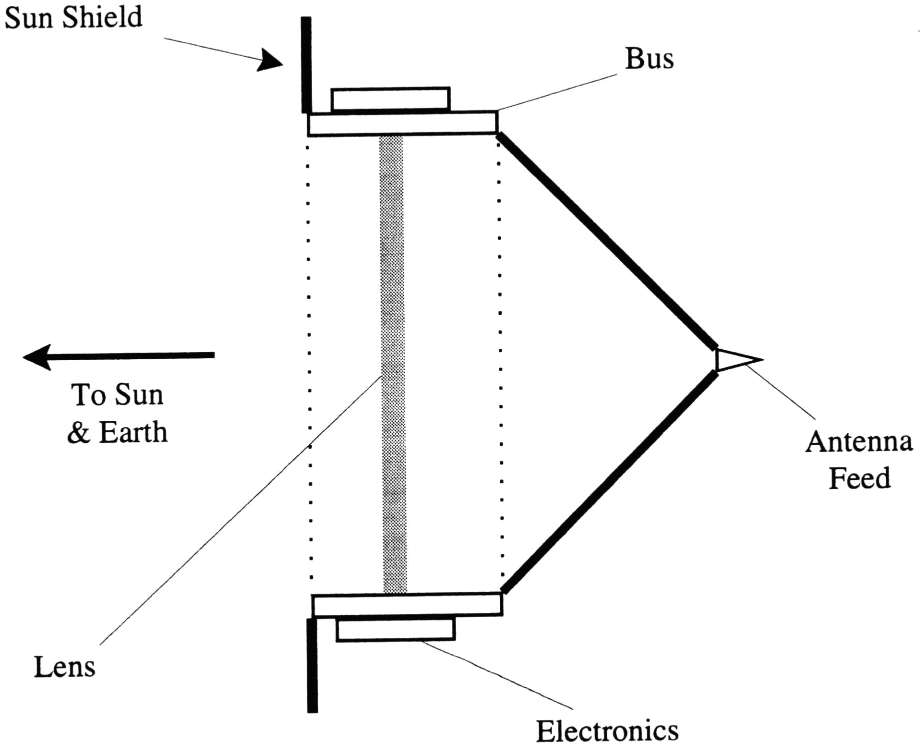
Sun Shield
Bus
To Sun
& Earth
Antenna
Feed
Lens
Electronics

Figure 9-16: Schematic Diagram of the Lens Based Spacecraft in Flight

9.13.3 Thermal Control Concepts

The thermal control concepts that are suitable for the PFF spacecraft are:

- Louvres
- Cold biased heater based system
- Hot biased petia cooling
- Hot biased heat pipe control.

9.13.4 Louvres

A louvre based design would control the system temperature by effectively controlling the thermal emissivity of the surface[18]. The typical thermal dissipation of a louvre system varies between 430 W/m^2 and 54 W/m^2 [46, page 413]. The spacecraft would therefore need an louvre area of 0.1 m^2. Additional power would be required from the spacecraft power subsystem to drive the louvre motors.

9.13.5 Cold Biased System with Heaters

The normal method of thermal control on the propulsion system is to cold bias the system. Thus, if the system were not actively controlled it would cool below the desired temperature. To maintain the system within the temperature limits, electrical heaters are used to heat the subsystem. This concept is very attractive for the PFF spacecraft. If the spacecraft is biased so that the subsystems operate at their optimum temperature when active, the system is cold biased. Then when the subsystem is inactive, the power which would have been drawn by the subsystem can be routed to heaters. This has the additional advantage of minimising the variation of power drawn from the power subsystem. This concept is available to the PFF because it has a constant power source, unlike Earth based spacecraft which must rely on batteries during eclipse operation.

---

[18] It might be interesting to explore whether LCD surfaces could be used for a similar purpose. However, the exploration of this idea is beyond the scope of this thesis

Some additional power must be allocated to each subsystem to allow for the spacecraft to be cold biased. Let us assume that the thermal balance for each subsystem can be achieved to 10% of its power requirement. Then an additional 10% per subsystem is required from the power subsystem. The additional electrical power should allow the spacecraft to maintain the equipment temperatures within the desired range during mid-course correction burns and Pluto flyby.

9.13.6 Hot Biased Petia Cooling

If the subsystems are hot biased using Radio-isotope Heater Units (RHU) then the spacecraft could control the temperature of the subsystem by connecting the equipment to a radiator via a petia cooler. This device can be used as a form of thermal transistor, and thus can be used to control the temperature of the equipment. The disadvantage of this system is that electrical power for the thermal control mechanism is required when the equipment is active. This, in turn, would increase the mass of the power supply. An additional mass penalty comes from the requirement for RHUs.

9.13.7 Hot Biased Heat Pipe Control

The heat pipe based control system is similar to the petia system in that the spacecraft is hot biased. However, rather than use an active control system a passive one is used. By selecting the working fluid of a heat pipe to vaporise at 25 deg C, the heat pipe would only become active when the temperature is above this. When the electronics are active, the heat pipe would be active and can therefore be assumed to be capable of conducting more heat[19] than the subsystem and RHU can generate. Therefore, we can assume that the subsystem will maintain a temperature of 25 deg C. The challenge in this design is to find a material that has the appropriate properties, and a life time commensurate with the PFFs mission. The disadvantage of this type of system is in the mass of the heat pipes and the RHUs required to control the system.

If the heat pipe based system is adopted then the spacecraft would appear as a series of bands. Black or dark bands of thermal radiators, and reflective MIL covered areas where the electronic boxes are mounted. The two areas would be connected to one another via heat pipes built into the structure of the spacecraft.

9.13.8 Preferred Thermal Control System

The selection criteria for the thermal control concept is to select the design which has the minimum mass impact and minimum risk. From the above discussion of the various designs, the preferred thermal control system is a cold biased spacecraft, using the excess electrical power to heat the spacecraft.

9.13.9 MLI

The basic thermal balance of the spacecraft is established by the surface material of the spacecraft. Traditionally, in non-radiative areas, this is achieved by covering the spacecraft in MLI blankets. This is the technique adopted by the PFF. The remaining question is therefore how many layers of MLI are required for the equipment blankets?

The temperature of the surface blanket of the spacecraft can be calculated from:

$$T^4_{surface} = T^4_{space} + \frac{q}{A\sigma\epsilon}$$

---

[19] A typical heat pipe can conduct 5080 W/cm, thus a 0.5 m heat pipe can dissipate in excess of 100 W.

Where q is the thermal energy output by the spacecraft (43.8 W). Thus if we assume that the temperature of deep space is 5 K, the surface emissivity is that of gold (0.023), and the surface area of the spacecraft is 7 m^2. The temperature of the outermost blanket is 263 K.

The temperature difference between two sheets of MLI is given by:

$$q = \sigma\epsilon_{\text{eff}}(T_1^4 - T_2^4)$$

Therefore if there are n layers of blanket the temperature difference is given by:

$$T_n^4 = T_1^4 - \frac{(n-1)q}{A\sigma\epsilon_{eff}}$$

and rearranging, the number of blankets required is given by:

$$n = \frac{A\sigma\epsilon_{\text{eff}}}{q}\left(T_1^4 - T_{surface}^4\right) + 1$$

Therefore, if the inside temperature of the spacecraft is 293 K, and the outer surface is 263 K. Then the number of MLI layers required is six.

If we assume that mylar has a similar density to Kevlar (1.38×10^3kg/m^3) and that each sheet is 0.00025 inch thick (or 0.006 mm) [15, page 367], the mass of the thermal blankets for the spacecraft is 0.23 kg. This figure does not include the sheet spacers or the attachments therefore an allowance of 0.5 kg should be allocated.

9.13.10 Power Regulator Radiator

The regulator of the power subsystem requires a radiator surface to dissipate the excess power generated by the system. Currently this power is minimal as when subsystems are switched off, the power they would have consumed is used by the thermal control subsystem. It is proposed to use the outer surface of the spacecraft structure as the primary radiator surface. If the black epoxy surface is left un-painted then the surface can radiate 275 W/m^2 at 0 deg Centigrade, rising to 446 W/m^2 at 35 deg C.

9.13.11 Sun Shade

During the cruise phase of the mission the spacecraft is in an Earth tracking mode. Therefore, the orientation relative to the Sun oscillates from side to side. This in turn means that one side of the spacecraft will be subject to direct sunlight. To avoid this affecting the thermal control, a sun shield must be added to the back of the spacecraft. This is expected to be only a thin reflective thermal blanket with support wires.

At 1 Au the incident energy on the sun shade will be 1358W/m^2. If the shade is coated with white paint then the solar absorption will be 0.2. Thus the shade will absorb 1494 W. The sun shade can be regarded as radiating to free space. Therefore if we initially assume that the sunshade does not let any thermal energy pass, then the temperature of the front surface of the sunshade will be 270 K. This assumes an emittance of 0.9.

If we assume that the shade is 0.5 m wide, then the total surface area of the shade is 5.5m^2. If the shade is made out of the same material as the thermal insulation blanket, then the mass of the shade taking into account the support rods will be approximately 0.5 kg.

9.13.12 Thermal Control Mass

The proposed thermal control system consists of three elements, the sun shade, the MLI blankets, and the heater circuits. If an initial allocation of 1.0 kg is made for the heaters and the controllers, then the total mass of the thermal control subsystem is 2.0 kg.

9.13.13 Thermal Control Power Requirement

The thermal control subsystem is assumed to require an additional 10% of the total spacecraft's power requirement to ensure that the spacecraft is maintained at the correct temperature. Thus 4.7 W will be required.

9.13.14 Thermal Control Risk

The proposed thermal control system is a low risk design, however careful modeling of the spacecraft will be required to ensure that the spacecraft is only marginally cold biased. This is believed to be well within the bounds of current design capabilities. Areas of particular importance will be the initial injection sequence, near Earth operation and the mid-course guidance maneuvers.

9.13.15 Cost

The parametric cost equation for the thermal control system is based on the mass of the thermal control system X via:

$$\text{Cost} = 0 + 416X^{0.66} + 86X^{0.65}$$

The base offset cost of the thermal control system has been set to zero as the equation is based on estimating the cost of the structure and control system together, and thus the base offset is already included in the cost of the spacecraft support structure. The cost of the thermal control system is estimated as $ 0.79 million.

Item		Comment
Concept	Cold biased with heaters Sun shade 6 layer MLI	
Antenna	Thermally isolated from the spacecraft bus	
Subsystem Mass	2.0 kg	
Power Requirement	4.7 W	
Cost	$ 0.79 M	Partially supported by structural costs.

Table 9.33: Thermal Control Subsystem Characteristics

9.13.16 Thermal Control System Summary

The main thermal control subsystem characteristics are summarised in Table 9.33.

9.14 Instrument Configuration

9.14.1 Introduction

The science instruments will be attached to the spacecraft, and will use the spacecraft attitude control to point them at the desired imaging targets rather than being on an independently pointed scan platform. The instruments can be mounted on the spacecraft in 3 basic possible directions:

1. Parallel to main antenna axis

2. Perpendicular to the main antenna axis

3. Some intermediate angle

9.14.2 Solar and Earth Occultation

The science mission requires that the spacecraft carry out two occultation experiments. The first is the solar occultation using the UV spectrometer to measure the atmospheric absorption. The second is the radio occultation experiment, where the spacecraft passes into Pluto's shadow as seen from the Earth. If the instruments are mounted perpendicular to the axis of the main mission antenna then the spacecraft must execute a 90 degree rotation maneuver between the two occultations. However, if the instruments are mounted such that they are parallel to the main antenna then the spacecraft, by tracking Pluto, will already point in the correct direction for observing the occultation. In this configuration the position of the Earth relative to the Sun, as viewed from Pluto, does not place any constraints on the orbit past Pluto. For the perpendicular arrangement the time between Solar and Earth occultation must be large enough to allow the spacecraft to be rotated 90 degrees. This imposes an additional constraint on either the orbit past Pluto or the AOCS subsystem.

9.14.3 Spin Axis

If the instruments are mounted perpendicular to the main antenna axis, then the spacecraft must be rotated about the main antenna axis. This axis has the largest moment of inertia of the possible axes and will therefore require the maximum amount of fuel to achieve the desired pointing change in a given time. This suggests that the instruments should be aligned parallel to the main axis of the antenna.

9.14.4 Preferred Instrument Mounting Direction

The simplest orientation for the instruments is parallel to the main axis of the spacecraft. This solution is adopted; however care will be required in designing the thermal control system to allow for the solar energy absorbed by the instruments during cruise phase.

9.15 First Iteration Design Summary

9.15.1 Introduction

This section presents a summary of all the budgets using figures calculated from the detailed systems work presented earlier in this chapter. It should be noted that these figures are not consistent and represent only the first round of the systems design activities.

9.15.2 Budgets

The mass, power, and cost budgets are presented in tables 9.34, 9.36 and 9.37 respectively. The tables show both the initial allocations and the figures which resulted from the detailed study.

Program level costs are typically equivalent to 35% of the hardware costs of the program[20]. Similarly, a factor of 11% is added to cover the Electrical and Mechanical Ground Support Equipment (EGSE & MGSE).

---

[20] The factor of 35% is a weighted average of the 36% factor for the design and development costs, and 33% factor for the first unit costs [46].

Subsystem	Initial Value (kg)	Systems Calculated (kg)	Comment
Payload	6.0	6.0	Project baseline
Propulsion	3	2.4	Dry mass
GN&C	0.0	0.0	Ground based or allocated to AOCS
AOCS	7.8	19.4	
Communications	6	57.3	Including antenna
C&DH	0.0	25.0	
Thermal Control	2	2.0	Passive system
Electrical Power	13	13.0	
Structure	10	17.9	
Integration	4	8.3	5%
Margin	5.5	15.1	10 %
Total Dry Mass	60.3	166.4	

Table 9.34: Spacecraft mass budget after initial systems design work

Subsystem	Initially Allocated Value (kg)	Preliminary Systems Calculated (kg)	Comment
Dry Mass	60.3	166.4	
Propellant	-	8.2	
On Orbit Mass	-	174.6	
Spacecraft adapter	-	21.3	Including margin
Upper Stage	-	668	Star 30 E
Launch Interface	-	20.3	Including margin
Pad Mass	-	884.2	

Table 9.35: Spacecraft Final Systems-Level Pad Mass Budget

Subsystem	Initial Value (W)	Systems Calculated (W)	Comment
Payload	6.0	6.0	Project baseline
Propulsion	0	3.0	
GN&C	0.0	0.0	
AOCS	9	56.8	
Communications	7.2	24.0	
C&DH	9	32.0	
Thermal Control	0	4.7	
Electrical Power	7.8	31.6	80 % efficient
Margin	7.8	31.6	20 %
Total	46.8	189.7	

Table 9.36: Spacecraft power budget after initial systems design work

Subsystem	Initial Value ($ M)	Systems Calculated ($ M)	Comment
Payload	0	0	from separate budget
Propulsion	25	1.29	
GN&C	0.0	0.20	assumed ground based
AOCS	25	27.85	
Communications	25	23.81	
C&DH	25	32.80	
Thermal Control	5	0.79	
Electrical Power	25	7.99	
Structure	25	13.46	
MGSE & EGSE	-	11.90	11%
Program Level	-	42.03	35%
Margin	32	32.42	(20 %)
Launcher	200	228.0	
Total	392	422.54	

Table 9.37: Spacecraft cost budget after initial systems design work

Chapter 10

Design Iteration Changes

10.1 Introduction

As noted in Section 9.1.1, the design work carried out in the previous chapter represents only the first pass through the systems design activity. The design process started with a set of initial budget allocations to each subsystem and in the process of the design work more accurate figures were generated. Changes in elements, such as the overall mass of the spacecraft, require that all the calculations be repeated to achieve a set of budgets that are more coherent. This process of iterating through the subsystem designs must be repeated until the spacecraft budgets reach a internally consistent state.

The current chapter presents a summary of the final output of the iteration process along with several additional trade studies now possible because of the higher level of knowledge of the system.

Antenna Radius m	Bus Mass kg	Lens Mass kg	Tx Power W	Power[2] Supply Mass kg	Total Mass kg
2.0	23.8	39.8	1.75	1.4	65.0
1.75	20.9	30.5	2.2	1.8	53.2
1.5	17.9	22.4	3.0	2.4	42.7
1.25	14.9	15.6	4.3	3.4	33.9
1.0	11.9	10.0	6.5	5.2	27.1
0.8	9.6	6.4	10.5	8.4	24.4
0.5	6.0	2.5	27	21.6	30.1

Table 10.1: Variation in spacecraft mass with different antenna diameters

10.2 Variation of Structure and Antenna Gain

The diameter of the main mission antenna was assumed to be 1.5 m. There is a trade off between the gain of the antenna and the power from the HPA. This trade off can be arbitrated in terms of the total mass of the spacecraft for a given downlink data rate. Let us assume that the data rate from the communications system is to be kept constant. By increasing the transmit power from the HPA the required antenna gain, and hence the antenna's diameter, can be reduced. Table 10.1 shows the variation in overall mass[1] of the spacecraft for different spacecraft diameters.

From the table it is clear at this level that for a given transmission rate a smaller antenna diameter gives an overall lighter spacecraft. This is primarily a result of the low base power of the HPA. Doubling the transmit power is, therefore, not very expensive in terms of the power required, but has a large effect on the required antenna diameter. To allow sufficient mounting space for the electronics, a radius of 0.8 m has been chosen.

---

[1] The antenna is assumed to be a composite based lens antenna operating at X band.

10.3 Instruments

The baselined instruments will not change in the process of harmonising the systems-level design. In a definitive project it is possible that these figures would change as a result of further detailed study, however because the instruments are taken as an external input into the design work carried out, this is not the case here.

10.4 Command and Data Management Subsystem

The CDMS is generally not affected by changing the mass and power budgets. This is because its primary design drivers are the number of equipments and their command and data generation capacity. Thus, like the instruments, the subsystem has the same budget allocation that was generated after the first systems level activity.

10.5 Attitude and Orbit Control

The sensor elements of the AOCS subsystem, like the CDMS, are independent of the spacecraft mass and power requirements. The only modification proposed to the system is to combine the cold gas supply used by the AOCS system and the gas supply required by the propulsion system. The tank mass allocated to the propulsion system is assumed to be sufficient to cover the additional cold gas mass required for AOCS operation. Therefore the tankage mass required by the AOCS system has been removed. Consideration was given to replacing the roll thrusters with mono-propellant thrusters utilising the MMH in conjunction with the propulsion system tank pressurisation. A potential 1.7 kg could be saved by using a MMH based system with its higher Isp when compared to the cold gas system proposed earlier. However this must be additional hydrazine, whereas the cold gas would be drawn from pressurisation gas and therefore potentially has no mass penalty. The actual mass savings from the use of MMH roll thrusters needs to be studied in more detail during the design of the propulsion system.

10.6 Communication Subsystem

The only change in the communications subsystem is the change in the transmit power necessitated by the change in the antenna diameter; the new transmit power is set at 10 W. A 10 W HPA is proposed over a 10.5 W system because this is an integer number for which designs exist. Also the figure of 10.5 W was established to keep the data rates constant against a changed antenna size, however, the effect of changing the HPA power to 10 W has a minimal effect on the data rate while providing some potential cost savings. To make allowance for this increased power requirement the HPA mass allowance has been increased to 1.6 kg per HPA. The revised link budgets are shown in Appendix G.

10.7 Thermal Control

The thermal control system concept is unchanged from the baseline. However the mass of the blankets is reduced due to the reduced size of the spacecraft bus. The power required for thermal control has been updated to remain at 10% of the nominal power requirement for each subsystem.

10.8 Power Supply

The power budget is altered mainly by two factors - first the change in the antenna gain and subsequent change in transmit power; second, and most noticeably, the high power requirement from the AOCS sensors, such as the INS system. The RTG is now required to generate 3,108.6 W of thermal power. The spacecraft now requires 7.1 kg of Sr90.

10.9 Propulsion System

The tankage mass of the propulsion system has been increased to 3.5 kg. This includes the tank mass necessary to support the AOCS cold gas requirement. The tankage increase was necessitated by the increase in the dry mass of the spacecraft. The spacecraft now carries 20.1 kg of bi-propellant because of the increased dry mass of the spacecraft from 60.3 kg to 148.1 kg.

10.10 Launch System and Upper Stage

The baselined launch system is still the Titan IV augmented by a Centaur G upper stage, however the optimum upper stage is a stack of two Star 30 BP motors. The total system provides a total C_3 of 187 km^2/sec^2 from the adjusted mass cited in section 10.9. This will give a transfer time of approximately 13 years, though this can be reduced if some of the ΔV available from the onboard propulsion system can be used to increase the orbital velocity rather than to correct the orbital velocity and path. The Star 30E originally would only provide a C_3 of 181 km^2/sec^2.

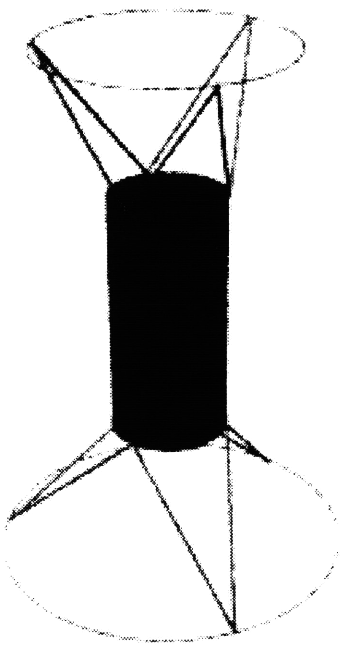

Figure 10-1: Revised launch interface and upper stages support

10.11 Launch Support Structure

The mid support structure separating the two upper stages is a composite cylinder since the rod design is not favorable when the shape of the structure is purely cylindrical. The cylinder has a radius of 0.381 m and is 1.6 m tall. The new launch support configuration is shown in figure 10-1.

The upper stage will exert an acceleration of 13 g. The rods proposed earlier will withstand these loads, however because of the change in the spacecraft diameter the rod are now only required to be 1.45 m long. This reduces the upper truss assembly mass to 2.9 kg per rod. The lower structure is as previously described.

10.12 Final System Budgets

The final system mass budget is shown in tables 10.2 and 10.3, while the final power and cost budgets are shown in tables 10.4 and 10.5 respectively.

10.13 Risk Summary

The two areas considered to be the risk drivers for the spacecraft are the micro-thrusters required by the AOCS system and the lens antenna. The micro-thrusters are considered a risk because there are no thrusters this small currently available. To reduce the system level risk the project team should also initiate development of valves capable of pulsing for periods shorter than the current limit of 5 ms.

The lens antenna is the other major risk area of this design. The risk stems from the fact that this type of antenna has not been used for this type of mission in the past. It is suggested that a demonstration program should be initiated to ensure that the antenna can be built and to validate the performance and physical characteristics derived in this document.

Subsystem	Initially Allocated Value (kg)	Preliminary Systems Calculated (kg)	Final Systems Allocation (kg)	Comment
Payload	6.0	6.0	6.0	Project baseline
Propulsion	3	2.4	5.2	Dry mass
GN&C	0.0	0.0	0.0	Ground based or allocated to AOCS
AOCS	7.8	19.4	18.0	
Communications	6	4.8	5.6	10 W Tx power
Antenna	-	52.5	6.4	0.8 m diameter
C&DH	0.0	25.0	25.0	
Thermal Control	2.0	2.0	2.0	Passive system
Electrical Power	13	13.0	49.4	247.2 W
Spacecraft Bus	10	17.9	9.6	0.8 m diameter
Integration	4	8.3	7.4	5% of dry mass
Margin	5.5	15.1	13.5	10 %
Dry Mass	60.3	166.4	148.1	

Table 10.2: Spacecraft Final Systems Level Mass Budget

Subsystem	Initially Allocated Value (kg)	Preliminary Systems Calculated (kg)	Final Systems Allocation (kg)	Comment
Dry Mass	60.3	166.4	148.1	
Propellant	-	8.2	20.1	
On Orbit Mass	-	174.6	168.2	
Spacecraft adapter	-	21.3	21.1	Including margin
Top Upper Stage	-	668	542.8	Star 30 BP
Upper Stage adapter	-	-	14.7	
Bottom Upper Stage	-	-	542.8	Star 30 BP
Launch interface	-	20.3	22.0	Including margin
Pad Mass	-	884.2	1311.6	

Table 10.3: Spacecraft Final Systems Level Pad Mass Budget

Subsystem	Initially Allocated Value (W)	Preliminary Systems Calculated (W)	Final Systems Allocation (W)	Comment
Payload	6.0	6.0	6.0	Project baseline
Propulsion	0	3.0	3.0	Valve operation
GN&C	0.0	0.0	0.0	Ground based or allocated to AOCS
AOCS	9	56.8	56.8	
Communications	7.2	24.0	52.0	10 W Tx power
C&DH	9	32.0	32.0	
Thermal Control	0	4.7	15.0	Cold Biased
Structure	0.0	0.0	0.0	
Electrical Power	7.8	31.6	41.2	80 % efficient
Margin	7.8	31.6	41.2	20 %
Total	46.8	189.7	247.2	

Table 10.4: Spacecraft Final Systems Level Power Budget

Subsystem	Initially Allocated Value ($ M)	Preliminary Systems Calculated ($ M)	Final Systems Allocation ($ M)	Comment
Payload	0	0	0	from separate budget
Propulsion	25	1.29	1.99	
GN&C	0.0	0.2	0.2	Interface and planning activities
AOCS	25	27.85	27.51	
Communications	25	23.81	11.45	
C&DH	25	32.80	32.80	
Thermal Control	5	0.79	0.79	
Electrical Power	25	7.99	8.34	
Structure	25	13.46	14.33	
Integration	5	-	-	
MGSE & EGSE	-	11.90	10.72	11%
Program Level	-	42.03	37.85	35%
Margin	32	32.42	29.20	(20 %)
Launcher	200	228.0	228.8	
Total	392	422.54	403.98	

Table 10.5: Spacecraft cost budget after initial systems design work

Chapter 11

NASA Engineering Handbook Critique

11.1 Introduction

The design methodology used to design the Pluto Fast Flyby spacecraft was taken in a general fashion from the guidelines set out in the NASA Systems Engineering Handbook [31]. The Handbook is intended primarily as a teaching aid and it is therefore difficult to critique its usefulness as a tool for developing a project at the conceptual level. However there are a number of points that can be drawn from the attempt. This analysis concentrates on chapters 1, 2 and 5, which are the the chapters relevant to a system designed outside the normal NASA project structure, as this thesis illustrates.

11.2 Objective of Systems Engineering

The NASA systems engineering handbook implies that the objective of systems engineering is to develop a project in the most cost-effective manner. This exaggerates the significance of the the cost parameter. Though cost is an important parameter, and growing more important in the current climate, it is just one parameter. The handbook does discuss the concept of minimising the cost function of a project, but here the concept of a cost function is different from that of the monetary cost of the project, and involves a number of other factors such as safety. This balance is not clear in the handbook's presentation.

See section 4.4 of this thesis for a discussion on the relative importance of the different parameters on the PFF mission.

11.3 Systems Engineering: Science or Art

The tone of the opening chapters of the handbook suggests that the concepts behind systems engineering are highly analytical and compose an exact science. This is contrasted by two primary references for the handbook. Griffin and French [15, page 4] state:

> "The key ingredient in systems design and in engineering the compromises [discussed earlier] is sound engineering judgment. Not everything can be analyzed, sometimes because data or tools are not available and sometimes because of time or funding limitations. Very often results are ambiguous or can only be understood in context. The judgment of the team and ultimately of the systems engineer must be the final decision mechanism in such cases."

Wertz and Larson [46, page 66] add:

> "The top-level trades in concept selection are usually not fully quantitative, and we should not force them to be. The purpose of the trade study [and utility analysis] is to make the decision, not quantify the decision making. In other words, we should not undervalue the decision maker's judgment by attempting to replace it with a simplistic formula or rule."

And from the handbook itself:

> "Because doing trade studies is part art, part science, the composition and experience of the teams is an important determinant of the study's ultimate usefulness."

Unfortunately this blend of science and art does not come across in the opening sections.

11.4 Systems Engineering and Systems Management

The NASA Handbook states that there is a difference between systems engineering and systems management:

> "[Systems] engineering is an analytical, advisory and planning function, while management is the decision-making function."

This could be misleading, though the handbook goes on to state that the same individual may perform both roles. Particularly the idea that a basic function of engineering is decision making, particularly with respect to resource allocation [14, Engineering Design and Decision Making] appears to be lost.

> "**Systems engineering** is the treatment of engineering design as a decision-making process."

and

> "The system engineer naturally is forced to make decisions in which system concepts are studied, the way in which interface problems are handled, and resources allocated."

The handbook's definition is particularly interesting, given the large number of pages they devote to the management issues and project phases, which at their root are management issues.

11.5 Mission Philosophy to Concept Development

11.5.1 Mission Objective

One of the most significant omissions from the handbook is the lack of a discussion of the concept of a Mission Objective. This concept, as stated in section 4.3 of this thesis, is the starting point for any mission design.

11.5.2 Program Philosophy

As with the Mission Objective, the handbook makes no reference to the program philosophy. This may in part stem from the implicit assumption in the handbook that cost is the key driver for the mission. The program philosophy that establishes the program priorities are then reflected in the system trades, and the trade study selection criteria.

11.5.3 Identifying Goals

The goals of a space system are presented as part of the trade study process. This is not really the case when the goals and requirements mainly come from higher levels in the successive refinement spiral. For example, the system design activity accepts as its inputs the system design requirements. These are not strictly part of the trade study process. There is, however, an element of requirements flowdown. For example, in the PFF AOCS design, the pointing requirements were translated into specific torque requirements.

11.5.4 Systems Concepts

The handbook offers no advice on how to generate the system concepts. This, I would suggest, would be of assistance, particularly as it is one of the key activities of the trade study process. The proposed design concepts strongly influence the final system.

11.6 The Doctrine of Successive Refinement

The concept of successive refinement is well introduced. The problem is that there is no sense of decision making and option elimination. This is particularly true of the diagram the handbook uses. The design of the PFF carried out in this thesis was primarily based on the diagram shown in figure 3-3. The shaded boxes represent the added elements. Though this is buried in the successive refinement spiral, it is not clear where. it is suggested that the way to resolve this problem is to introduce the system hierarchy which the handbook introduces in its first side bar. The second problem with the refinement spiral is that there is no sense of requirements flow down. This, it should be noted, is one of the key activities of the systems engineer in the early phases of the design process. A proposed revision of the successive refinement spiral is shown in figure 11-1.

11.6.1 Requirements Flow Down

To develop the PFF design, it was initially necessary to define the top level flow of requirements. This was shown graphically in figure 3-3. The addition of a diagram such as this would clarify the process of the flow down of requirements, and assist the reader in understanding the systems engineering process. It would also clarify where systems engineering affects the design process.

11.6.2 Iteration

The concept of successive refinement at a particular resolution is not well developed. The key word which seems to be missing from the discussion is that of iteration. An example of what they mean could clarify the situation for the reader.

The simplest example of this is the power system. Let us assume that the spacecraft definition has reached the point where it is sensible to break the spacecraft down into subsystems. For each of these subsystems the systems engineer will be able to estimate the likely power requirement. This stage is very much an experience-based estimate. The various power requirements can now be merged to form a power budget, which tells the designer the total power requirement for the spacecraft (within a suitable margin). This figure can then be given to the engineer responsible for conducting the trade study on the power subsystem. This initial evaluation will define the preferred generation mechanism, be it solar cells or RTG, along with the mass, thermal and structural impact. At the same time as the power subsystem is being refined, the other sub-systems are undergoing a similar process. The result of this work is an improved estimate of the spacecraft's power requirement. This estimate

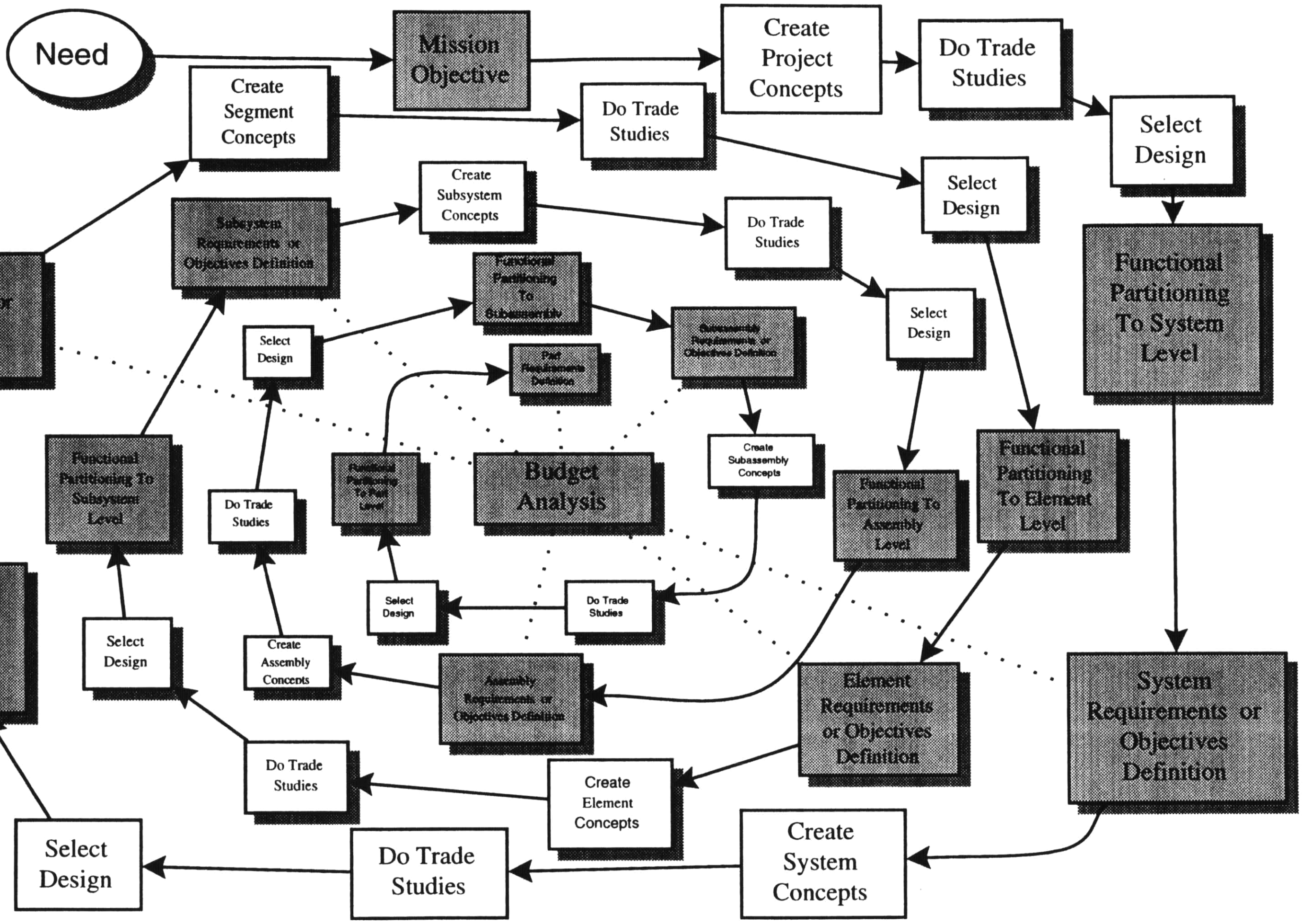
Need
Mission Objective
Create Project Concepts
Do Trade Studies
Select Design
Create Segment Concepts
Do Trade Studies
Select Design
Functional Partitioning To System Level
Segment Requirements or Objectives Definition
Subsystem Requirements or Objectives Definition
Create Subsystem Concepts
Do Trade Studies
Select Design
Functional Partitioning To Subassembly
Subassembly Requirements or Objectives Definition
Select Design
Part Requirements Definition
Functional Partitioning To Subsystem Level
Do Trade Studies
Functional Partitioning To Part Level
Budget Analysis
Create Subassembly Concepts
Functional Partitioning To Assembly Level
Functional Partitioning To Element Level
Functional Partitioning To Segment Level
Select Design
Select Design
Do Trade Studies
Create Assembly Concepts
Assembly Requirements or Objectives Definition
Element Requirements or Objectives Definition
System Requirements or Objectives Definition
Do Trade Studies
Create Element Concepts
Select Design
Do Trade Studies
Create System Concepts

Figure 11-1: Revised Successive Refinement Spiral Shaded boxes represent changes or additions to the NASA Handbook

can then be used to iterate the power system design. These changes will naturally require that the trade studies be revisited. This approach is seen in the design of the PFF spacecraft in chapter 10.

11.6.3 Defining Goals and Constraints

It is assumed that defining the goals and constraints means the establishment of the system/subsystem requirements. Furthermore the functional analysis is assumed to include some division of tasks to apportion the requirements to the appropriate functional blocks. The meaning of "defining goals and constraints" needs to be clarified.

11.6.4 Budgets

One concept that the handbook omitted is system budgets. The handbook only mentions them in the context of the cost budget. This is an important omission since they are the key tools that the systems engineer uses to monitor the compliance of the design with the requirements, and to ensure that the system is self consistent. Figure 11-1 introduces this as an additional box at the centre of the spiral, like a spider at the centre of its web. The systems budgets are linked to the requirements allocation, which is where the requirements at each level are most visible. An idea associated with budgets, that of system margins, is also not discussed in the NASA Handbook.

11.6.5 Loop Unrolling

The handbook introduces the idea of loop unrolling as the process of working back up the design spiral. The idea they appear to be trying to establish is that of taking the design parameters of the various subsystems and bringing them together to show that they will achieve the desired goals. This is surely where the concept of system budgets should be introduced.

11.6.6 Increase the Resolution of the Design

In the section on increasing the design resolution, the handbook introduces the concept of sub-dividing the system into subsystems. However the handbook fails to point out that in order to design these subsystems the Objectives/Requirements need to be apportioned to the various subsystems. For example, as noted earlier, the engineer responsible for designing the power subsystem will need to know an estimate of the power required by the spacecraft. This is a simple flow down of a requirement, but one which the power engineer cannot be expected to detail for themselves. The apportionment provides a starting point for the scheme of successive refinement. Another example of an apportionment is the pointing budget, which defines the pointing accuracy required of the platform, the instruments and so on.

11.7 Design Trade Studies

In general, the reader's attention is drawn to the comments on the subject of trade-off analysis presented by Griffin, *et al* [15, page 9], which puts the whole trade-off process into perspective.

11.7.1 Trade Studies and the Doctrine of Successive Refinement

There is a large overlap between the section on the philosophy of successive refinement and that of trade studies. Activities such as Identifying and Quantifying Goals appear in both (page 7 and page 65), leaving the reader to wonder to which area this belongs.

11.7.2 Functional Analysis

The handbook describes functional analysis as follows:

> "Functional analysis is the systematic process of identifying, describing, and relating the functions a system must perform in order to fulfill its goals and objectives."

The handbook goes on to discuss such techniques as Functional Flow Block Diagrams and Time Linear Analysis. This has the potential of limiting these flows to sequential systems where one action follows from another. However, spacecraft functions often involve parallel systems. For example, using the techniques described to break down the top level of the spacecraft into propulsion, instruments, etc., one could easily forget that the spacecraft must provide power to all these subsystems simultaneously. A lower level example is the communications subsystem whose basic functions can be well developed using a flow block diagram. However this will not capture the parallel requirement for active target ranging which goes on in parallel with the communications activity.

11.7.3 When to trade or not to trade–that is the question

The question of what constitutes a true trade and when it is appropriate to just list the pros and cons of a situation is never really addressed.

The selection criteria are critical to any decision making process within the trade study. Yet there are often few grounds for setting these, particularly determining the most important measurement variables. Sensitivity analysis helps to determine if the criteria are good, but often for high level trades there is no quantitative data, just subjective data divided into broad categories, so sensitivity analysis is impossible at this level.

11.7.4 Making a Tentative Selection

In figure 21 of the handbook (The Trade Study Process) the outcome of the analytical portion of the trade study involves making a tentative selection. This should not preclude selecting several candidates that are acceptable since there are often circumstances for which the level of a particular trade study is not detailed enough. An example of this in the design of the PFF is the choice between a lens based and a reflector based spacecraft.

11.8 Technical Terms

11.8.1 Definitions

In the preface to the handbook the authors note:

> "There are legitimate differences of opinion on basic definitions, content, and techniques."

It is therefore unfortunate that the handbook has a habit of using terms and concepts before defining them. This is particularly true of Chapters 3 and 4. The addition of a glossary of terms would be useful in this respect. It would also be helpful for the user who has read the manual and is referring to it at a later date as they could then refer to the glossary to confirm the interpretation of the term.

11.8.2 Project Phases

Given the above quotation it is interesting to note that the handbook does not have a consistent definition of the different phases of a project. Chapters 3 and 4 have somewhat conflicting definitions of what the output of Phase B is, for example.

11.9 Conclusion

The NASA Systems Engineering Handbook makes an excellent start on the process of defining the mechanisms by which a system engineer should work and the techniques available to them. However the handbook omits such aspects as the Mission Objective, Requirements Flowdown, System Engineering Budgets, and Program Philosophy from its discussion. These are central to much of the work of a systems engineer and a discussion of these topics should be added to the handbook. The above comments would, the author believes, add to the document's readability and assist anyone undertaking a systems development.

Chapter 12

Technology Development Program

12.1 Introduction

When the question of which spacecraft should be used to test the design methodology was first considered, it was decided that one of the new small missions should be selected. This was done for two reasons. The first is that the small missions are likely to be the type of missions which will use the handbook's methodology. Secondly, because the small missions are likely to make up the majority of the future spacecraft built by NASA. Thus this choice of spacecraft would also provided the opportunity to comment on the technology development activities within NASA. The particular emphasis of this idea was that the payload to spacecraft fraction in recent years has been shrinking as advanced technology has been applied preferentially to the instruments, shrinking, thus, their mass faster than that of the other subsystems.

The PFF spacecraft was chosen over one of the discovery missions, because of its better defined requirements and more challenging mission.

12.2 Is the PFF a Fair Comparison?

It is normally expected that the payload will constitute between 15 and 50 % of the dry mass of the spacecraft. For example, the Galileo spacecraft has a payload fraction of 15%. However, in the PFF case the payload fraction is down to 4.6%. The question must be raised as to whether this is a fair comparison. Most normal missions, without putting any additional requirements on the rest of the system except the structure, and power supply, would have a very much larger compliment of instruments. Thus, the architecture of the PFF is capable of supporting a much larger suit of instruments than is possible because of weight restrictions. To add additional instruments the only effects on the system would be to require additional power from the RTG, a possible increase in the fuel required for pointing, and an increase in data storage capacity or a reduction in the amount of data taken from the currently existing instruments.

Thus the PFF is an example of the basic problem of utilising simple statistics. There is a base mass penalty for such a system which does not correspond well to the artificial pure ratio tests.

12.3 Technology Required for PFF

12.3.1 Introduction

In developing the design of the PFF spacecraft, a number of advanced technologies have either been assumed or proposed for development. These technologies are critical for the design of the PFF as envisaged and in many cases mirror technologies required by the PFF spacecraft proposed by JPL.

12.3.2 Micro-Thrusters

The one major new piece of technology that the PFF spacecraft requires is the micro-thrusters required for station-keeping. As noted in Section 10.13, valves with a shorter pulse duration than those currently available should also be developed.

12.3.3 Inertial Navigation System

The inertial navigation system is the largest user of power on the spacecraft. The development of smaller and lighter systems, therefore must be considered a high priority. The author must admit puzzlement at why a strap-down system such as the one proposed for the PFF has such a high power requirement. One possible area that has not been developed is the control electronics for the RLGs. The possibility of integrating the computations associated with the RLGs into the main onboard computer should be explored.

12.3.4 Star Mappers

The star mappers used for updating the INS are currently under development. The biggest change that could be desired from these devices is to reduce their power requirement. An additional area could be to off load the processing requirement of the sensor onto the main computer.

12.3.5 Communications Subsystem

The key area for development in the communications subsystem is the efficiency of the HPA. Currently the efficiency is only 25% for X band and lower for Ka band. Considering that high linearity L band HPA's are currently achieving better than 30%, the improvement of HPA efficiency at higher bands is therefore a likely candidate for continued development.

The other elements of the communications subsystem are currently undergoing miniaturisation, a trend that is likely to continue. Therefore, miniaturisation is not seen as a critical area.

12.3.6 Onboard Computer

The computer proposed for the PFF has some excess capacity. The possibility of using this spare capacity to subsume some of the processing carried out by the star mappers and INS system may allow the mass of the spacecraft to be further reduced.

12.3.7 Data Storage

The proposed PFF spacecraft uses a new type, for space applications, of storage system. This has been developed by the BMO. This concept shows great promise of being able to utilise commercial development of storage systems for space applications. The imaging capability of the PFF is ultimately controlled by the onboard storage capacity of the spacecraft; and as such, the bigger the storage capacity the better. This data storage technology should also find application in Earth-sensing spacecraft. It will be worth while for NASA to ensure that systems are compatible with the latest large storage disks and with predicted systems, to ensure that the maximum capacity is always available in a spaceflight compatible packaging. This may not require much direction from NASA as current development in the commercialisation of photographic satellites is likely to drive this goal from a commercial stand point.

12.3.8 RTG

The single largest mass on the spacecraft is the RTG. Any development work that could reduce the size of this element of the spacecraft would be extremely beneficial to the spacecraft. This element may well present problems with balancing the spacecraft. JPL has proposed a programme to develop a smaller and lighter version of the current RTG design; however this programme is not scheduled to start until 1996. It is suggested that this activity be brought forward in time and its schedule accelerated.

12.3.9 Composite Materials

The spacecraft structure and launch supports proposed use carbon fibre epoxy face skins over an aluminium honeycomb core. The configuration and designs are not technologically challenging, since this type of design is an industry standard solution. The challenge for the American industry is that it is proposed to use composite face skins, which while a common solution for European satellites, because of the mass advantage it offers, are not regularly used by their American counter parts. The author must admit to being surprised at the low use of composites in American spacecraft design. The introduction of this type of material is currently under development. [8]. Their introduction is more an educational issue than a development one. The technology exists to build the materials, so all that is required is its introduction into the production facilities. The bigger challenge is in educating the structure designers in the use of these materials, which have complex properties resulting from their non-isomorphic nature. This requires the provision of appropriate training to the mechanical engineers and then building their experience and confidence in the materials and the appropriate safety factors. Some progress is being made in this area, however, for example the structure on the new Hughes HS-601 is primarily composite based.

12.3.10 Lens Antenna

The spacecraft is based around the novel use of a lens antenna as the main mission antenna. This is very different from the antennas used by conventional deep space vehicles developed by JPL, which tend to be based around reflector antenna designs. Optimum lens mass suggests that the lens be built about an X band system. The trade off is between lens thickness and the fill factor of support material to cavity size. Trades must be made with Ka band gains as noted in Section 9.11.4. Lens antenna have been used in spacecraft, LES 6 and 7 being examples. Their use is normally for multi-beam systems rather than the single-beam system proposed here and for which the unknowns have yet to be identified.

It should be noted that one of the beauties of the lens design is the ease of access that is given to the spacecraft electronics for integration.

12.3.11 Thermal Control

The PFF spacecraft proposed in this thesis uses a very different thermal control concept from the JPL craft, which uses a louvre based system. The design proposed here takes advantage of the constant electrical power availability and should be both simple and reliable while using current technology. No technology development proposals derive from of the thermal design.

12.3.12 Electronic Packaging

To reduce the mass of the electronics packaging, proposals have been made to integrate the packaging into the structure. For the PFF it is suggested that a five sided box design for the electronics packaging be utilised. The package will then be mounted to the structure so that the structure forms the sixth side. This may present problems with thermal design and testing of the electronics. Because of the ease of integration an all up test may be possible, thus minimising the individual electronics testing, apart from functional and burn in testing.

12.3.13 Flight Operations

One of the biggest challenges faced by the "smaller, faster, cheaper" missions is that of operations support. JPL have proposed for the PFF mission to pass the control of the spacecraft to a university, which, because of its structure, and the availability low cost student labour, will minimise operating costs. This solution is, of course, not consistent with current operating practices.

There are four areas of interest of this problem:

1. Normal operations monitoring
2. Activity planning
3. Problem resolution
4. Data processing

Opportunities for the use of AI on the ground and in the OBC failure identification and correction systems show promise of reducing the currently high demand for operator assistance. The current deep spacecraft already have a degree of autonomy. Ways to increase this should be explored with some urgency. This is likely to be one of the largest technological problems faced by the designers of discovery missions.

12.4 General Comments on NASA Technology Development

12.4.1 Distress Beacon

With the development of more autonomous spacecraft, there will need to be a method developed for the spacecraft to alert the ground users that it requires attention. This should be something akin to the emergency distress frequencies used in civil aviation. As an example, consider the scenario in which the PFF spacecraft is designed to have a fully autonomous flight system. It would carry out its own navigation and rendezvous with Pluto. The only planned contact with the spacecraft would be just prior to encounter, with Pluto, to upload the imaging plan. In the event of a failure outside the spacecraft's autonomy system's capability to correct, the spacecraft will enter a safeing mode. At this point, the spacecraft will require a mechanism to inform the Earth that it requires assistance. This could be done by issuing a distress message on a specific frequency. This frequency could be a common distress channel used by all satellites. Onto the carrier frequency, the spacecraft would modulate a identification pattern to allow the PFF to be identified as the sending spacecraft, and thus its "operators" to be notified of its request for attention.

12.4.2 Reaction Wheels

Although the PFF spacecraft in this thesis used a thruster only solution, future discovery missions, of which the PFF is a for runner, are likely to include reaction wheels. JPL states that the emerging technology in reaction wheels is a unit capable of generating 0.02 Nm of torque, storing 4 Nms momentum, weighing 3.5 kg and requiring 20 W at peak torque [25, (Ithaco T-Wheel]. However, if we compare this to currently available technology from Europe, noting that Teldex of Germany has a device available which is flight proven, can generate a torque of 0.09 Nm, has a maximum momentum of 3 Nms, weighs 3.35 kg, and requires only 16.3 W at maximum torque [47, RDR 3]; this suggests that NASA's development program has some catching up to do in this area.

12.4.3 AOCS

If the current generation of small satellites, such as the UOS spacecraft, are compared with current commercial spacecraft, one of the major differences that can be noticed is that the small spacecraft tend to use gravity gradient stabilisation. Thus their AOCS mass is extremely low. The use of gravity gradient stabilisation leads to a very low pointing accuracy. If this level of accuracy is compared with those of planned spacecraft, we note that they require much higher accuracies, particularly the PFF mission which requires almost state of the art pointing systems. Therefore to achieve the mass reductions desired, and the scale factors that are often promised by the use of small satellites, the development of small and lightweight AOCS equipment must be considered a priority.

12.4.4 Spreading the Butter too Thin

NASA and in particular OATC has an extremely wide set of goals and missions to cover projects ranging from deep space probes, through scientific research, to low earth orbiting satellites. It is trying to develop technology for all these mission, yet its 1993 budget for technology is a mere $111.7 million. This seems to be a case of spreading its extremely limited resources extremely thinly. For example, the Pluto Fast Flyby mission has twelve activities in active development, yet[1], only $5 Million to spend on these activities.

---

[1] from a side note on a presentation

12.4.5 Project Personnel

It is interesting to review the different opinions on how to build small advanced spacecraft. From NASA's GSFC [43] we have the following comments on the myths of small spacecraft construction:

> **Myth #3** - Small spacecraft are easy to design and require no prior experience to build.
>
> **Au Contraire!** SMEX spacecraft have required considerable expertise to design and assemble.
>
> - Weight optimization (0.1 Lbs. sensitivity, < 10% margin)
> - Power optimization (0.1 W sensitivity, < 15% margin)
> - Many packaging trades
> - Space/ground segment partitioning
> - High density/high rate data systems
> - Fully digital ACS
>
> **Myth # 4** - Small spacecraft manufactures must "cut corners" in order to meet cost and schedule constraints.
>
> **Au Contraire!** SMEX has found that attention to detail, proper documentation, and aggressive quality assurance are critically important to maintaining schedule and reducing costs.
>
> - Proper procedures ensure thoroughness and reduce errors

- Documentation requirements are reduced because the team size is reduced and co-located, thereby improving communications.

Myth # 5 - Because of the small number of components in small spacecraft, the observatory can be qualified through extensive component level testing.

Au Contraire! Several critical flaws were discovered on SAMPEX during flight integration testing. The faults were system level faults.

SDI list under the MSTI Scout-1 program accomplishments [28]:

Spacecraft ATP to PDR in 1 month (record time)

- Systems trades and evaluations stressed engineering judgment over optimization analysis

While Hughes says, on the source of operational inefficiencies [10]:

Personnel are not working 8 hours a day on useful tasks due to:

1. Transitions from one task to another
2. Waiting for parts, kits, assemblies, etc.

The key ingredient to developing "smaller, faster, cheaper" mission is the use of small integrated team, co-located and with the minimum of extraneous activities. Although to some extent the TQM process now implemented in most industries will improve the performance of each individual, this will not deal with government-imposed bureaucracy. It has been suggested that one of the reasons the BMO has achieved its high level of success is that because it is a new organisation, it has imposed far less oversight on the contractors than would have been the case for a NASA project.

The author suggests that the whole project process of spacecraft development needs to be "re-engineered" to form an integrated process rather than the system that is currently used.

Design Tools

Every unit of flight hardware has a very high added value. This added value is primarily in the form of design, analysis and testing. As is recognised by many groups in NASA and aerospace companies, one of the key activities to reducing the cost of spacecraft is reducing the number of personnel and the duration of the projects. OACT summarised this as, "Fewer people spending less time is key for missions at a lower cost." However, this is to be contrasted to the push for more advanced technologies in spacecraft to reduce the weight. By increasing the performance and reducing the size of the components, the amount of design work is also increased due to two factors. Firstly, higher performance components require more analysis to ensure that all error sources are understood and designed for. Secondly, with smaller components the rework cost exponentially increases; thus, more up front design work must be carried out to ensure that the design is right the first time. Both of these lead to increased man-power requirements. The only way to control this is to increase the level of design automation and the number of design tools available to assist engineers in their work and to minimise the number of low skill activities, which add little value to the project yet cost the project at high skill activity rates. This area appears to have had little development assistance from NASA.

There is a trend in computerised tools to develop new tools to improve the level of accuracy and modeling available to the engineer. It may be that this is the wrong approach. A more cost effective approach may be to automate the current design simulation techniques, without attempting to improve their accuracy. That is to say do not make the models any more accurate or complex than those currently used, but merely reduce the time the current models require to generate the desired output.

12.4.6 Government Review Process

A long touted problem which may hinder the the development of the "smaller, faster, cheaper" missions is the continual review process and cost capping imposed by the current system of year-to-year funding by Congress. This places a large overhead on the project to support the funding request, rather than expending the manpower to design the final system. It would be an interesting study to apply the TQM principle to the whole process and compute the cost of congressional oversight to a project.

12.4.7 Software Cost

The development of highly automated spacecraft with more complex instruments, even if packaged in smaller boxes, requires vastly more software development. It has been suggested that:

> "As the computers get smaller and faster, so the software gets bigger and less efficient."

In association with this requirement for more advanced design tools and applications will place a large burden on project costs. It is easily possible to foresee a time when the cost of any new advanced project will be dominated by the software costs. Therefore, NASA needs to enact the necessary activities to decrease the cost of software development.

Software development is still very much at the stage of making each nut and bolt afresh for each project. The use of standard functions and techniques has not yet reached the level of standard components. For example, an electrical engineer will not re-invent the opamp every time they need one but will merely use the standard components available. This is the level that software engineering needs to reach to reduce the cost. The author would suggest that the DoD made a bold start with the mandating of Ada as the *de facto* standard. However, the cost of using Ada is still high due to the lack of available software programmers experienced in using it. This is in part a problem at the university level; for example, at MIT the only languages taught are C and Fortran, while modern programming languages are not available. One possible solution is to require that all DoD funded or Space Grant universities teach Ada.

There have been suggestions within the military hierarchy to remove the requirement of the use of Ada, on the grounds of its expense when compared with more commercial languages such as C. However, this could well be a serious mistake, given that C lacks the inherent features, such as strong type checking, that are essential to time and mission critical applications. It must be remembered that there is no such thing as bug free code and thus in these applications the use of a "hardened" language must be considered essential. It must be remembered that NASA has already lost one spacecraft through faulty computer code.

As noted in the costing of the CDMS, over two-thirds of the subsystem costs are associated with the flight software. There are currently tools and techniques to increase the rate of code generation and to improve the reuse of code under development. This is particularly relevant to the development of prototype systems, which are currently developed using simpler languages to limit the cost. The development of these tools and techniques needs to be accelerated to ensure that the cost of a given mission is not dominated by the cost of its software.

12.5 Conclusion

The shift to "Smaller, Faster, Cheaper" missions will present the spacecraft engineering establishment with many new challenges. The most critical of these will be in the cost element of the equation. The technical challenges are the engineer's life blood and as such only require funding and a political will to be solved. The programmatic and "cultural" issues will be the most challenging and their resolution will be the most critical to the success of the whole process.

Chapter 13

Future Work

13.1 Introduction

The previous chapters of this thesis have described the design and development of a Pluto spacecraft, reviewed the proposed NASA systems engineering handbook methodology, and commented on the NASA technology program from the prospective of the PFF mission. One remaining question is, what areas of future study are likely to be of interest.

13.2 Pluto Fast Flyby Spacecraft

The design of the PFF spacecraft documented in this thesis has been developed to a level where initial subsystem requirement specifications could be written. However a spacecraft which will carry out the mission to Pluto is currently under development by JPL. The micro-thruster and the lens antenna technologies both suggest that a review of their requirements and assumptions could be of potential use for either the JPL PFF spacecraft, or other spacecraft in the future. The micro-thrusters in particular could prove to be an interesting topic for future research and development.

13.3 NASA Systems Engineering Handbook

The comments generated by this thesis on the systems engineering handbook will be submitted to the authors of the NASA Systems Engineering Handbook. This will conclude the activities with respect to the handbook for this thesis. However, consideration should be given to utilising the revised handbook in a similar manner to that executed here on a different spacecraft project to develop additional comments.

One area of the handbook that the work carried out here did not address is the management planning and project cycle. Both of these sections would also benefit from comments resulting from the use of these sections on a real project.

13.4 NASA's Discovery Programs

The technology analysis was directed at developing comments on NASA's technology support for the 'smaller, faster, cheaper" missions. The result of this work was a concern that the programmatic aspect will dominate the chance of success of the programs. It is therefore suggested that a thorough study of these aspects be carried out. The inherent problem with this task is that it must blend management science and political science to achieve its objective. The execution of such an analysis may fit nicely under an extended "Lean Aircraft Initiative".

13.5 Conclusions

The largest area for future exploration generated by this thesis is the proposal to study the management and funding issues that will drive the discovery missions. It is therefore suggested that this would be an interesting area for exploration, but would require a diverse combination of talents to study.

Chapter 14

Conclusion

This thesis investigated three topics. The first and largest of the tasks was to develop an independent design of a spacecraft capable of being launched using conventional launch vehicles and arriving at Pluto before the atmosphere condensed onto the planets surface. The second area the thesis considered was the systems engineering design methodology proposed in the draft edition of the NASA Systems Engineering Handbook. By using the design methodology outlined in the handbook, experience with its use in practice was established which resulted in some practical comments for the handbooks improvement. The third and final topic for this thesis investigated the NASA technology development program, from the perspective of the "smaller, faster, cheaper" discovery missions. The basis of this review was that the Pluto Fast Flyby (PFF) mission is a good example of the type of missions that will be carried out under this slogan.

The PFF spacecraft proposed by this thesis has a dry mass of 130 kg, which compares very closely with that of the actual spacecraft currently under development by NASA's Jet Propulsion Lab. However, the spacecraft proposed here is very different from JPL's in a number of key areas. The most significant of these is that of the main mission antenna. The craft proposed within this document is based around the use of a lens antenna. The estimated overall on orbit cost of the spacecraft is approximately \$404 million. This is very close to the \$400 M that NASA has budgeted for the mission.

The NASA Systems Engineering Handbook methodology was found to provide moderate suitability for the design of the PFF spacecraft; however, a number of areas were identified which were omitted from the Handbook's discussion. For example the concepts of mission objective, system budgets and requirements flowdown were not included in the Handbook. Also identified where a number of areas were the handbook's explanation was unclear.

In reviewing NASA's technology development program, it was noted that the problems the discovery missions will face will be more at the programmatical level than at the technological level. The latter problems appear solvable, even given the limited availability of the appropriate funds and manpower. However, the programmatic problems reach into the very way in which NASA operates and is funded. These aspects, unfortunately, cannot be so easily remedied.

In summary this thesis has achieved its three main objectives, of developing a spacecraft using the NASA Systems Engineering Handbook, of critiquing the Handbook, and of reviewing NASA's technology development program.

Appendix A

Minimum Energy Transfer Orbit

If the orbits of Pluto and the Earth are approximated by Circular Co-planar Orbits then The optimum single impulse transfer orbit can be calculated using Battin's Equations 11.12 to 11.15 [3] which state that:

$$\begin{aligned} p = \quad & \tfrac{p_m}{8}\left(\tfrac{\eta^2+8+\eta\sqrt{\eta^2+4}}{3\eta^2+16}\right)^2\left(\eta+2\sqrt{\eta^2+4}\right) \\ & \times\left[2\eta^2+8+\eta\sqrt{\Big(3\eta^2+16)(\eta^2+2\eta\sqrt{\eta^2+4}\Big)}\right] \end{aligned}$$

where:

$$p_m = \frac{2r_1r_2}{c\sin^2\frac{\theta}{2}}$$

$$\eta = \frac{3}{4}\frac{AQ^2}{(1+A+A^2)}$$

$$A = \left(\sqrt{1+B^2}+B\right)^{\frac{2}{3}}$$

$$B = \frac{3}{16}\sqrt{3}Q^2$$

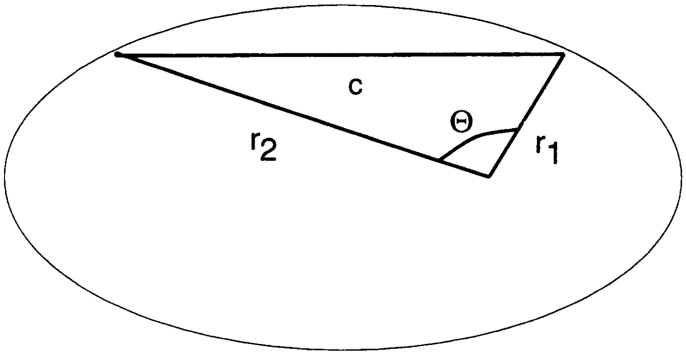

Figure A-1: Single Impulse Orbit Transfer

$$Q^2 = \left(\frac{r_2}{c}\right)^3 (1 + \cos\theta)\sin^2\theta$$

$$c^2 = r_1^2 + r_2^2 - 2r_1r_2\cos\theta$$

from Equation 6.15 we have:

$$v_c = \frac{c\sqrt{\mu p}}{r_1r_2\sin\theta}$$

and

$$v_\rho = \sqrt{\frac{\mu}{p}}\left(\frac{1-\cos\theta}{\sin\theta}\right)$$

Using figure A-1, the circumferential and radial velocities can be calculated as:

$$v_\theta = v_c\sin\beta$$

$$v_r = v_\rho - v_c\cos\beta$$

substituting in the values of v_c and v_ρ gives:

$$v_\theta = \frac{\sqrt{\mu p}}{r_1}$$

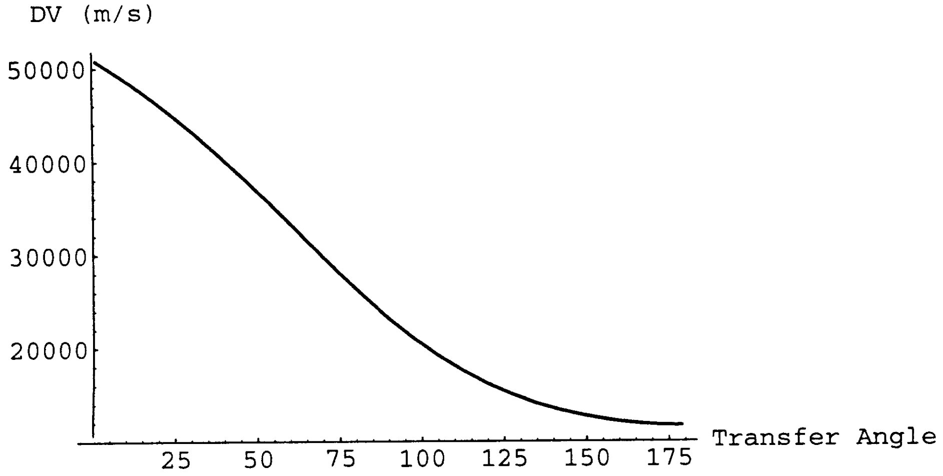

Figure A-2: Plot of the variation of ΔV with transfer angle

$$v_r = \frac{1}{r_1 r_2 \sin\theta}\sqrt{\frac{\mu}{p}}[r_1(r_2 - p) - r_2\cos\theta(r_1 - p)]$$

The ΔV can be then calculated from:

$$\Delta V = \sqrt{\left(v_\theta - \sqrt{\frac{\mu}{r_1}}\right)^2 + v_r^2}$$

The variation of the ΔV with the transfer angle is shown in figure A-2. As can be seen the optimum launch time, as with a hohmann transfer is when the planets are 180 degrees apart. This gives rise to an optimum launch window approximately once every year. The minimum energy[1](C_3) required is approximately 144 Km^2/s^2. This figure does not include any plane change burns, however because of the large magnitude of the ΔV this is likely to be only a small delta on this figure.

To compute the flight times for the optimum single impulse transfer, the eccentricity of the transfer orbit must first be computed. This can be achieved by rearranging Battin's Equation 3.15 and substituting $v^2 = v_\theta^2 + v_r^2$:

---

[1] The Mathematica Notebook used to calculate this figure is shown in Appendix B

$$e = sqrt1 - p\left(\frac{2}{r_1} - \frac{v_r^2 + v_\theta^2}{\mu}\right)$$

similarly, the mean motion can be calculated from:

$$n = \sqrt{\frac{\mu(1-e^2)^3}{p^3}}$$

and hence the eccentric anomaly and mean anomaly are

$$\cos E = \frac{1}{e}\left(1 - \frac{r(1-e^2)}{p}\right)$$

$$M = E - e\sin E$$

or, if the orbit is hyperbolic:

$$\cosh H = \frac{1}{e}\left(1 - \frac{r}{a}\right)$$
$$\sqrt{\frac{\mu}{(-a)^3}}(t - \tau) = e\sinh H - H$$

The flight time is then given by

$$\mathrm{FlightTime} = \frac{1}{n}(M_2 - M_1)$$

The flight time against transfer angle is plotted in Figure A-3. It is interesting to note that launching on a minimum energy trajectory will cause the spacecraft to arrive in approximately 31 years.

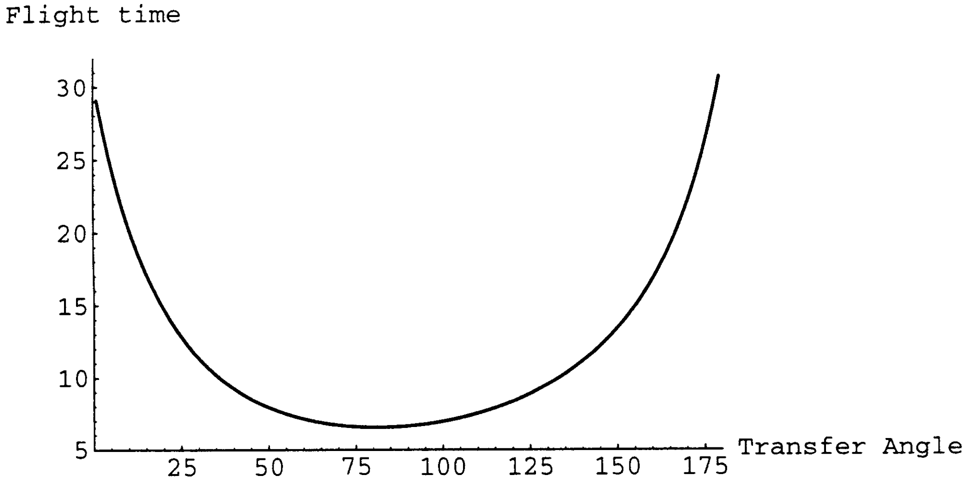

Figure A-3: Plot of the variation of flight time with transfer angle

Appendix B

Minimum Impulse Transfer Notebook

This Mathematica notebook looks at the minimum DeltaV required to inject a spacecraft into a direct transfer orbit to Pluto.

From Chapter 11 of Battin, page 521, we find the formula for the optimum transfer from a circular Orbit (Equations 11-9 to 11-15).

r1 is the radius from the sun of the point of depature.

```
r1 = 1;
```

r2 is the radius from the sun of the target point

```
r2 = 31;
```

Theta is the transfer angle between the departure point and the arrival point. See figure 6.1 in Battin

mu is the gravitational constant of the focal body.

```
mu = 4*Pi^2;
Alpha = Table[x,{x,1,179}];
```

Convert Theta into a degree measurement. For this introduce the angle Alpha.

```
Theta = Alpha *Pi/180;
```

Using figure 6.1 and some elementary trig,

```
c = N[Sqrt[r1^ 2+r2^ 2 - 2*r1*r2*Cos[Theta]]];
```

Equation 6.24 gives

```
Pm = N[(2*r1*r2)/c*(Sin[Theta/2])^2];
```

From Equation 11.10 we have

```
Q2 = N[(r2/c)^3*(1+Cos[Theta])(Sin[Theta])^2];
```

From Eqns 11.13 we have

```
B= N[3/16*Sqrt[3]*Q2];
A = N[(Sqrt[1+B^2]+B)^(2/3)];
n = N[3/4 A*Q2/(1+A+A^2)];
```

Equation 11.15 gives

```
P = N[Pm/8((n^2 + 8 + n*Sqrt[n^2+4]) / (3n^2 + 16))^2 * (n + 2
Sqrt[n^2+4])* (2n^2+8+n * Sqrt[n^2+4]+ Sqrt[(3n^2+16)* (n^2+2n *
Sqrt[n^2 + 4])])];
```

From Equation 6.3, the circumferential velocity of an orbit is given by:

```
Vt = Sqrt[mu*P]/r1;
```

The radial velocity may be calculated using the equations of 6.15 and developing an expression to link Vr , Vc and Vrho.

```
Vr = Sqrt[mu/P] * 1/(r1 * r2 * Sin[Theta]) * (r1(r2-P) - r2 * Cos[Theta]
* (r1-P));

DeltaV = Sqrt[(Vt - Sqrt[mu/r1])^2 + Vr^2];
```

Convert the DeltaV from AU/year into m/s (1 Au/year = 4740.4 m/s)

```
DV = N[DeltaV*4740.4]; plot1 = ListPlot[DV,PlotJoined->True];
```

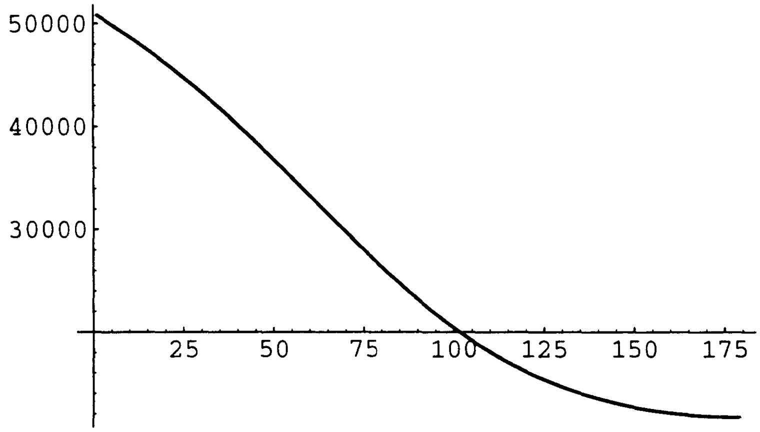

Show[plot1,AxesLabel->{"Transfer Angle","DV (m/s)"}, AxesOrigin->{0,10000}];

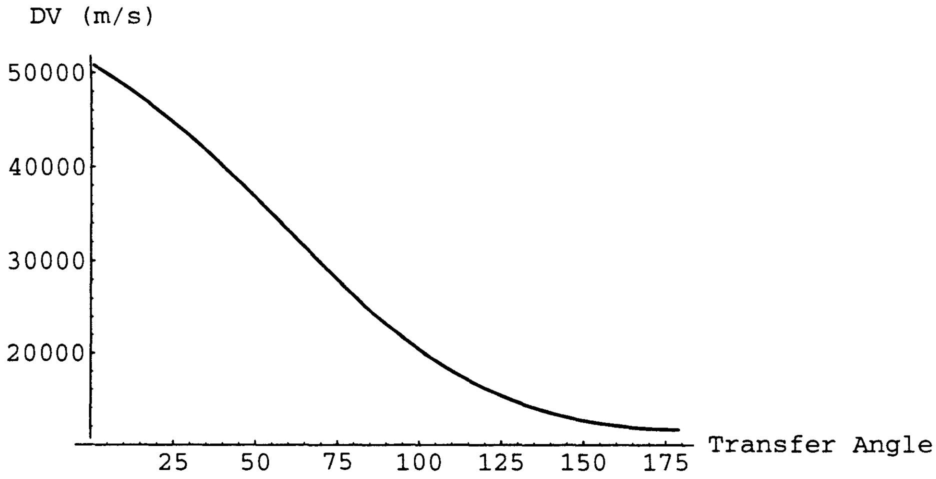

Compute the eccentricity of the orbit using a version of Eqn 3.15

e =N[Sqrt[1-P*(2/r1 - (Vr^2 + Vt^2)/mu)]];

plot3 = ListPlot[e,PlotJoined->True];

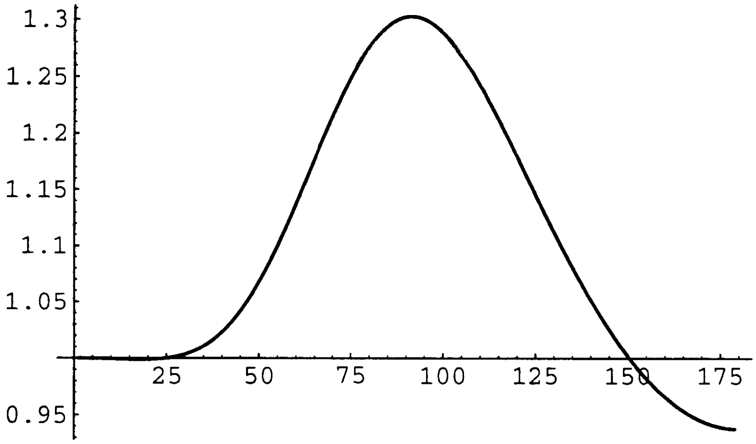

Calculate the mean motion of the orbit (n)

```
mm = N[Sqrt[Abs[mu*(1-e^2)^3/P^3]]];
plot3 = ListPlot[mm,PlotJoined->True];
```

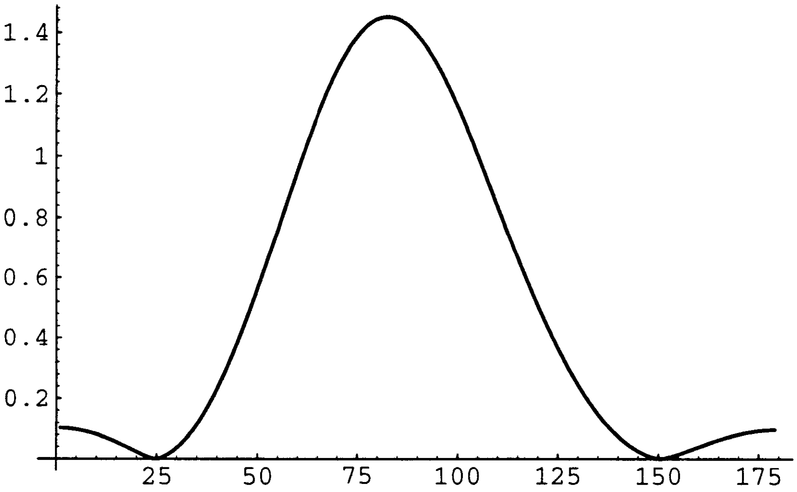

Calculate the two eccentric anomalies for the launch and arrival positions using Eqn 4.28 rearranged

The MapThread command substitutes e for # and P for #2. The command has to have this form because P and e are stored in arrays(vectors)

```
E1 = MapThread[Which[# < 1, ArcCos[1/#*(1-r1(1-#^2)/#2)],
        # > 1, ArcCosh[1/#*(1-r1(1-#^2)/#2)],
        True, ArcCos[1/#*(1-r1(1-#^2)/#2)]]&,{e,P}] ;

E2 = MapThread[Which[# < 1, ArcCos[1/#*(1-r2(1-#^2)/#2)],
        # > 1, ArcCosh[1/#*(1-r2(1-#^2)/#2)],
        True, ArcCos[1/#*(1-r2(1-#^2)/#2)]]&,{e,P}];
```

```
  plot5 = ListPlot[E1,PlotJoined->True];
```

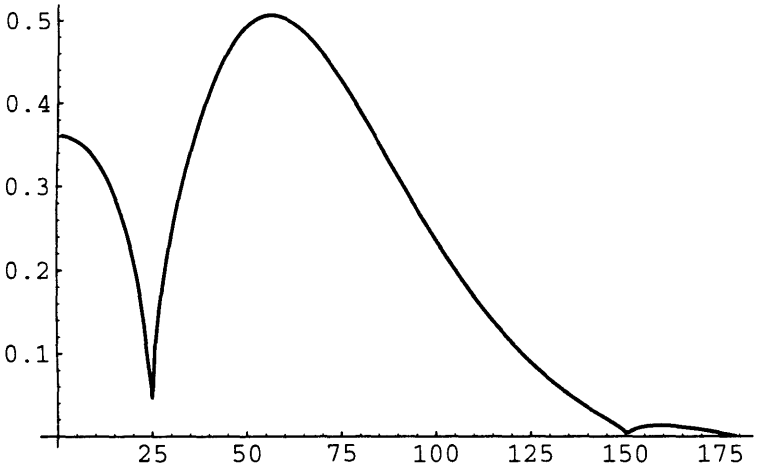

Compute the mean anomaly for both positions using Eqn 4.34

```
M1 = MapThread[Which[# < 1, #2 - #*Sin[#2],
        # > 1, #*Sinh[#2] - #2,
        True, #2 - #*Sin[#2]]&,{e,E1}];

M2 = MapThread[Which[# < 1, #2 - #*Sin[#2],
        # > 1, #*Sinh[#2] - #2,
        True, #2 - #*Sin[#2]]&,{e,E2}];
```

Compute the flight time in years:

```
  FlightTime = N[1/mm*(M2-M1)];
  plot2 = ListPlot[FlightTime,PlotJoined->True];
```

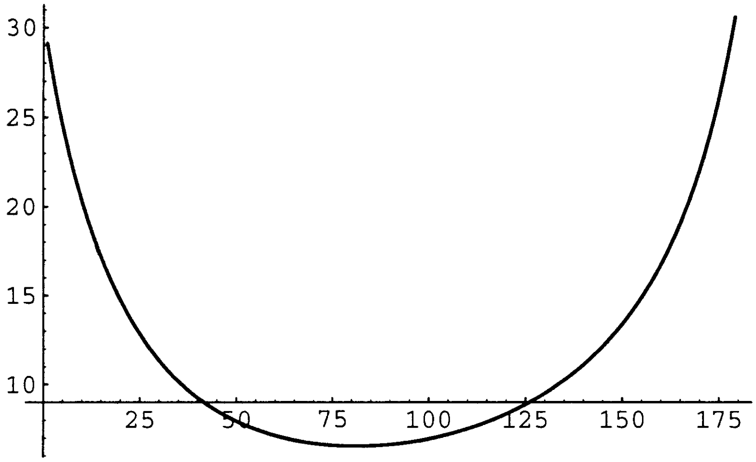

Show[plot2,AxesLabel->{"Transfer Angle","Flight time"}, PlotRange->{{0,180},{5,32}}];

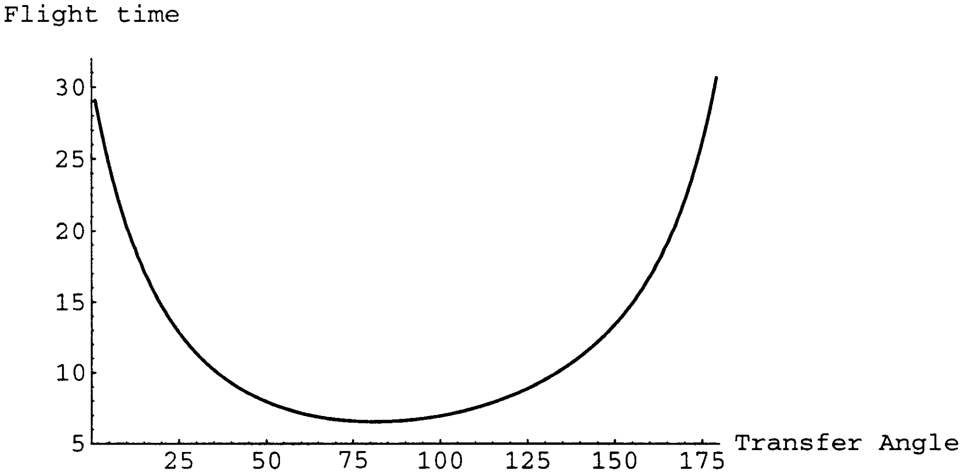

FlightTime[[179]]

30.675

Appendix C

Solar Radiation Induced Torque Notebook

This Mathematica Notebook computes the position of the spacecraft relative to the sun as a vector. It is used to calculate the solar radiation torque.

Establish the basic orbital parameters. Flight time is in years. Note that the programm is sensitive to inacuracies in e and P

```
e = 0.9375716913454446;
P = 1.937560343908667;
FlightTime = 32;
r1 = 1;
mu = 4 *Pi^2;
```

Set the step size for the time interval.

```
StepSize = 0.1;
```

C.ompute the time space between the sample points in seconds. (This is used in the integration later on)

```
h = StepSize*365.25*24*60*60
3.1557610^6
```

Compute a for the orbit.

```
a = P/(1-e^2)
16.0183
```

Calculate the mean motion of the orbit (n)

```
mm = N[Sqrt[Abs[mu*(1-e^2)^3/P^3]]];
```

Compute the intial conditions of the orbit.

```
E1 = Which[e < 1, ArcCos[1/e*(1-r1(1-e^2)/P)],
        e > 1, ArcCosh[1/e*(1-r1(1-e^2)/P)],
        True, ArcCos[1/e*(1-r1(1-e^2)/P)]] ;

M1 = Which[e < 1, E1 - e*Sin[E1],
        e > 1, e*Sinh[#2] - E1,
        True, E1 - e*Sin[E1]];
```

Compute the current value of the mean anomaly where t is zero at departure from earth.

```
t = Range[0,FlightTime,0.1];
M2 = mm*(t) + M1;
InvKepler[EccenAnom_] := M2+Sin[EccenAnom];
```

Nest is the iteration function. Basically this iterates the call to invKepler to compute E2. It is done this way because Mathematica can't solve Keplers equation (not that I can blame it for that). The number of iterations is limited to ensure that the machine doesn't hang. It would probably be faster to call each element of the array separately.

```
E2 = Nest[InvKepler,0,1000];
r2 = a(1- e*Cos[E2]);
```

```
Phi = 0;
```

Calculate the initial orbital velocity direction.

```
ro = Cos[Phi],Sin[Phi],0;
Vr = Sqrt[(mu/P)*(e^2 - (P/rl-1)^2)];
Vt = Sqrt[mu*P];
So = Vr/Sqrt[mu];
Vo = Vr*ro + Vt*{-Sin[Phi],Cos[Phi],0};
```

Compute the Lagrangian coefficients.

```
F = 1- a(1-Cos[E2-El]);
G = a*So/Sqrt[mu]*(1-Cos[E2-El]) + Sqrt[a/mu]*Sin[E2-El];
```

Compute the spacecraft's position as a vector.

```
Rt = Outer[Times,F,ro] + Outer[Times,G,Vo];
```

Plot the orbital trajectory for informational purposes

```
<<Graphics`Graphics3D`
Plotl = ScatterPlot3D[Rt,PlotJoined ->True, Boxed->False];
```

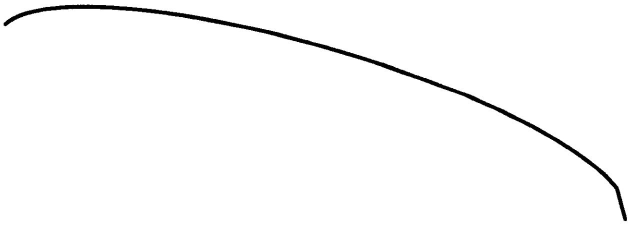

Compute the position of the Earth as a function of time.

```
Rearth = Transpose[Cos[Phi+ 2*Pi*t],Sin[Phi+ 2*Pi*t],0*t];
```

Compute the vector joining the Earth to the probe

```
Rl = Rearth - Rt;
```

Define a function to compute the magnitude of a vector.

```
Mag[{a_,b_,c_}] := Sqrt[a^2 + b^2 + c^2]
```

Calculate the angle between the Sun and the Earth vector.

```
<<Calculus‘VectorAnalysis‘
Cosi = MapThread[Dot,{Rl,-1*Rt}]/(Map[Mag,Rl]*Map[Mag,Rt]);
crossprod =N[MapThread[CrossProduct[#,#2,Cartesian]&,
{Rl,-1*Rt}]];
Sini = Transpose[Map[Sign,crossprod]][[3]]*
(Map[Mag,crossprod]/(Map[Mag,Rl]*Map[Mag,Rt]));
i = ArcTan[Cosi,Sini];
ListPlot[i,PlotJoined -> True];
```

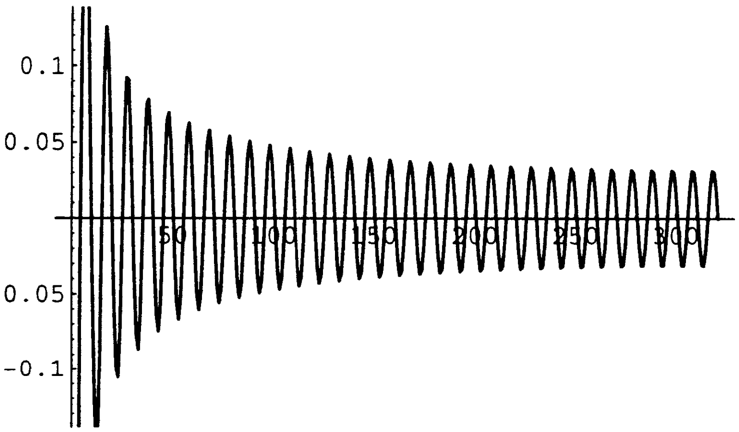

The solar pressure at a range of R (assuming a simple square law affect)

```
Fs = 4.644 * 10ˆ(-6)/(r2)ˆ2;
```

Components of solar radiation pressure in the plane of the illuminated surface and normal to it.

Alpha is the surface reflectivity

```
alpha = 0.2;
Psn = Fs(2-alpha)Cos[i];
Psp = Fs*alpha*Sin[i];
```

A is the area of the spacecraft which is iluminated. Assuming normal shroud dimensions, then this could have a diameter of 3m, which we shall assume.

```
A = Pi*1.5^2;
```

If we assume that the center of mass is directly behind the center of the antenna, which is the illuminated surface, then the disturbance torque is the pressure in the plane of the reflector, ie Psp. The moment arm of the force we shall assume is 1 m (which is large).

```
Ts = A*Psp*1 ;
ListPlot[Ts,PlotJoined-> True];
```

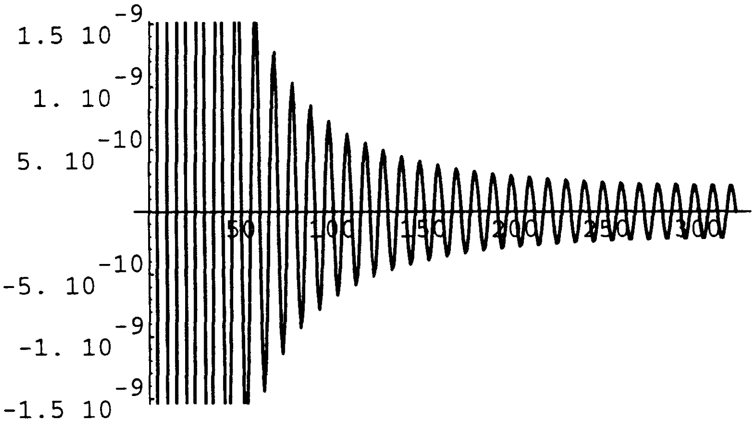

Take the data from above and pass it through a simple low pass filter. This basically removes the oscillatory effects and selects out the bias data, which is what we are interested in for DV calculations. The max variation would give the amount of momentum the AOC needs to absorb once this is integrated.

```
<<Statistics`DescriptiveStatistics`
Td = N[Abs[Take[Ts,4]]];
```

Modify the list to cope with some irregularities in the data that make filtering it dificult.

```
Tsmod = Drop[Ts,4];
Tsmod = Drop[Tsmod,{16,16}];
```

```
zz = Partition[Tsmod,11,10];
Filtered = N[Thread[Mean[zz]]];
Plotdata = Join[Td,Filtered];
ListPlot[Plotdata,PlotJoined -> True];
```

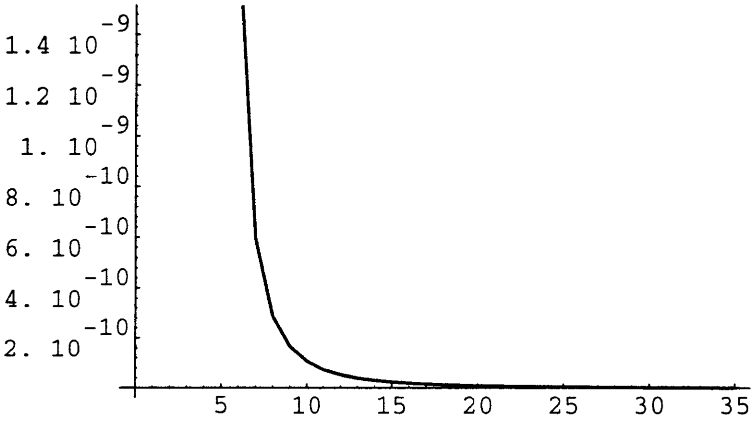

Create a function to implement Simpson's rule.

```
Simpson[{a_,b_,c_}]:= h*(a + 4*b + c)/3
```

Integrate the filtered function to give the total momentum transferred to the spacecraft.

```
zzp = Partition[Filtered,3,2];
zzsimp = Thread[Simpson[zzp]];
Apply[Plus,zzsimp]
0.0287916
```

Compute the total integrated torque on the spacecraft. This number is needed to calculate the fuel required for pure thruster-based pointing.

```
Thrust = Abs[N[Ts]];
ThrustPart = Partition[Thrust,3,2];
TotalTorque = Apply[Plus,Thread[Simpson[ThrustPart]]]
11.7509
```

Appendix D

Communication Link Budgets

D.1 L Band Down Link

Frequency	GHz	1.668	
Wavelength	m	0.18	
HPA Output Power	W	3	
HPA Power	dBW		4.77
Isolator Loss	dB		0.1
Waveguide Loss	dB		0.05
Diplexor Loss	dB		0.1
Waveguide Loss	dB		0.1
O/P Power at Horn	dB		4.42
Antenna Diameter	m	3	
Antenna Beamwidth	deg	4.19	

Antenna Efficiency	%	70	
Antenna Gain	dB		32.84
EIRP	dBi		37.27
pointing Accuracy	Deg	0.1	
Pointing Loss	dB		0.001
Path Length	AU	31	
Free Space Loss	dBm-2		-290.22
Atmospheric Loss	dB		0.03
Power at DSN Antenna	dBm-2		-252.98
Receive Antenna Gain	dBi		60.2
System Noise Temp	K	35	
System Noise Temp	dBK		15.44
Boltzmann's Constant	dBK-1		228.6
C/No	dB		20.38
Data Rate	Bps	19	
Eb/No	dB		7.59
Required BER		10^{-6}	

Required Eb/No	dBHz	10.2
Coding Gain	dB	7.6
Implementation Loss	dB	2
Margin	dB	2.99

L Band Down Link

D.2 S Band Up Link

Frequency	GHz	2.115	
Wavelength	m	0.14	
HPA Power	dBW		43
Waveguide Loss	dB		0.2
O/P Power at Horn	dB		42.8
Antenna Gain	dB		62.7
EIRP	dBi		105.5
Pointing Loss	dB		0.001
Atmospheric Loss	dB		0.46

Path Length	AU	31	
Free Space Loss	dBm-2		-292.28
Power at Spacecraft	dBm-2		-187.24
Antenna Diameter	m	3	
Antenna Beamwidth	deg	3.31	
Antenna Efficiency	%	65	
Antenna Gain	dB		34.58
Pointing Accuracy	Deg	0.1	
Pointing Loss	dB		0.003
WaveGuide Loss	dB		0.1
Diplexor Loss	dB		0.1
LNA Noise Figure	dB	1.6	
System Noise Temp	K	153.93	
System Noise Temp	dBK		21.87
Boltzmann's Constant	dBK-1		228.6
C/No	dB		54.07
Data Rate	Bps	18000	
Eb/No	dB		11.51

Required BER		10^{-6}	
Required Eb/No	dBHz		10.2
Coding Gain	dB		3.8
Implementation loss	dB		2
Margin	dB		3.11

S Band Up Link

D.3 S Band Down Link

Frequency	GHz	2.295	
Wavelength	m	0.13	
HPA Output Power	W	3	
HPA Power	dBW		4.77
Isolator Loss	dB		0.1
WaveGuide Loss	dB		0.05
Diplexor Loss	dB		0.1
WaveGuide Loss	dB		0.1
O/P Power at Horn	dB		4.42

Antenna Diameter	m	3	
Antenna Beamwidth	deg	3.05	
Antenna Efficiency	%	70	
Antenna Gain	dB		35.62
EIRP	dBi		40.04
Pointing Accuracy	deg	0.1	
Pointing Loss	dB		0.003
Path Length	AU	31	
Free Space Loss	dBm-2		-292.99
Atmospheric Loss	dB		0.03
Power at DSN Antenna	dBm-2		-252.99
Receive Antenna Gain	dBi		63.28
System Noise Temp	K	18.5	
System Noise Temp	dBK		12.67
Boltzmann's Constant	dBK-1		228.6
C/No	dB		26.22
Data Rate	Bps	72	
Eb/No	dB		7.65

Required BER		10^{-6}	
Required Eb/No	dBHz		10.2
Coding Gain	dB		7.6
Implementation Loss	dB		2
Margin	dB		3.05

S Band Down Link

D.4 X Band Up Link

Frequency	GHz	7.145	
Wavelength	m	0.04	
HPA Power	dBW		43
Waveguide Loss	dB		0.25
O/P Power at Horn	dB		42.75
Antenna Gain	dB		67.1
EIRP	dBi		109.85

Pointing Loss	dB		0.1
Atmospheric Loss	dB		0.06
Path Length	AU	31	
Free Space Loss	dBm-2		-302.85
Power at Spacecraft	dBm-2		-193.16
Antenna Diameter	m	3	
Antenna Beamwidth	deg	0.98	
Antenna Efficiency	%	65	
Antenna Gain	dB		45.16
Pointing Accuracy	Deg	0.1	
Pointing Loss	dB		0.03
Waveguide Loss	dB		0.1
Diplexor Loss	dB		0.1
LNA Noise Figure	dB	1.6	
System Noise Temp	K	153.93	
System Noise Temp	dBK		21.87
Boltzmann's Constant	dBK-1		228.6
C/No	dB		58.69
Data Rate	KBps	53	

Eb/No	dB		11.45
Required BER		10^{-6}	
Required Eb/No	dBHz		10.2
Coding Gain	dB		3.8
Implementation loss	dB		2
Margin	dB		3.05

X Band Up Link

D.5 X Band Down Link

Frequency	GHz	8.42	
Wavelength	m	0.04	
HPA Output Power	W	3	
HPA Power	dBW		4.77
Isolator Loss	dB		0.1
Waveguide Loss	dB		0.05
Diplexor Loss	dB		0.1
Waveguide Loss	dB		0.1

O/P Power at Horn	dB		4.42
Antenna Diameter	m	3	
Antenna Beamwidth	deg	0.83	
Antenna Efficiency	%	70	
Antenna Gain	dB		46.91
EIRP	dBi		51.33
Pointing Error	Deg	0.1	
Pointing Loss	dB		0.04
Path Length	AU	31	
Free Space Loss	dBm-2		-304.28
Atmospheric Loss	dB		0.06
Power at DSN Antenna	dBm-2		-253.06
Receive Antenna Gain	dBi		74.1
System Noise Temp	K	31.56	
System Noise Temp	dBK		14.99
Boltzmann's Constant	dBK-1		228.6
C/No	dB		34.65
Data Rate	Bps	500	

Eb/No	dB		7.66
Required BER		10^{-6}	
Required Eb/No	dBHz		10.2
Coding Gain	dB		7.6
Implementation Loss	dB		2
Margin	dB		3.06

X Band Down Link

D.6 Ka Band Up Link

Frequency	GHz	32	
Wavelength	m	0.01	
HPA Power	dBW		43
Waveguide Loss	dB		0.25
O/P Power at Horn	dB		42.75
Antenna Gain	dB		74.86

EIRP	dBi		117.61
Pointing Loss	dB		0.1
Atmospheric Loss	dB		0.46
Path Length	AU	31	
Free Space Loss	dBm-2		-315.88
Power at Spacecraft	dBm-2		-198.83
Antenna Diameter	m	3	
Antenna Beamwidth	deg	0.22	
Antenna Efficiency	%	65	
Antenna Gain	dB		58.18
Pointing Accuracy	Deg	0.1	
Pointing Loss	dB		0.63
Waveguide Loss	dB		0.15
Diplexor Loss	dB		0.1
LNA Noise Figure	dB	1.6	
System Noise Temp	K	159.02	
System Noise Temp	dBK		22.01
Boltzmann's Constant	dBK-1		228.6
C/No	dB		65.31

Data Rate	KBps	245	
Eb/No	dB		11.42
Required BER		10^{-6}	
Required Eb/No	dBHz		10.2
Coding Gain	dB		3.8
Implementation loss	dB		2
Margin	dB		3.02

Ka Band Up Link

D.7 Ka Band Down Link

Frequency	GHz	32	
Wavelength	m	0.01	
HPA Output Power	W	3	
HPA Power	dBW		4.77
Isolator Loss	dB		0.1
Waveguide Loss	dB		0.05
Diplexor Loss	dB		0.1

Waveguide Loss	dB		0.1
O/P power at Horn	dB		4.42
Antenna Diameter	m	3	
Antenna Beamwidth	deg	0.22	
Antenna Efficiency	%	65	
Antenna Gain	dB		58.18
EIRP	dBi		62.60
Pointing Error	Deg	0.1	
Pointing Loss	dB		0.63
Path Length	AU	31	
Free Space Loss	dBm-2		-315.88
Atmospheric Loss	dB		0.46
Power at DSN Antenna	dBm-2		-254.36
Receive Antenna Gain	dBi		74.86
System Noise Temp	K	53.31	
System Noise Temp	dBK		17.27
Boltzmann's Constant	dBK-1		228.6
C/No	dB		31.83

Data Rate	Bps	260	
Eb/No	dB		7.68
Required BER		10^{-6}	
Required Eb/No	dBHz		10.2
Coding Gain	dB		7.6
Implementation Loss	dB		2
Margin	dB		3.08

Ka Band Down Link

Appendix E

Computer Program To calculate C_3

E.1 Make File

```
OBJS =    Transfer.time.o \
          Initialise.Planet.o \
          Compute.transfer.angle.o \
          Lamberts.problem.o \
          vector.o \
           rec.to.clasical.o\
          universal.o

CFLAGS = −g −ansi

LIBS = definitions.h array.def.h

ADJUNCT = /john/Library/c_progs/julday.o /john/Library/c_progs/nrutil.o \
            /john/Library/c_progs/caldat.o
```

```
MAKEFILE = Make.Transfer.time

Program: ${LIBS} ${FRC} ${OBJS} ${MAKEFILE}
        ${CC} -o Transfer.time ${CFLAGS} ${OBJS} ${ADJUNCT}

Transfer.time.o : Transfer.time.c ${LIBS} ${FRC} ${MAKEFILE}
        ${CC} -c ${CFLAGS} $<

Initialise.Planet.o : Initialise.Planet.c ${LIBS} ${FRC} ${MAKEFILE}
        ${CC} -c ${CFLAGS} $<

Compute.transfer.angle.o : Compute.transfer.angle.c ${LIBS} ${FRC} ${MAKEFILE}
        ${CC} -c ${CFLAGS} $<

Lamberts.problem.o : Lamberts.problem.c ${LIBS} ${FRC} ${MAKEFILE}
        ${CC} -c ${CFLAGS} $<

vector.o : vector.c ${LIBS} ${FRC} ${MAKEFILE}
        ${CC} -c ${CFLAGS} $<

rec.to.clasical.o : rec.to.clasical.c ${LIBS} ${FRC} ${MAKEFILE}
        ${CC} -c ${CFLAGS} $<

universal.o : universal.c ${LIBS} ${FRC} ${MAKEFILE}
        ${CC} -c ${CFLAGS} $<
```

E.2 array.def.h

```
/* This file contains the variables used by all the programs. */
/* this file contains the definition of the orbit structure and the position
structure for use in the modeling of satellite systems */

/* note that the perigee radius is included even though this can be calculated
 from the Semi major axis, so that parabolic orbits can be handled, ie when
e = 1 and the semi major axis = infinity */


typedef struct ORBIT {double Semi_major_axis;
                      double Eccentricity;
                      double Inclination;              /* degs */
                      double Long_ascending_node;      /* degs */
                      double Argument_of_perigee;      /* rads */
                      double Time_of_perigee;
                      double Perigee_radius;} orbit;

/* Define the Sub Satellite position in Lat, long coordinates */
typedef struct SUB_SAT_POSITION { double Longitude;
                                  double Latitude;} Sub_Sat_Position;

/*Define a 3D vector */
typedef struct VECTOR_3_D { double x,y,z;} vector_3_D;

/* define an orbit in terms of position and velocity */
typedef struct REC_ORBIT { vector_3_D pos,vel;} Rec_Orbit;
```

E.3 definitions.h

```
/* This header file contains standard definitions used by the various
   modules */
```

```
/* This is mu in Au per day */
#define mu 0.0002959113664

#define accuracy 1e-15          /* accuracy to which Kepler's eqn is solved
                                    to*/

/* define the accuracy to which Lamberts problem is solved to */
#define limiting_accuracy 1e-16

enum Planets {Mercury, Venus, Earth, Mars, Jupiter, Saturn,
              Uranus, Neptune, Pluto};
```

E.4 Transfer.time.c

```
/* This program computes the optimum launch time within a given year to arrive
at Pluto a given period after launch. The year is searched for the day on
which the minimum energy is required to launch a spacecraft. The answer is
output as a C3 value. */

#include <stdio.h>
#include <errno.h>
#include <math.h>
#include "definitions.h"
#include "array.def.h"

#define years 366

orbit Initialise_Planet_Orbit(int Name);
double Compute_transfer_angle(vector_3_D r1,vector_3_D v1, vector_3_D r2 );
vector_3_D Solve_Lamberts_problem( vector_3_D r1, vector_3_D r2, double theta,
 double transfer_time);
orbit rectalinear_to_clasical(Rec_Orbit body_status,double current_date);
```

```
Rec_Orbit Compute_Satellite_Position(orbit sat_orbit, double current_time);
void print_orbit(orbit satellite);
void caldat(long julian, int *mm, int *id, int *iyyy);


main()
{
  double transfer_angle,pi,transfer_time,E,f,e;
  vector_3_D r1,r2,v1,Plutos_position, Earths_position, v_parabolic;
  orbit new_orbit,Earth_orbit,Pluto_orbit;
  double launch_time,arrival_time, arrival_year, launch_year;
  double temp1,Delta_V,C3,initial_v;
  double Smallest_Delta_V, optimum_launch_date,optimum_arrival_date;
  int launch_index, arrival_index,count,day,month,year;
  Rec_Orbit rec_Earth, rec_Pluto,r3,spacecraft;
  float requested_transfer_time;
  FILE *fp1;

  pi = 2.0*acos(0.0);

 /* output to the user what the program does */

  printf("This program computes the minimum C3 for a given transfer time,\n");
  printf("and launching in a given year.\n");
  printf("Thus the program computes the best launch date in that year\n");
  printf("So that the spacecraft arrives the required time later.\n");
  printf("The output is stored in ./data/Transfer.time.dat\n\n");

  /* this file contains a summery of the C3 values for the entered year */
  fp1 = fopen("/john/thesis/Broken.plane/data/Transfer.time.dat","w");

  /* initialise the orbits of the two planets */
  Earth_orbit = Initialise_Planet_Orbit(Earth);
  Pluto_orbit = Initialise_Planet_Orbit(Pluto);

  /* write header for the full info file */
  fprintf(fp1,"Record of direct transfer from Earth to Pluto C3 requirements\n");


  printf("please input required launch year yyyy:");
  count = scanf("%i",&year);
  fprintf(fp1,"Departing Earth in the year %i\n",year);

  /* convert date into julian calander and then correct to make it at midnight
which is when the tables are set for on that particular day */
  month = 1;
  day =1;
  launch_year = (double)julday(month,day,year) +0.5;
  printf("departure date = %f\n",launch_year);

  printf("please input required transfer time in years:");
  count = scanf("%e",&requested_transfer_time);
  printf("Transfer time requested:  %e\n",requested_transfer_time);
  fprintf(fp1,"For a %e year(s) transfer time \n",requested_transfer_time);


  /* convert date into julian calander and then correct to make it at midnight
which is when the tables are set for on that particular day */

  arrival_time = (double)launch_year + (double)requested_transfer_time*365.25;
  printf("arrival date = %f\n",arrival_time);

  /* print file header */
  fprintf(fp1,"Departure Date  Arrival date  transfer Angle    C3 (Km^2/Sec^2) \n");
```

```
/* initialise the value of the min C3 */
Smallest_Delta_V = 1E6;


for (launch_index = 0; launch_index <= 1*years; ++launch_index) {


  /* compute launch and arrival dates */
    launch_time = launch_year + launch_index;
    arrival_time = (double)launch_time +
                              (double)requested_transfer_time*365.25;


  /* compute Eath and Pluto position and velocity at required dates */
    rec_Earth = Compute_Satellite_Position(Earth_orbit,launch_time);
    rec_Pluto = Compute_Satellite_Position(Pluto_orbit,arrival_time);


    Earths_position = rec_Earth.pos;
    Plutos_position = rec_Pluto.pos;


    /* compute the transfer angle */
    transfer_angle = Compute_transfer_angle(Earths_position,v1,
                                                  Plutos_position);
    /* printf("transfer angle = %f\n",transfer_angle*180/pi); */


    transfer_time = arrival_time - launch_time;


    /* Solve lamberts problem for the reuired initial velocity */
    v1 = Solve_Lamberts_problem(Earths_position,Plutos_position,
                                        transfer_angle,transfer_time);


    /* compute the velocity change required */


    v_parabolic.x = v1.x - rec_Earth.vel.x;
    v_parabolic.y = v1.y - rec_Earth.vel.y;
    v_parabolic.z = v1.z − rec_Earth.vel.z;



    Delta_V = sqrt(temp1*temp1 + v_parabolic.z*v_parabolic.z);
    Delta_V = v_parabolic.x*v_parabolic.x + v_parabolic.y*v_parabolic.y
                + v_parabolic.z*v_parabolic.z;
    /* convert into km^2/s^2 */
    C3 = Delta_V*2.997942747E6;



    /*printf("day %i,date %f C3 required = %f km^2/s^2 \n", launch_index,
                                          launch_time, Delta_V);*/

    /* update the smallest value of C3 */
    if (C3 < Smallest_Delta_V) {
      optimum_launch_date = launch_time;
      optimum_arrival_date = arrival_time;
      Smallest_Delta_V = C3;
    }

    /* write the computed results to file */
    caldat(launch_time,&month,&day,&year);
    fprintf(fp1,"%i %i %i ",day,month,year);

    caldat(arrival_time,&month,&day,&year);
    fprintf(fp1,"%i %i %i ",day,month,year);

    fprintf(fp1,"%f                              ",transfer_angle*180/pi);

    fprintf(fp1,"%f\n",C3);
  }
```

```
    C/* print the optimum lanch date and C3 */
    fprintf(fp1,"optimum launch date ");
    caldat(optimum_launch_date,&month,&day,&year);
    fprintf(fp1,"%i %i %i \n",day,month,year);
    printf("optimum launch date ");
    printf("%i %i %i \n",day,month,year);

    fprintf(fp1,"arrival date");
    caldat(optimum_arrival_date,&month,&day,&year);
    fprintf(fp1,"%i %i %i \n",day,month,year);
    printf("arrival date ");
    printf("%i %i %i \n",day,month,year);

    fprintf(fp1,"C3 ");
    fprintf(fp1,"%6.2f Km^2/Sec^2", Smallest_Delta_V);
    fprintf(fp1,"\n");

    printf("C3 ");
    printf("%6.2f Km^2/Sec^2", Smallest_Delta_V);
    printf("\n");


  /* close files */
  fclose(fp1);

}

/* print the orbit details...used for debuging */
void print_orbit(orbit satellite)
{

  double pi;
  pi = 2.0*acos(0.0);

  printf(" Semi_major_axis  = %f\n",satellite.Semi_major_axis);
  printf(" Eccentricity  = %f\n",satellite.Eccentricity);
  printf(" Inclination = %f\n",satellite.Inclination);
  printf(" Longitude of the Asscending node= %f\n",
                                   satellite.Long_ascending_node);
  printf(" Argument of perigee  = %f\n",
       satellite.Argument_of_perigee*180/pi);
  printf(" Time of perigee passage  = %f\n",satellite.Time_of_perigee);
  printf(" Perigee radius = %f\n",satellite.Perigee_radius);

}
```

E.5 Initialise.Planet.c

```
/* This program initialises the orbital data for use in computing the planets
position at a later time.  The data is stored here to make it more generally
available and to allow easy change in the target planet.  */

/* the data is taken from the astronomical almanac 1992 page E3 */

/* julian date for 27 Feb 1992 */
#define date_of_data 2448680.5

#include <stdio.h>
#include <errno.h>
#include <math.h>
#include "definitions.h"
#include "array.def.h"
```

```
orbit rectalinear_to_clasical(Rec_Orbit body_status,double current_date);
void print_orbit(orbit satellite);

orbit Initialise_Planet_Orbit(int Name)
{
  Rec_Orbit rec_Planet;
  orbit Planet_orbit;




  switch(Name){
    case Mercury:
      /* Mercury's Orbital Data */
      rec_Planet.pos.x = 0.2603940;
      rec_Planet.pos.y = 0.1760307;
      rec_Planet.pos.z = 0.0670142;

      rec_Planet.vel.x = −0.02199915;
      rec_Planet.vel.y = 0.02045990;
      rec_Planet.vel.z = 0.01321070;
      break;
    case Venus:
      /* Venus's Orbital Data */
      rec_Planet.pos.x = 0.0397435;
      rec_Planet.pos.y = −0.6611896;
      rec_Planet.pos.z = −0.2999574;

      rec_Planet.vel.x = 0.02006091;
      rec_Planet.vel.y = 0.00140209;
      rec_Planet.vel.z = −0.00063895;
      break;
```

```
case Earth:
  /* Earth's Orbital data */
  rec_Planet.pos.x = -0.9231630;
  rec_Planet.pos.y = 0.3291685;
  rec_Planet.pos.z = 0.1427190;

  rec_Planet.vel.x = -0.00651264;
  rec_Planet.vel.y = -0.01477166;
  rec_Planet.vel.z = -0.00640462;
  break;

case Mars:
  /* Mars's Orbital Data */
  rec_Planet.pos.x = 0.4055621;
  rec_Planet.pos.y = -1.2364320;
  rec_Planet.pos.z = -0.5780814;

  rec_Planet.vel.x = 0.01394412;
  rec_Planet.vel.y = 0.00485505;
  rec_Planet.vel.z = 0.00184965;
  break;

case Jupiter:
  /* Jupiter's Orbital Data */
  rec_Planet.pos.x = -5.065706;
  rec_Planet.pos.y = 1.676754;
  rec_Planet.pos.z = 0.842162;

  rec_Planet.vel.x = -0.002716756;
  rec_Planet.vel.y = -0.006213551;
  rec_Planet.vel.z = -0.002597219;
  break;
```

```
case Saturn:
  /* Saturn's Orbital Data */
  rec_Planet.pos.x = 6.412183;
  rec_Planet.pos.y = -6.901778;
  rec_Planet.pos.z = -3.126276;

  rec_Planet.vel.x = 0.003953559;
  rec_Planet.vel.y = 0.003378972;
  rec_Planet.vel.z = 0.001225329;
  break;

case Uranus:
  /* Uranus's Orbital Data */
  rec_Planet.pos.x = 4.93542;
  rec_Planet.pos.y = -17.27300;
  rec_Planet.pos.z = -7.63484;

  rec_Planet.vel.x = 0.003774668;
  rec_Planet.vel.y = 0.000758884;
  rec_Planet.vel.z = 0.000278988;
  break;

case Neptune:
  /* Neptune's Orbital Data */
  rec_Planet.pos.x = 8.76753;
  rec_Planet.pos.y = -26.66235;
  rec_Planet.pos.z = -11.13138;

  rec_Planet.vel.x = 0.002982380;
  rec_Planet.vel.y = 0.000882759;
  rec_Planet.vel.z = 0.000286949;
```

```
      break;

    case Pluto:
      /* Pluto's Orbital data */

      rec_Planet.pos.x = −18.00345;
      rec_Planet.pos.y = −23.53273;
      rec_Planet.pos.z = −1.92050;
      rec_Planet.vel.x = 0.002585865;
      rec_Planet.vel.y = −0.001962502;
      rec_Planet.vel.z = −0.001392448;
      break;

    default:
      printf("Bad call to initialise Planetary Orbit\n");
    }

  /* convert the orbital data to classical orbital elements such as
  the inclination, right ascending node etc. */
  Planet_orbit = rectalinear_to_clasical(rec_Planet,date_of_data);

  return Planet_orbit;
}
```

E.6 Compute.transfer.angle.c

```
/* Compute transfer angle for an orbit between two terminal vectors.
This procedure is required to be able to solve Lambert's problem.  The output of
this procedure is required as an input to the Lambert problem solver.
The program requires the imput of three vectors, the two terminal vectors and a
```

```
third vector used to calculate the orbit plane normal.  The third vector can be
the initial velocity of the vechile at its starting terminal.
*/

#include <stdio.h>
#include <errno.h>
#include <math.h>
#include "definitions.h"
#include "array.def.h"

vector_3_D cross_product(vector_3_D,vector_3_D);
double dot_product(vector_3_D,vector_3_D);
double vector_length(vector_3_D );
vector_3_D Normalise_vector( vector_3_D a);

/* Compute the transfer angle.  This algorithm computes an angle between 0
and 360.  to define the rotation direction, it requires the velocity vector of
the first planet.  Alternativly the Z axis could be used but I think using the
velocity makes more sense. There is a posible problem when the two axes lie at
90 deg to each other. Though currently it work with the negative velocity vector
 as defining the rotation direction.  However it may be able to get a plane
through r1 and r2 in such a way as to mess up both the normal and velocity
 definition, but to get this I think the planet must be on a rectalinear
 orbit so this is probably not worth dealing with.*/

double Compute_transfer_angle(vector_3_D r1, vector_3_D v1, vector_3_D r2 )
{

  double answer, cos_theta, sin_theta;
  double length_r1,length_r2,test;
  vector_3_D plane_normal,pos_rotation_axis;
  length_r1 = vector_length(r1);
  length_r2 = vector_length(r2);

/* printf("|r1| = %f \n",length_r1);
  printf("|r2| = %f \n",length_r2); */

  /* compute the transfer plane normal */
  plane_normal = Normalise_vector( cross_product(r1,r2));
  pos_rotation_axis = Normalise_vector(cross_product(r1,v1));

 /* Test to see if the transfer angle is greater than 180 degrees.
   In which case solve the problem as a rotation in the opposite direction */
  test = dot_product(plane_normal,pos_rotation_axis);
  if (test < -limiting_accuracy){
    /* transfer angle is greater than 180 deg */
    plane_normal.x = - plane_normal.x;
    plane_normal.y = - plane_normal.y;
    plane_normal.z = - plane_normal.z;
  }


    /* test to see if the transfer plane is at right angles to the current
      orbital plane. In this event use the velocity vector to define the
      negative reference for rotation
    */
  if (fabs(test) < limiting_accuracy ){
    test = dot_product(plane_normal,v1);
    if (test  > 0.0 ){
      plane_normal.x = - plane_normal.x;
      plane_normal.y = - plane_normal.y;
      plane_normal.z = - plane_normal.z;
    }
  }

  /* compute the transfer angle using arctan2 to get quadrant */
  cos_theta = dot_product(r1,r2)/(length_r1*length_r2);

  sin_theta = dot_product(cross_product(r1,r2),plane_normal)/
                    (length_r1*length_r2);

  /*printf("sin theta = %f\n",sin_theta);
  printf("cos_theta = %f\n",cos_theta);*/

  answer = atan2(sin_theta,cos_theta);

  return answer;
}
```

E.7 Lamberts.problem.c

```
/* Solve Lamberts Problem */
/* This program takes in the start point vector, the destination vector, the
   transfer angle and the required transfer time.  It returns the velocity vector
   at the start point required to reach the target at the specified time.
   The position and velocity can then be fed into the rectaliniar to orbital
   elements program to calculate the orbital elements. */


/* Because the program returns the velocity it has real problems with 180 deg
transfers as the orbit normal is undefined. */

/* this version also contains a simple cubic solver introduced during problems
with the one suggested by Battin. These problems have now been resolved. */
```

```
/* Equation references are to Battins Astrodynamics book */

#include <stdio.h>
#include <errno.h>
#include <math.h>
#include "definitions.h"
#include "array.def.h"

vector_3_D cross_product(vector_3_D,vector_3_D);
double dot_product(vector_3_D,vector_3_D);
double vector_length(vector_3_D );
vector_3_D Normalise_vector( vector_3_D a);

long double compute_zeta(long double x);
long double compute_K(long double);
long double excentricity_a_p(long double a, long double p );
int sign(double x);
long double cubrt(long double x);
long double cubic_solver(long double a1,long double a2,long double a3);



vector_3_D Solve_Lamberts_problem( vector_3_D r1, vector_3_D r2, double theta, double transfer_time)
{
  long double length_r1,length_r2;
  long double c,s,lambda,T,Tp,l,m,x,error,zeta,h1,h2;
  long double B,u,K,y,old_x;
  vector_3_D answer;
  long double a,e,p,A1,A2,A11,A12,r0;
  long double c1,c2,c3,L,pi;
  long double epsilon,e_squared,temp1,temp2;
  pi = 2.0*acos(0.0);

 /* Compute the length of the sides of the transfer triangle */
  length_r1 = vector_length(r1);
  length_r2 = vector_length(r2);
  c = sqrt((length_r1+ length_r2)*(length_r1+length_r2) -
                        4*length_r1*length_r2*cos(theta/2)*cos(theta/2));

  /* printf("|r1| = %f \n",length_r1);
  printf("|r2| = %f \n",length_r2);
  printf("c = %f \n",c);*/

  /* Compute the 1/2 cucumference and Lambda */
  s = 0.5*(length_r1 + length_r2 + c);
  lambda = sqrt((s - c)/s);

/* printf("s = %f \n",s);
  printf("lambda = %e \n",lambda);*/


  T = sqrt(8*mu/(s*s*s))*transfer_time;

  /* Compute the transfer time for a parabolic orbit between the two points
    page 340 */

  Tp = 4/3*(1-lambda*lambda*lambda);

  l = (1-lambda)*(1-lambda)/((1+lambda)*(1+lambda));
/* printf("l = %e \n",l);*/

  m = T*T/(pow((1+lambda),6));
/* printf("m = %e \n",m); */
```

```
L = (1-l)/2;

/* initialise value of x */

if (T > Tp ){
  /* if T > Tp then looking for an eliptic orbit */
  x = l;
} else {
  /* if T < Tp then looking for a hypobolic orbit */
  x = 0.0;
}

/* need an initial guess at y */
y = sqrt(m/((l+x)*(1+x)));

error = 1.0;
while (fabs(error) > accuracy){

  old_x = x;

  zeta = compute_zeta(x);

  /* equations from page 339 */

  c1 = sqrt(L*L+m/(y*y))+L;
  c2 = c1-L-L;
  c3 = c1+c1-L-L;

  /* eqn 7.111 */
  h1 = c2*c2*(1.0+3.0*x+zeta)/(c3*(4.0*x+zeta*(x+3.0)));
```

```
    /* eqn 7.112 */
    h2 = m*(x - l + zeta)/(c3*(4.0*x+zeta*(3.0+x)));

    B = 27*h2/(4*(1+h1)*(1+h1)*(1+h1));

    u = B/(2.0*(sqrt(B+1.0)+1.0));

    K = compute_K(u);

    y = ((1.0+h1)/3.0)*(2.0+ (sqrt(1.0+B))/(1.0+2.0*u*K*K));

    /* As an alternative to using Battins Cubic solver there is a simple
technique, which is commented out in this example */

    /* y = cubic_solver(-1*(1+h1),0.0,-1.0*h2); */

    x = sqrt( (1-l)*(1-l)/4 + m/(y*y)) - (1+l)/2;

    error = fabs(x - old_x);

  }

  /* test code used to monitor the performance of the solution */
  /*zeta = compute_zeta(x);
  temp1 = sqrt((1.0-l)*(1.0-l)/4.0 + m/(y*y)) - (1+l)/2.0 - x;

  c1 = sqrt(L*L+m/(y*y))+L;
  c2 = c1-L-L;
  c3 = c1+c1-L-L;

  h1 = c2*c2*(1.0+3.0*x+zeta)/(c3*(4.0*x+zeta*(x+3.0)));
```

```
h2 = m*(x - l + zeta)/(c3*(4.0*x+zeta*(3.0+x)));

temp2 = y*y*y - y*y - h1*y*y - h2;

printf("eqn 1 = %e   eqn 2 = %e \n",temp1,temp2);

printf("zeta = %f\n",zeta);
printf(" x = %e   y = %f  h1 = %e   h2 = %e\n",x,y,h1,h2); */

/* having computed x can compute the orbit */

p = 2*length_r1*length_r2*y*y*(1+x)*(1+x)*sin(theta/2)*sin(theta/2)/
             (m*s*(1+lambda)*(1+lambda));

/*printf("Semi Latice rectum %f\n",p); */

a = m*s*(1+lambda)*(1+lambda)/(8*x*y*y);

/*printf("mean anomaly = %f\n",a); */


/*  compute the eccentricity */
epsilon = length_r2/length_r1 - 1.0;

c1 = 4.0*length_r2*sin(theta/2.0)*sin(theta/2.0)/length_r1;

e_squared = (epsilon*epsilon + c1 *(l-x)*(l-x)/((l+x)*(l+x)))/
                                                   (epsilon*epsilon+c1);

e = sqrt(e_squared);

/*printf("eccentricity = %f\n",e); */
```

```
  /* Computation of V1 is from derivation in thesis notes.*/
  r0 = 0.25*s*(1+lambda)*(1+lambda)*(1+x);

  /*printf(”r0 = %f\n”,r0);*/

  A11 = 2*y*(length_r1*(r0−0.5*(length_r1+length_r2)) + (r0−length_r1)*lambda*s)/(length_r1*length_r1*transfer_

  A2 = y*r0/(s*lambda*transfer_time);

  A12 = A2*length_r2*cos(theta)/length_r1;

  A1 = A11 −A12;

  /*printf(”A1 = %f A2 = %f \n”,A1,A2);*/

  answer.x = A1*r1.x + A2*r2.x;
  answer.y = A1*r1.y + A2*r2.y;
  answer.z = A1*r1.z + A2*r2.z;

  return answer;
}

long double compute_zeta(long double x)
{
  long double delta,sum,u,a,eta,answer;
  int count;

  eta = x/((sqrt(1+x)+1)*(sqrt(1+x)+1));

  delta = 1.0;
  sum = 9.0*eta/7.0;
  u = 9.0*eta/7.0;
  count = 1;

  /* derive the required accuracy and do at least a number of iterations */
  while ((u > limiting_accuracy)|| (count < 10)){

    a = (count+3)*(count+3)*eta/(4*(count+3)*(count+3) -1);

    delta = 1/(1+ a*delta);

    u = u*(delta-1);

    sum = sum + u;

    count = count +1;
  }

  answer = 8*(sqrt(1+x)+1)/(3+1/(5+eta+sum));

  return answer;

}

/* compute the continued fraction K eqn 7.125 using eqn 1.51 */
long double compute_K(long double x)
{
  long double delta,sum,u,a,remainder;
  double test_number,n;
  int count;

  delta = 1.0;
  sum = 1.0/3.0;
  u = 1.0/3.0;
  count = 1;

  /* derive the required accuracy and do at least a number of iterations */
  while ((u > limiting_accuracy) || (count < 10)){

    test_number = count/2.0;
    remainder = 2.0*modf(test_number,&n);
    if (remainder == 0)
      a = 2*(3*n+1)*(6*n−1)/(9*(4*n−1)*(4*n+1));
    else
      a = 2*(3*n+2)*(6*n+1)/(9*(4*n+1)*(4*n+3));

    delta = 1/(1+ a*x*delta);

    u = u*(delta−1);

    sum = sum + u;

    count = count +1;
  }

  return sum;
}

long double excentricity_a_p(long double a,long double p )
{

  long double answer;

  answer = sqrt(1−p/a);
  return answer;
}


long double cubic_solver(long double a1,long double a2,long double a3)
/* solves a general cubic of the form y^3+a1.y^2+a2.y +a3 = 0 and returns the
largest of the roots, or if only one real root that root.
it uses the routine in Numerical recipes page 164 eqns 5.5.6-5.5.10*/
{

  long double Q,R,x1,x2,x3,theta,pi,temp,answer;

  pi = 2.0*acos(0.0);

  Q = (a1*a1-3.0*a2)/9.0;
  R = (2.0*a1*a1*a1 -9.0*a1*a2 +27.0*a3)/54.0;

  if ((Q*Q*Q-R*R) >= 0.0){
    theta = acos(R/sqrt(Q*Q*Q));
    x1 = -2.0*sqrt(Q)*cos(theta/3.0) - a1/3.0;
    x2 = -2.0*sqrt(Q)*cos((theta+2.0*pi)/3.0) - a1/3.0;
    x3 = -2.0*sqrt(Q)*cos((theta+4.0*pi)/3.0) - a1/3.0;
    if (x1 > x2) {
      if  (x1 > x3)
        answer = x1;
      else
        answer = x3;
      }
    else {
      if (x2 > x3)
        answer =x2;
      else
        answer = x3;
    }

  }
  else{
    temp = cubrt(sqrt(R*R−Q*Q*Q)+fabs(R));
    x1 = −1.0*sign(R)*(temp+Q/temp) − a1/3.0;
    x2 = 0.0;
    x3 = 0.0;
    answer = x1;
  }

  return answer;

}

long double cubrt(long double x)
/* compute the cube root of a number */
{

  long double answer;

  answer = exp(log(x)/3.0);

  return answer;

}
```

E.8 vector.c

```
#include <stdio.h>
#include <errno.h>
#include <math.h>
```

```
#include "definitions.h"
#include "array.def.h"

vector_3_D cross_product(vector_3_D a,vector_3_D b)
{

  vector_3_D answer;

  answer.x = a.y*b.z − b.y*a.z;
  answer.y = a.z*b.x − a.x*b.z;
  answer.z = a.x*b.y − a.y*b.x;

  if (fabs(answer.x) < limiting_accuracy)
    answer.x = 0.0;
  if (fabs(answer.y) < limiting_accuracy)
    answer.y = 0.0;
  if (fabs(answer.z) < limiting_accuracy)
    answer.z = 0.0;

  return answer;

}

double dot_product(vector_3_D a,vector_3_D b)
{

  double answer;

  answer = a.x*b.x + a.y*b.y + a.z*b.z;

  if (fabs(answer) < limiting_accuracy)
    answer = 0.0;
  return answer;

}

double vector_length(vector_3_D a)
{

  double answer;
  answer = sqrt(a.x*a.x + a.y*a.y +a.z*a.z);

  return answer;
}

vector_3_D Normalise_vector( vector_3_D a)
{

  vector_3_D answer;
  double length;

  length = vector_length(a);
  if (length > limiting_accuracy){
    answer.x = a.x/length;
    answer.y = a.y/length;
    answer.z = a.z/length;}
  else{
    answer.x = 0.0;
    answer.y = 0.0;
    answer.z = 0.0;
  }

  return answer;
```

```
}
```

E.9 rec.to.clasical.c

```
/* This program converts rectangular orbital position and velocity into
   Classical Orbital Elements */

/* the formulas used for the most part come from Orbital Mechanics, Vladimir A
Chobotov editor, page 79& 80.  note the formulas for the sin of an angle are a
little different as his notation is confusing */

#include <stdio.h>
#include <errno.h>
#include <math.h>
#include "definitions.h"
#include "array.def.h"

vector_3_D cross_product(vector_3_D,vector_3_D);
double dot_product(vector_3_D,vector_3_D);
double vector_length(vector_3_D );
vector_3_D Normalise_vector( vector_3_D a);

orbit rectalinear_to_clasical(Rec_Orbit body_status,double current_date)
{
  vector_3_D vec_r,vec_v;
  vector_3_D W,vec_e,vec_k,vec_i,vec_N,N_hat,vec_temp,vec_Z;
  double r,v,e,a,mod_W,pi,cos_Omega,sin_Omega;
  double cos_omega,sin_omega;
  double cos_f,sin_f,f;
  double number_1,number_2;
  double M,E,delta_time,time, Semi_latice_rectum;
  orbit answer;
```

```
pi = 2.0*acos(0.0);


vec_r = body_status.pos;
vec_v = body_status.vel;


r = vector_length(vec_r);


v = vector_length(vec_v);


/* compute the Orbits Semi-major Axis */
a = 1/(2/r - v*v/mu);
answer.Semi_major_axis = a;


/* compute the Orbit Normal W */


W = cross_product(vec_r,vec_v);
W = Normalise_vector(W);
/*printf("Vector W = %f %f %f\n",W.x,W.y,W.z);  */


/* compute the Orbits inclination */
answer.Inclination = acos(W.z)*180/pi;



/* compute the eccentricity */


number_1 = 1/mu*(v*v - mu/r);
number_2 = 1/mu*dot_product(vec_r,vec_v);


vec_e.x = number_1*vec_r.x - number_2*vec_v.x;
vec_e.y = number_1*vec_r.y - number_2*vec_v.y;
vec_e.z = number_1*vec_r.z - number_2*vec_v.z;
```

```
/*              printf(”vector e = %f %f %f\n”,vec_e.x,vec_e.y,vec_e.z); */

e = vector_length(vec_e);
answer.Eccentricity = e;

if (e ==1.0){
    /* if the orbit is parabolic then tidy up a */
  a = 1.0/0.0;
  answer.Semi_major_axis = a;
}

/* Compute omega */

vec_k.x = 0.0;
vec_k.y = 0.0;
vec_k.z = 1.0;

/* Compute the longitude of the ascending Node */
/* N is the vector which defines the line of node */
vec_N = cross_product(vec_k,W);
N_hat = Normalise_vector(vec_N);
/*printf(”vector N = %f %f %f\n”,N_hat.x,N_hat.y,N_hat.z);*/

cos_Omega = N_hat.x;

vec_i.x = 1.0;
vec_i.y = 0.0;
vec_i.z = 0.0;

vec_temp = cross_product(vec_i,N_hat);

sin_Omega = vec_temp.z;
```

```
answer.Long_ascending_node = atan2(sin_Omega,cos_Omega)*180/pi;


vec_Z = Normalise_vector(cross_product(W,N_hat));

/* compute omega */

cos_omega = dot_product(N_hat,vec_e)/e;

/* this is modified from the book as it is not clear in the book */

vec_e = Normalise_vector(vec_e);
sin_omega = dot_product(W,cross_product(N_hat,vec_e));

answer.Argument_of_perigee = atan2(sin_omega,cos_omega);

/* compute f note this is theta in the book */

cos_f = dot_product(vec_e,Normalise_vector(vec_r));

sin_f = dot_product(W,cross_product(vec_e,Normalise_vector(vec_r)));

f = atan2(sin_f,cos_f);

printf("true Anomaly = %f\n",f*180/pi);

/* compute Semi Latice Rectum.  this is used to avoid having to work with the
   mean anomaly to get the perigee radius and also for parabolic orbits. */

Semi_latice_rectum = mu*(1+e*e+2*e*cos(f))/(v*v);
```

```
  answer.Perigee_radius = Semi_latice_rectum/(1+e);

  /* compute time of perigee passage */
  /* note this algorithm may have problems as approach e = 1.0 but currently no
  universal algorithm appears to be workable and so this is implemented
  in the mean time */
  if (e < 1.0) {
    /* compute E */
    E = 2.0*atan(sqrt((1-e)/(1+e))*tan(f/2));
    M = E - e*sin(E);
    delta_time = sqrt(a*a*a/mu)*M;
  }
  else {
    if ( e == 1.0){
      E = sqrt(Semi_latice_rectum)*tan(f/2.0);
      delta_time = (Semi_latice_rectum*E + E*E*E/3.0)/(2.0*sqrt(mu));
    }
    else {
      /* hypobolic orbit.  therefore use Battins eqn 4.48, 4.50 & 4.51 */
      E = 2.0*atan(sqrt((e-1.0)/(e+1.0))*tan(f/2.0));
      delta_time = sqrt(-1.0*a*a*a/mu)*(e*tan(E)-log(tan(E/2.0+pi/4.0)));
    }
  }

  answer.Time_of_perigee = current_date - delta_time;


  return answer;
}
```

E.10 universal.c

```
/*This routine computes the position of the satellite
  given the orbital elements and the time. It basically solves Kepler's
equation. It uses the algorithm proposed by Bates, White et al and expanded by
Chobotov */
/* for convenience if the orbit is circular then the program doesn't bother with
solving Keplers equation but goes straight to the answer.  This is done to speed
up the solution of Walker constellation problems. */

/* Note the program currently seems to have a problem with small values of e
and appears to be unstable. However this may have been fixed by replacing the
Chobotov iteration scheme with Bate et al's Newtonian solver which appears to
work well.  The problem with Chobotov's technique is unknown but seems to diverge
in some cases.  See univesal.ma*/

/* I'm a little concerned about the use of perigee as the definition of T0 but
not sure that it will be a problem */

/*If the orbit gets to hyperbolic then the C function fails. similarly the
program has problems initialising X if a position on the orbit before perigee
is required.*/

#define required_accuracy 1e-15

#include <stdio.h>
#include <errno.h>
#include <math.h>
#include "definitions.h"
#include "array.def.h"
```

```
#define required_accuracy2 1e−20

int sign(double x);
int integer(double x);
double compute_S(double Z);
double compute_C(double Z);
double vector_length(vector_3_D a);
double dot_product(vector_3_D a,vector_3_D b);
double cosh(double x);
double sinh(double x);

Rec_Orbit Compute_Satellite_Position(orbit sat_orbit, double current_time)
{

  double pi, e, inc, t0, r_0, alpha, semi_latice_rectum, Delta_t;
  double sigma_0,Period, X,Z,C,S, f,f1,f2,delta,delta_X,error;
  double g,Omega,omega,h, true_anomaly,r;
  double temp1,temp2,temp3,f_dot,g_dot;
  vector_3_D vector_r_0,vector_V_0, vector_r,vector_v;
  Rec_Orbit answer;
  int loop_counter;

  pi = 2.0*acos(0.0);
  e = sat_orbit.Eccentricity;
  inc = sat_orbit.Inclination *pi/180;
  t0 = sat_orbit.Time_of_perigee;

  r_0 = fabs(sat_orbit.Perigee_radius);

  /* alpha = 1/a */

  alpha = ( 1− e)/r_0;
```

```
semi_latice_rectum = r_0*(1+e);

/* compute the initial position and velocity */

Omega = sat_orbit.Long_ascending_node * pi/180;
omega = sat_orbit.Argument_of_perigee;

/* from problem 3-21 in Battins book */

vector_r_0.x = r_0*(cos(Omega)*cos(omega) - sin(Omega)*sin(omega)*cos(inc));
vector_r_0.y = r_0*(sin(Omega)*cos(omega) + cos(Omega)*sin(omega)*cos(inc));
vector_r_0.z = r_0*(sin(omega)*sin(inc));

/*printf("x0 = %f ", vector_r_0.x);
printf("y0 = %f ", vector_r_0.y);
printf("z0 = %f \n", vector_r_0.z); */

h = sqrt(mu*semi_latice_rectum);

Omega = sat_orbit.Long_ascending_node * pi/180;
omega = sat_orbit.Argument_of_perigee;

vector_V_0.x = -mu/h*(cos(Omega)*(sin(omega)+e*sin(omega)) +
                        sin(Omega)*(cos(omega)+e*cos(omega))*cos(inc));
vector_V_0.y = -mu/h*(sin(Omega)*(sin(omega)+e*sin(omega)) -
                        cos(Omega)*(cos(omega)+e*cos(omega))*cos(inc));

vector_V_0.z = mu/h*(cos(omega)+e*cos(omega))*sin(inc);
sigma_0 = dot_product(vector_r_0, vector_V_0);
if (fabs(sigma_0) > accuracy)
  printf("sigma = %e and should zero therefore there is a problem\n",
            sigma_0);

sigma_0 = 0.0;          /* this is because the base position is taken as perigee */

Delta_t = current_time − t0;

if (alpha > 0.0) {

  /* if an elliptical orbit then make the time a fraction of the period */
  Period = 2 * pi * sqrt(1/(alpha*alpha*alpha))/sqrt(mu);

  Delta_t = Delta_t − sign(Delta_t)*integer(fabs(Delta_t)/Period)*Period;
}

/* initialise the value of X */

if (e <= 1.0)
  X = sqrt(mu)*Delta_t*fabs(alpha);
else {
  temp1 = sign(Delta_t);
  temp2 = sqrt(−1.0/alpha);
  if (Delta_t == 0)
    temp3 = 0.0;
  else
    temp3 = log(2.0*mu*Delta_t/(sign(Delta_t)*
                          sqrt(−mu/alpha)*(1.0−r_0*alpha)));
  X = temp1*temp2*temp3;
}

/* down iteration to compute the correct value of X */
error = 1;
loop_counter = 0;
```

```
  while (error >required_accuracy){

    Z = X*X*alpha;

/*  C = 0.5 - (Z/24.0) +(Z*Z/720.0) - (Z*Z*Z/40320.0); */
    C = compute_C(Z);

/*  S = (1/6.0) - (Z/120.0) + (Z*Z/5040.0) - (Z*Z*Z/362880.0);*/

    S = compute_S(Z);

    /* Chobotov proposes a solution technique based around Laguere's Method.
In practice however this seems to give problems with stability.  Bates et al
propose a different solution technique which seems to work and is implemented
next.  The problem  associated with Chobotov's method is shown in universal.ma,
and is associated with a = 1, e =0.5 f = 45 deg.  Note this may just be a
coding problem but in tests using universal seems to be consistent problem*/

    /*f = (1- r_0*alpha)*S*X*X*X + sigma_0*C*X*X + r_0*X - sqrt(mu)*Delta_t;

    f1 = C*X*X + sigma_0*(1-C*Z);

    f2 = (1.0-r_0*alpha)*(1-S*Z)*X + sigma_0*(1-C*Z);
    printf(" C = %f  S = %f f = %f f1 = %f  f2 = %f \n",C,S,f,f1,f2);

    delta = 2*sqrt(fabs(4*f1*f1 - 5*f*f2));*/

    /* the if statement is required to deal with the case of Delta_t = 0 */
    /* if (( f < 1e-12) && (( delta < 1e-12)||(f1 <1e-12)))
      delta_X = 0.0;
    else
      delta_X = 5*f/(f1+sign(f1)*delta);
  X = X− delta_X;
  error = fabs(delta_X*delta_X*alpha); */

  /* The following calculation is based arround the method proposed by Bates
  et al, and uses a simple Newton iteration to solve for X */

  delta_X = (sqrt(mu)*Delta_t − (1.0−r_0*alpha)*X*X*X*S − r_0*X)/
                      (X*X*C + r_0*(1.0−Z*C));

  X = X + delta_X;
  error = fabs(delta_X);
  /*printf(”loop error = %e\n”,error);*/

  ++loop_counter;
  if (modf((double)loop_counter/20.0,&temp1) == 0 )
    printf("in uinversal %i\n",loop_counter);
}

Z = X*X*alpha;
C = compute_C(Z);
S = compute_S(Z);

/*printf(”x = %f  Z = %12.9f  C = %f  S = %f\n”,X,Z,C,S); */

error = ((1.0−r_0*alpha)*X*X*X*S + r_0*X)/sqrt(mu) − Delta_t;
if (fabs(error) > (1E3 *accuracy))
  printf("larger than expected error in reverse computed time = %e\n",error);

f = 1.0 − X*X*C/r_0;

/*g = Delta_t − X*X*X*S/sqrt(mu); */
g = r_0*X*(1.0−Z*S)/sqrt(mu);
```

```
  /*printf("f = %f,  g = %f\n",f,g); */

  /* compute the position and velocity at perigee */
  /* see Battin page 125 */

  vector_r.x = f*vector_r_0.x + g*vector_V_0.x;
  vector_r.y = f*vector_r_0.y + g*vector_V_0.y;
  vector_r.z = f*vector_r_0.z + g*vector_V_0.z;

/* printf("Position 0= %f %f %f\n", vector_r_0.x, vector_r_0.y, vector_r_0.z);
  printf("Velocity 0 = %f %f %f\n", vector_V_0.x, vector_V_0.y, vector_V_0.z);
*/
  /* compute the true anomaly...this is a good test of the accuracy */

  r = fabs(vector_length(vector_r));

  g_dot = 1.0 - X*X*C/r;
  f_dot = sqrt(mu)*X*(Z*S-1.0)/(r_0*r);

  vector_v.x = f_dot*vector_r_0.x + g_dot*vector_V_0.x;
  vector_v.y = f_dot*vector_r_0.y + g_dot*vector_V_0.y;
  vector_v.z = f_dot*vector_r_0.z + g_dot*vector_V_0.z;

  error = f*g_dot -f_dot*g;

  if (fabs(error -1.0) > (100.0 *accuracy)){
    printf("generating large error in Lagrangian multipliers = %e\n",
                                                            (error-1.0));
    printf("This Suggest that the results are in ERROR \n");
  }
  true_anomaly = acos(1.0− semi_latice_rectum*X*X*C/
                 (r*r_0));
  /*printf(”true anomaly 1 = %f\n”,true_anomaly*180/pi); */

  error = cos(true_anomaly)*cos(true_anomaly);

  true_anomaly = asin(g*sqrt(mu*semi_latice_rectum)/(r*r_0));
  /* printf(”true anomaly 2 = %f\n”,true_anomaly*180/pi); */

  error = error +sin(true_anomaly)*sin(true_anomaly);

  if (fabs(error −1.0) > (100.0 *accuracy)){
    printf("generating large error in true anomaly = %e\n",(error−1.0));
    printf("This Suggest that the results are in ERROR \n");
  }

  /* copy answer for return to calling program */

  answer.pos = vector_r;
  answer.vel = vector_v;

  return answer;

}

int sign(double x)
{
  int answer;

  if ( x >= 0.0 )
    answer = 1;
  else
```

```
    answer = -1;

  return answer;
}

int integer(double x)
{
  int answer;
  double temp,temp2;

  temp = modf(x, &temp2);
  answer = (int)temp2;
  return answer;
}

/* S and C are computed using the following functions as one has to be careful
    of the number of terms required for a decent accuracy
    The implementation is to avoid problems with dividing large numbers by
    large numbers with the danger of overflows etc
    */
double compute_S(double Z)
{

  long double delta, answer,temp;
  int index;

  if (fabs(Z) < 5.0){
    answer = 1/6.0;
    delta = answer;
    index = 1;
    while ((delta > required_accuracy2)|| (index < 8)){
      delta = delta * Z/((2*index +2)*(2*index+3));
      if ( fmod(index,2) == 0 )
        answer = answer + delta;
      else
        answer = answer - delta;

      ++index;
    }
  }
  else{
    if ( Z > 0){
      temp = sqrt(Z);
      answer = (temp - sin(temp))/(Z*temp);
    }
    else{
      temp = sqrt(-1.0*Z);
      answer = (sinh(temp)-temp)/(-1*Z*temp);
    }
  }
/*  printf(”Z = %f answer =%e\n”,Z,answer);*/

  return answer;
}

double compute_C(double Z)
{
  /* there seems to be a problem with these series as they initially diverge for large X */
  long double delta, answer;
  double reply;
  int index;


  if (fabs(Z) < 5.0){
    answer = 0.5;
    delta = answer;
    index = 1;
    while ((delta > required_accuracy2)|| (index < 8)){
      delta = delta * Z/((2*index +1)*(2*index+2));
      if ( fmod(index,2) == 0 )
        answer = answer + delta;
      else
        answer = answer - delta;

      ++index;
    }
    reply = answer;
    /* printf("index = %i ",index); */
  }
  else{
    if ( Z > 0)
      reply = (1.0 - cos(sqrt(Z)))/Z;
    else {
      answer = sqrt(-1.0*Z);
      reply = (1.0-cosh(answer))/Z;
    }
    /*                    printf("Z = %f answer =%e\n",Z,reply); */
  }
  return reply;
}

double cosh(double x)
{
  long double answer,temp;

  temp = exp(x);
  answer = (temp+1/temp)/2;

  return answer;
}

double sinh(double x)
{
  long double answer,temp;

  temp = exp(x);
  answer = (temp-1/temp)/2;

  return answer;
}
```

Appendix F

Lens Mass Calculation

F.1 Assumptions

Let us assume that the lens is created using circular waveguide channels. Furthermore let us assume that the lens can be modeled as a grid of hexagonal pieces joined together, each piece containing a single waveguide passage. Figure F-1 shows these assumptions schematically.

F.2 Circular Cavity Segment Mass

A single lens segment is shown in figure F-2. r is the radius of the waveguide cavity. t is the half minimum thickness of the support material between the cavities.

The area of the surrounding hexagon is given by:

$$\text{Area} = 6 \times \frac{s}{2} \times (r + t)$$

Where

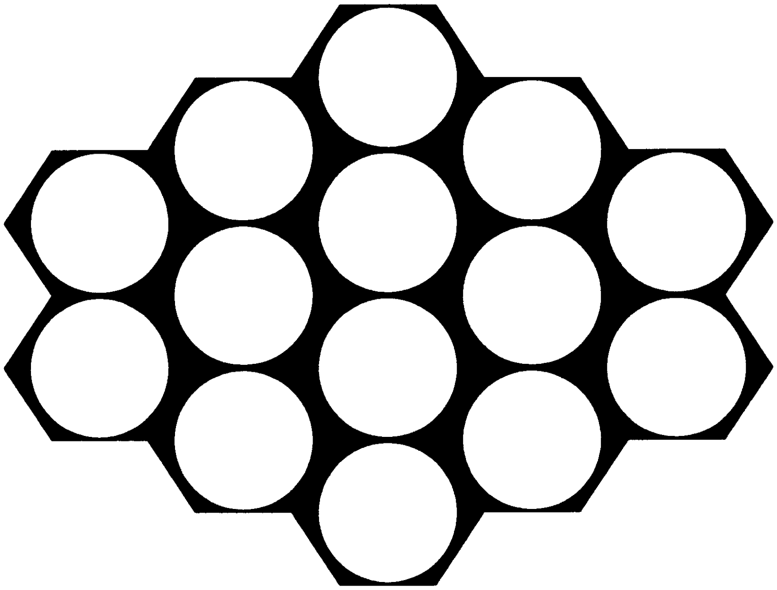

Figure F-1: Segment of Antenna Lens

$$s = \frac{(r+t)}{\cos 30}$$

If h is the depth of the lens and ρ is the density of the support material then the mass of a single segment is given by:

$$\mathrm{M,ass}_{\mathrm{cavity}} = h\rho\left(\frac{3(r+t)^2}{\cos 30} - \pi r^2\right)$$

F.3 Rectangular Cavity Segment Mass

If the cavity has internal dimensions of a and b and a wall thickness of t, the mass of a single segment is given by:

$$\mathrm{Mass}_{\mathrm{r}} = 2\rho h t(b + a + t)$$

The area of each cavity is:

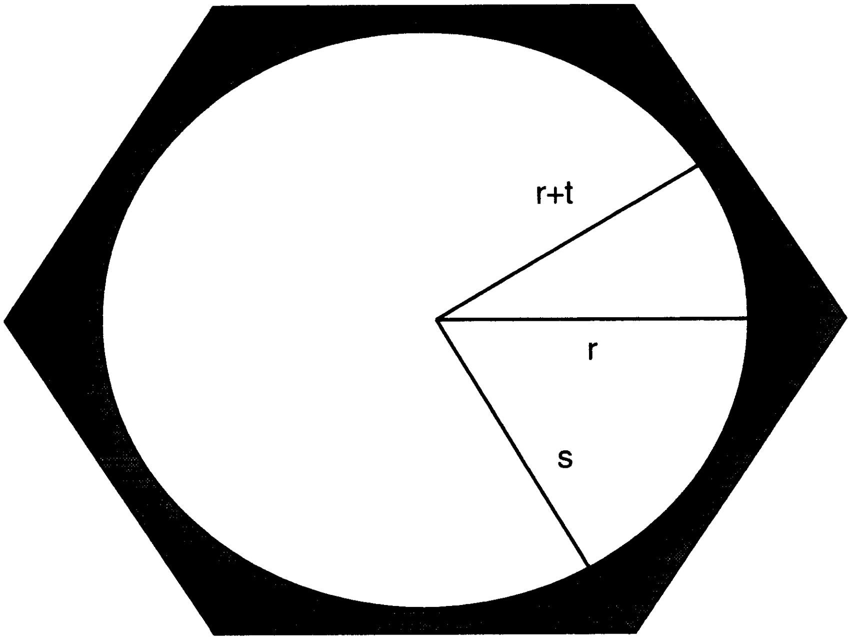

Figure F-2: Segment of Antenna Lens

$$\text{Area}_r = (a + 2t) \times (b + 2t)$$

F.4 Waveguide Diameter

A circular waveguide has a cut off frequency controlled by the propagation of the TE_{11} mode. The cut-off wavelength is given by [24]:

$$\lambda_c = 3.41r$$

Because the antenna is operating in vacuum we can assume that the waveguide permittivity is the same as the free space permittivity. Therefore, to propagate a signal at 32 GHz, a waveguide greater than 3 mm is required.

For rectangular waveguide the cut off frequency is given by:

$$f_c = c\left(\left(\frac{m\pi}{a}\right)^2 + \left(\frac{n\pi}{b}\right)^2\right)^{\frac{1}{2}}$$

For a rectangular waveguide the lowest order mode is the TE_{10} mode. Thus, if $a > b$, this simplifies to:

$$f_c = \frac{c}{2a}$$

To cut off all frequencies below 32 GHz, a = 4.6 mm.

F.5 Circular Cavity Based Lens Mass

Let us assume that the total area of the lens is much larger than that of a single waveguide segment. The number of segments required for a lens of radius R is simply given by:

$$n = \frac{\pi R^2 \cos 30}{3(r+t)^2}$$

The mass of the lens is:

$$\text{Mass} = \frac{\pi R^2 \cos 30}{3(r+t)^2} \times h\rho\left(\frac{3(r+t)^2}{\cos 30} - \pi r^2\right)$$

For an aluminium structure $\rho = 2.8 \times 10^3 \text{Kg/m}^3$ [1]. For a lens with a cutoff frequency of 32 GHz then $r = 0.002$ m. If we assume that the minimum thickness between cavities is 1 mm, then a 1.5 m lens with an average thickness of 0.01 m weighs 69.4 Kg.

F.6 Rectangular Cavity Based Lens Mass

Let us again assume that the total area of the lens is much larger than that of a single waveguide segment. The number of segments required for a lens is therefore:

$$n = \frac{\pi R^2}{(a + 2t) \times (b + 2t)}$$

Therefore the mass of the lens is:

$$\text{Mass} = \left(\frac{\pi R^2}{(a + 2t) \times (b + 2t)} \right) 2\rho h t(b + a + t)$$

For a lens with a cutoff frequency of 32 GHz, a average thickness of 0.01 m and a diameter of 1.5 m, the mass is 62.7 Kg. This suggests that a rectangular cavity based lens is preferable.

Appendix G

Final Spacecraft Communication Link Budgets

G.1 X Band Up Link

Frequency	GHz	7.145	
Wavelength	m	0.04	
Tx Power	dBW		43
Waveguide Loss	dB		0.25
O/P Power at Horn	dB		42.75
Antenna Gain	dB		67.1
EIRP	dBi		109.85

Pointing Loss	dB		0.1
Atmospheric Loss	dB		0.06
Path Length	AU	31	
Free Space Loss	dBm-2		-302.85
Power at Spacecraft	dBm-2		-193.16
Antenna Diameter	m	1.6	
Antenna Beamwidth	deg	1.84	
Antenna Efficiency	%	65	
Antenna Gain	dB		39.70
Pointing Accuracy	deg	0.1	
Pointing Loss	dB		0.01
Waveguide Loss	dB		0.15
Diplexor Loss	dB		0.1
LNA Noise Figure	dB	1.6	
System Noise Temp	K	159.02	
System Noise Temp	dBK		22.01
Boltzmann's Constant	dBK-1		228.6
C/No	dB		53.11
Data Rate	KBps	14.5	

Eb/No	dB		11.50
Required BER		10^{-6}	
Required Eb/No	dBHz		10.2
Coding Gain	dB		3.8
Implementation Loss	dB		2
Margin	dB		3.10

X Band Up Link

G.2 X Band Down Link

Frequency	GHz	8.42	
Wavelength	m	0.04	
HPA Output Power	W	10	
HPA Power	dBW		10
Isolator Loss	dB		0.1
Waveguide Loss	dB		0.05
Diplexor Loss	dB		0.1
Waveguide Loss	dB		0.1

O/P power at Horn	dB		9.65
Antenna Diameter	m	1.6	
Antenna Beamwidth	deg	1.56	
Antenna Efficiency	%	65	
Antenna Gain	dB		41.12
EIRP	dBi		50.77
Pointing Error	deg	0.1	
Pointing Loss	dB		0.01
Path Length	AU	31	
Free Space Loss	dBm-2		-304.28
Atmospheric Loss	dB		0.06
Power at DSN Antenna	dBm-2		-253.58
Receiver antenna Gain	dBi		74.1
System Noise Temp	K	31.56	
System Noise Temp	dBK		14.99
Boltzmann's Constant	dBK-1		228.6
C/No	dB		34.13
Data Rate	Bps	450	

Eb/No	dB		7.60
Required BER		10^{-6}	
Required Eb/No	dBHz		10.2
Coding Gain	dB		7.6
Implementation loss	dB		2
Margin	dB		3.00

X Band Down Link

G.3 Ka Band Up Link

Frequency	GHz	32	
Wavelength	m	0.01	
Tx Power	dBW		43
Waveguide Loss	dB		0.25
O/P Power at Horn	dB		42.75
Antenna Gain	dB		74.86
EIRP	dBi		117.61

Pointing Loss	dB		0.1
Atmospheric Loss	dB		0.46
Path Length	AU	31	
Free Space Loss	dBm-2		-315.88
Power at Spacecraft	dBm-2		-198.83
Antenna Diameter	m	1.6	
Antenna Beamwidth	deg	0.41	
Antenna Efficiency	%	65	
Antenna Gain	dB		52.72
Pointing Accuracy	deg	0.1	
Pointing Loss	dB		0.17
Waveguide Loss	dB		0.15
Diplexor Loss	dB		0.1
LNA Noise Figure	dB	1.6	
Antenna Noise Temp	K	5	
System Noise Temp	K	143.94	
System Noise Temp	dBK		21.58
Boltzmann's Constant	dBK-1		228.6
C/No	dB		60.73

Data Rate	KBps	85	
Eb/No	dB		11.44
Required BER		10^{-6}	
Required Eb/No	dBHz		10.2
Coding Gain	dB		3.8
Implementation Loss	dB		2
Margin	dB		3.04

Ka Band Up Link

G.4 Ka Band Down Link

Frequency	GHz	32	
Wavelength	m	0.01	
HPA Output Power	W	10	
HPA Power	dBW		10
Isolator Loss	dB		0.1
Waveguide Loss	dB		0.05
Diplexor Loss	dB		0.1
Waveguide Loss	dB		0.1

O/P Power at Horn	dB		9.65
Antenna Diameter	m	1.6	
Antenna Beamwidth	deg	0.41	
Antenna Efficiency	%	65	
Antenna Gain	dB		52.72
EIRP	dBi		62.37
Pointing Error	deg	0.1	
Pointing Loss	dB		0.18
Path Length	AU	31	
Free Space Loss	dBm-2		-315.88
Atmospheric Loss	dB		0.46
Receiver antenna Gain	dBi		74.86
System Noise Temp	K	53.31	
System Noise Temp	dBK		17.27
Boltzmann's Constant	dBK-1		228.6
C/No	dB		32.05
Data Rate	Bps	275	

Eb/No	dB		7.65
Required BER		10^{-6}	
Required Eb/No	dBHz		10.2
Coding Gain	dB		7.6
Implementation loss	dB		2
Margin	dB		3.05

Ka Band Down Link

Bibliography

[1] Brij N Agrawal. *Design of Geostationary Spacecraft.* Prentice-Hall, 1986.

[2] James R Asker. Pluto fast flyby slated for 2006. *Aviation Week & Space Technology*, pages 46–51, February 1993.

[3] Richard H Battin. *An Introduction to the Mathematics and Methods of Astrodynamics.* AIAA Education Series. American Institute of Aeronautics and Astronautics Inc, Washington, DC, first edition, 1987.

[4] Charles D Brown. *Spacecraft Mission Design.* AIAA Education Series. American Institute of Aeronautics and Astronautics Inc, Washington, DC, first edition, 1992.

[5] H S Chen. *Space Remote Sensing Systems: An Introduction.* Academic Press, 1985.

[6] Clarricoat and Poulton. High-efficiency microwave reflector antennas (a review). *Proceedings of the IEEE*, 65:1470–1504, October 1977.

[7] Lt Col Thomas M Davis. Space technologies for small satellites. Presentation by Phillips Laboratory to The NRC Advanced Space Technology Comittee Meeting on Small Satellite Technology., 1993.

[8] R W Davis. Emerging light sat capabilities. Presentation by TRW Space & Electronics Group, Spacecraft Technology division, to NRC/ASEB Committee on Advanced Space Technology, 1993.

[9] Richard de Neufville. *Applied Systems Analysis.* McGraw-Hill, 1990.

[10] Burton dobratz. Third annual hughes technology review. Presentation by Hughes Spacec and Communications Company, to NRC/ASEB Committee on Advanced Space Technology, on April 1st, 1993.

[11] J L Elliot et al. Pluto's atmosphere. *Icarus*, pages 148–170, 1989.

[12] W R Fimple. Optimum midcourse plane changes for ballistic interplanetary trajectories. In *American Rocket Society 17th Annual Meeting*, Los Angeles California, November 1962. American Rocket Society. ARS-2628-62.

[13] M Bousquet G Maral. *Satellite Communications Systems.* John Wiley & Sons, 1982.

[14] Joel S Greenburg and Henry R Hertzfeld, editors. *Space Economics.* Progress in Astronautics and Aeronautics. Americaan Institute of Aeronautics and Astronautics, 1992.

[15] Michael D Griffin and James R French. *Space Vechicle Design*, volume 1 of *AIAA Education Series.* American Institute of Aeronautics and Astronautics Inc, Washington, DC, first edition, 1991.

[16] Brantley R Hanks. Nasa miniature spacecraft technology development activities. Presentation by OACT to The NRC Advanced Space Technology Comittee Meeting on Small Satellite Technology., January 1993.

[17] Yeongming Hwang. Satellite antennas. *Proceedings of the IEEE*, 80(1):183–193, January 1992.

[18] Steven J Isakowitz. *International Reference Guide to Space Launch Systems.* AIAA, 1991.

[19] S N Williams J M Longuski. The last grand tour opportunity to pluto. *The Journal of the Astronautical Sciences*, 39:359–365, July-September 1991.

[20] Jerry I Porras James C Collins. Organizational vision and visionary organizations. *California Management Review*, pages 30–52, Fall 1991.

[21] JPL. *Deep Space Network/Flight Project Interface Desgin Handbook.* JPL, 1992. JPL Document 810-5 Rev D Volume I and II.

[22] Carl G Sauer Jr. The effect of parking orbit constraints on the optimization of ballistic planetary missions. In *AAS/AIAA Astrodynamics Specialist Conference*, Lake Placid New York, August 1983. AAS. AAS-83-311.

[23] P H Kellemeyn et al. Galileo orbit determination for the gaspera astroid encounter. In *AAS/AIAA Astrodynamics Specialist Conference*, 1992. AIAA paper AIAA-92-4523.

[24] Ronold W P King and Sheila Prasad, editors. *Fundamental Electromagnetic Theory and Applications.* Prentice-Hall Inc., Englewood Cliffs NJ, 1986.

[25] Jet Propulsion Laboratory. Small spacecraft control technology. Presentation by JPL May 13-14th to NRC/ASEB Committee on Advanced Space Technology, 1993.

[26] James R Lesh. Deep space optical communications program. Presentation by JPL to NRC/ASEB Committee on Advanced Space Technology, 1993.

[27] Dennis V Byrnes Louis A D'Amario. Interplanetry trajectory design for the galileo mission. Technical Report 83-0099, AIAA, 1983.

[28] Richard Matlock et al. Overview of sdio technology programs. Presentation by SDI, to NRC/ASEB Committee on Advanced Space Technology on 27-29 January, 1993.

[29] Frederick C. Mish, editor. *Webster's Ninth New Collegite Dictionary.* Merriam-Webster Inc, first digital edition, 1992.

[30] Dan Rascoe. Miniture spacecraft rf communications technology. Presentation by JPL May 13-14th to NRC/ASEB Committee on Advanced Space Technology, 1993.

[31] Robert G. Chamberlin Robert Shishko. *NASA Systems Engineering Handbook.* NASA, draft edition, September 1992.

[32] A W Rudge et al., editors. *The Handbook of Antenna Design*, volume 1 of *IEE Electromagnatic Waves Series.* Peter Peregrinus Ltd on behalf of the Institute of Electrical Engineers, 1982.

[33] Christopher G Salvo. Pluto fast flight system assumptions/guidelines. Presentation by JPL 16th November, 1992.

[34] Andrey B Sergeyevsky. Planetary mission departures from space station orbit. In *Aerospaces Science Meeting*, number 27th, Reno Nevada, 1989. AIAA, AIAA. AIAA-89-0345.

[35] Robert Staehle et al. Technology trades for the pluto fast flyby mission. Presentation to the National Research council, Aeronautics and Space Engineering Board, Advanced Space Technology Committee, January 1993.

[36] Robert L Staehle et al. Exploration of pluto. IAF, 1992. IAF Paper 92-0558.

[37] K A Stroud, editor. *Engineering Mathematics.* Macmillan Education Ltd, 3 edition, 1989.

[38] George P Sutton. *Rocket Propulsion Elements: An Introduction to the Engineering of Rockets.* John Wiley & Sons, sixth edition, 1992.

[39] Tomas Svitek et al. A low-cost, near-term pluto/charon flyby mission. In *AAS/AIAA Astrodynamics Specialist Conference*, pages 1395–1410. AAS, 1993. AAS-93-194.

[40] T.L.Staehle et al. Exploration of pluto: Search for applicable satellite technology. In Wizard V. Oz and Mihalis Yannakakis, editors, *Proc. Fifteenth Annual ACM 3 STOC*, number Sixth in Annual AIAA/Utah State University Conference on Small Satellites, pages 133–139, Logan Utah, September 1983. AIAA/Utah State University, AIAA.

[41] L M Trafton. Pluto's atmosphere near perihelion. *Geophysical Research Letters*, 16(11):1213–1216, Nov 1989.

[42] R M Vaughan et al. Optical navigation for the galileo gaspera encounter. In *AAS/AIAA Astrodynamics Specialist Conference*, 1992. AIAA paper AIAA-92-4522.

[43] Jim Watzin. Small satellite subsystem architecture: Systems engineering. Presentation by GSFC SMEX project, to NRC/ASEB Committee on Advanced Space Technology on June 1st, 1993.

[44] S S Weinstein. Pluto flyby mission concepts for very small and moderate spacecraft. Technical Report 92-4372-CP, AIAA, 1982.

[45] James R Wertz, editor. *Spacecraft Attitude Determination and Control.* Kluwer Academic Publishers, 1991.

[46] James R Wertz and Wiley J Larson, editors. *Space Mission Analysis and Design.* Space Technology Library. Kluwer Academic Publishers, 1991.

[47] Andrew Wilson, editor. *Jane's Space Directory 1993-94.* Jane's information group, 1993.

[48] D K Yeomans et al. Targetting an astroid: the galileo spacecraft's encounter with 951 gaspra. *The Astronomical Journal*, 105(4):1547–1552, April 1993.

5440-27